UC Santa Barbara

UC Santa Barbara Electronic Theses and Dissertations

Title

The influence of land use on river nutrient and sediment concentrations as well as benthic community composition on nearshore reefs around Moorea, French Polynesia, and the development of a low-cost, open-source autonomous water sampler

Permalink

https://escholarship.org/uc/item/0th60752

Author

Neumann, Kyle Christopher

Publication Date

2023

Peer reviewed|Thesis/dissertation

eScholarship.org Powered by the California Digital Library
University of California

UNIVERSITY OF CALIFORNIA

Santa Barbara

The influence of land use on river nutrient and sediment concentrations as well as benthic community composition on nearshore reefs around Moorea, French Polynesia, and the development of a low-cost, open-source autonomous water sampler

A dissertation submitted in partial satisfaction of the
requirements for the degree Doctor of Philosophy from the
Interdepartmental Graduate Program in Marine Science

by

Kyle Christoper Neumann

Committee in charge:

Professor Deron E. Burkepile, Chair

Professor John Melack

Professor Nicholas Nidzieko

December 2023

SIGNATURE PAGE

The dissertation of Kyle Neumann is approved.

_____

Dr. John Melack

_____

Dr. Nick Nidzieko

_____

Dr. Deron Burkepile, Committee Chair

September 2023

Acknowledgements

First and foremost I must express my immense gratitude for the island of Moorea and her people. As a young, naïve graduate student I was honored to be welcomed to the table with Polynesian educators, scientists, artists, musicians, fishers, and knowledge keepers. The work presented in this dissertation was born out of long conversations and the sharing of ideas, and was accomplished through long days in the field followed by the sharing of meals. Specifically and humbly I would like to thank Hinano Murphy for entertaining and welcoming the ideas of a young graduate student and fostering those ideas until they grew into something much larger than I could have imagined. Terava Atger and Tauira Punu, your incredible positivity, hard work and support truly made this work possible. I thank all of the members of Ati Vai including Sandrine Raparii, Sylvie Tuahu, Mariella Taumihau, Rauheno Taeahi, Anu Firiapu, Djelma Maono, Taaroa Maono, and Francis who so generously shared their knowledge, time and home with me. Thank you to Benoit Espiau for welcoming me into your laboratory and your home so many times. I am also incredibly grateful for Léna Marchal at the Teavaro school for the opportunity to give back in some small way to the place that has given me so much.

I could not have made through years of the ecologist lifecycle — months in the field followed by months behind a computer, repeat — without the Pile, and a few others. Thank you Deron for your guidance, Kelly for being such an incredible inspiration and friend, Cory for setting the example of following one's own path, and Christian for your generosity in knowledge and coffee. I now know that the grind of academia cannot be survived without letting off steam. Lily, I value every one of our late night vexation vents over Hinanos. Christie and Ryan, without the space that

you created to allow for the free creative expression through music and sailing, and your friendship overall, I am certain I would have lost my self.

Completing my PhD has truly been the single most difficult thing I have done in my life. The process is hard in and of itself, of that there is no doubt. However, the revelations about oneself catalyzed by the process can be even harder. It was through the process of completing the PhD that I came to understand how my brain might work differently than others. Through all of this, my wife Jordan has been in front of me as a beacon of inspiration and love, at my side encouraging and supporting, and when necessary behind me pushing me to be here, now. I love you. And I love the life we have built together with our son Owen in spite of (and sometimes, but only sometimes, because of) this path that I chose. I look forward to exploring our future together!

CV

Kyle C. Neumann

Ostrea Marine
Juneau, AK 99801
(503) 459-1730
kyle.neumann@ostreamarine.com

EDUCATION

Ph.D. Candidate in Marine Science, University of California Santa Barbara *2015 to 2023*
Graduate Student Researcher – Burkepile Marine Community Ecology Lab

Bachelor of Science in BioResource Research, Oregon State University *Graduated 2015*
Minor: Chemistry, Emphasis: Water Resources

PROFESSIONAL AND ACADEMIC APPOINTMENTS

Owner *2021 to Present*
Ostrea Marine

Research Fellow *2021 to 2022*
Alaska Sea Grant
NOAA Alaska Fisheries Science Center

Marine Engineer *Feb. 2020 to Present*
Steering Committee
Lab Manager Search Committee
Innovation Lab
Oregon State University

Lead Video Engineer *2017 to 2018*
Exploration Vessel Nautilus
Ocean Exploration Trust

Video Engineer *2014 to 2016*
Exploration Vessel Nautilus
Ocean Exploration Trust

Ocean Instrumentation Specialist *2014 to 2015*
The Sexton Corporation

Research Assistant *2013 to 2015*
Geomicrobiology Lab
Oregon State University

CEO/Camera Systems Engineer *2012 to 2013*
Remotely Operated Vehicle (ROV) Team
Linn Benton Community College

Camera/Production Assistant *2011 to 2013*
Oregon Field Guide
Oregon Public Broadcasting

TEACHING & MENTORING EXPERIENCE

Research Mentor *2016 to Present*
Total of 10 undergraduate students from Marine Science, Biology, Biochemistry, Geography and Mechanical, Electrical and Computer Engineering programs
UC Santa Barbara

Director and Founder *2017 to Present*
Ati Vai: An educational organization focused on watershed processes, pollution, and aquatic biology
Mo'orea, French Polynesia

Technical Advisor *2018 to Present*
Openly Published Environmental Sensing (OPEnS) Lab
Oregon State University

Advisor *2018 to 2019*
Undergraduate engineering senior capstone project: Drone Deployable CTD
UC Santa Barbara

Teaching Assistant *2017*
Introductory Biology Lab
UC Santa Barbara

Instructor - Volunteer *2016 to 2017*
Robotics
The Anacapa School

Classroom Lead – Volunteer *2015*
SciTrek
La Colina Junior High School

PUBLICATIONS & REPORTS

Neumann, K.C., Yoo, H., La, D., Burkepile, D.E. (2023). Programmable autonomous water sampler (PAWS) for aquatic research. *HardwareX. https://doi.org/10.1016/j.ohx.2022.e00392*

Hollarsmith, J. A., Ramírez-Ortiz, G., Winquist, T., Velasco-Lozano, M. DuBois, K., Reyes Bonilla, H., **Neumann, K.C.**, Grosholz., E.D. (2020). Habitats and fish communities at mesophotic depths in the Mexican Pacific. *Journal of Biogeography.*

Neumann, K.C., Tremblay, A., Lenihan, H. (2017) Crowdsourcing oceanographic data using novel small format sensors deployed on recreational and commercial vessels. *White Paper for the Honda Marine Foundation*

Torres, M., Colwell, F., Yang, J., Wishart, J., **Neumann, K.C**., Verba, C. (2014). Biogeochemical reactions that control tracer and contaminant release. *National Energy Technology Laboratory Unconventional Resources Final Report (EPACT)*

FELLOWSHIPS, GRANTS & AWARDS

2016 to 2020 - NSF Graduate Research Fellowship ($138,000)

2019 - Association for the Sciences of Limnology and Oceanography Global Outreach Initiative ($2,000)

2019 - Worster Award for Mentorship of Undergraduate Research ($5,000)

2019 - Schmidt Family Foundation Environmental Solutions Fellowship ($8,500)

2018 - Maria Carrillo High School Distinguished Alumni Award

2017 - Link Foundation Ocean Instrumentation Fellowship ($29,000)

2017 - Honda Marine Ocean Instrumentation Fellowship ($7,500)

2016 - 1st prize in the UC Santa Barbara New Ventures Competition ($12,500)

2016 - Marine Technology Society's ROV Committee Scholarship ($5,000)

2016 - UC Santa Barbara Coastal Fund Grant ($17,000)

SELECTED PRESENTATIONS

Neumann, K.C. *The influence of terrestrial runoff on the health of reefs around Mo'orea, French Polynesia, and how doing things the hard way inspired the development of new research tools.* Talk. Hatfield Marine Science Center Seminar Series, Oregon State University, June 11th, 2020 **(Invited seminar)**

Neumann, K.C., Zubia, M., Pierce, K., Underhill, W., Green, C. Burkepile, D.E. *Rivers, land use change, and the influence of rivers on reefs.* Talk. Mo'orea Coral Reef LTER All Investigators Meeting, Santa Barbara, CA, December 5th-6th, 2019

Neumann, K.C., Yoo, H., La, D., Burkepile, D.E. *Water-Corers: Low-cost, open source water samplers designed to study ecosystem dynamics in novel ways and with high resolution*. Speed talk. Western Society of Naturalists Meeting, Ensenada, MX, October 31st - November 3rd, 2019

Neumann, K.C., Burkepile, D.E. *Nutrients from Ridge to Reef on Mo'orea, A High Island in the South Pacific*. Poster. Western Society of Naturalists Meeting, Tacoma WA, November 8th-11th, 2018

Neumann, K.C. *Connexions montagne-récif à Moorea*. Talk. Teavaro Community Center, Mo'orea, French Polynesia, August 9th, 2018 **(Invited public seminar)**

Neumann, K.C. *Robotics in Undersea Research and Exploration*. Talk. Antarctic Circumnavigation Expedition Maritime University, R/V Akademik Tryoshnikov, December 18th, 2016 **(Invited seminar)**

Neumann, K.C. *Crowdsourcing Environmental Data*. Talk. Antarctic Circumnavigation Expedition Maritime University, R/V Akademik Tryoshnikov, December 6th, 2016 **(Invited seminar)**

Neumann, K.C., Wishart, J.R., Colwell, F.S., Thurber, A., Vega-Thurber, R. *Development of high resolution osmotically driven sampling systems to track nutrient flux in shallow marine environments.* Poster. Pacific Northwest Marine Technology Summit, Newport OR, October 20th-22nd, 2014 (**Winner of best Poster**)

Wishart, J.R., **Neumann, K.C.,** Edenborn, H.M., Hakala, J.A., Yang, J., Torres, M.E., Colwell, F.S. *Development of osmotic sampling systems for chemical and microbial characterization of Marcellus Shale flowback waters.* Poster. 4th Annual Hydrophiles Water Research Symposium, Corvallis OR, May 12th, 2014. (**Winner of second place poster**)

ABSTRACT

The influence of land use on river nutrient and sediment concentrations as well as benthic community composition on nearshore reefs around Moorea, French Polynesia, and the development of a low-cost, open-source autonomous water sampler

By

Kyle Christopher Neumann

Human development of watersheds has fundamentally altered nutrient (nitrogen and phosphorus) and sediment regimes in freshwater and marine ecosystems. Watersheds located on steep tropical islands can be particularly susceptible to increases in nutrient and sediment runoff following the replacement of native forest by agriculture, roadways, and buildings. Ultimately, much of this elevated runoff is deposited in the nearshore environment. On tropical islands the nearshore is often characterized by coral reefs. Generally, coral reefs tend to thrive in clear, low-nutrient waters. As such, nutrient enrichment and sediment runoff can have numerous deleterious impacts on the physiology and life cycle of corals and other reef organisms.

In Chapter 1, I test the impact of watershed development on nutrient and total suspended solid (TSS) concentrations on the island of Moorea, French Polynesia. To do this, I collected water samples during rainfall events in the rainy and dry

seasons in eleven watersheds on the island. Water samples were analyzed for dissolved inorganic nitrogen (DIN = nitrate + nitrite + ammonium) and phosphate concentrations and total suspended solids (TSS). I quantified land use in watersheds by analyzing satellite imagery for the percent of each watershed that is cleared of forest for agriculture or development, and used census data to determine the population of each watershed. PCA and regression analyses of these data indicate strong positive relationships between how much of a watershed is cleared and the nitrogen levels of the rivers, as well as a positive relationship between the amount of sediment in the river and both how much the watershed is cleared and the population of the watershed. Phosphate concentrations were not related directly to watershed development, but positively related to TSS. I then used DIN and TSS concentration thresholds established in similar tropical island ecosystems to assess watersheds on Moorea for potential concerns to human health and ecosystem function. I found that DIN and TSS concentrations in Moorea's rivers regularly exceed these thresholds.

In Chapter 2, I studied the impacts of land use on nearshore fringing reefs around Moorea. I used a combination of remote sensing, river water sampling, and reef photo transects to quantify land use, river nutrient and sediment concentrations, and reef community structure across a gradient of land use intensity. I found that the percentage of cleared land in a watershed has a negative relationship with coral cover on adjacent fringing reefs. Through ordination analysis I also revealed that land clearing, human population, and river nutrient and sediment concentrations are all correlated with the heterogeneity of community composition on fringing reefs. Reefs situated near more developed watersheds were exposed to higher nutrient and sediment runoff and were more homogenous than those with less anthro-

pogenic stress even hundreds of meters from river outflows.

In Chapter 3, I present a new research tool for water chemistry research. Water chemistry conditions in freshwater and marine environments can change rapidly over both space and time. This is especially true in environments that are exposed to anthropogenic impacts such as sedimentation, sewage, runoff and other types of pollution. Through the fieldwork and analyses for Chapters 2 and 3 the challenges associated with accurately collecting water samples across relevant spatial and temporal scales became abundantly clear. In response, I developed an inexpensive, open-source Programmable Autonomous Water Sampler (PAWS) that is compact, robust, highly adaptable and submersible to 40 meters. PAWS utilizes a time-integrated sampling approach by collecting a single sample in a syringe slowly over hours to days. Once analyzed, data from the sample collected represents an integrated average of water chemistry conditions over time. Due to its adaptability and low cost, PAWS has the potential to improve the spatial and temporal coverage of many freshwater and marine studies.

TABLE OF CONTENTS

I. Land use shapes riverine nutrient and sediment concentrations on Moorea, French Polynesia

Contributing Authors: *Terava Atger* — Local and traditional ecological knowledge, sample collection and laboratory assistance. *Tauira Punu* — Local and traditional ecological knowledge, sample collection and laboratory assistance. *Christian Green* — Satellite image analysis. *Will Underhill*—Satellite image analysis. *Jordan A. Hollarsmith* — Advising of statistical analyses, editing. *Deron E. Burkepile* — Advising.

A. Introduction

Human activity has altered approximately 75% of the Earth's surface in the last millennia (Winkler et al. 2021). Global land-use models indicate a 0.8 million km^2 loss in forest cover since 1960 and a corresponding increase of 0.9 to 1.0 million km^2 in agricultural land (Winkler et al. 2021). Hydrologic models estimate that ~50% of observed increases in river run-off globally between 1900 and 2000 were the result of changes in land use as deforestation reduced water retention capacity of landscapes. This makes land-use change as much or more impactful than climate driven changes in runoff patterns (Piao et al. 2007). In addition to the increases in water transport, human driven land use change has resulted in an increase in nutrient enrichment and sediment loading in rivers (Green et al. 2004; Kroon et al. 2012; Hoffmann et al. 2010).

Due to their steep slopes, highly erodible soils, and high precipitation, deforestation in mountainous tropical regions can have an outsized impact on riverine sediment loading and discharge (reviewed in: Labrière et al. 2015; Tanaka et al. 2021). One study of Kolombangara, a high tropical island in the Solomons, estimat-

ed that if no land management practices were put in place, a 10% increase in logging activity would result in an increase in sediment runoff of approximately 1500% island-wide equating to an annual transport of approximately 3,000 tons of sediment from land through rivers to the ocean (Wenger et al. 2020). If forests are replaced by agriculture or population centers in these regions, there will be a resulting increase in riverine nutrient loading. In a review of land-use impacts on the nitrogen cycle in tropical systems, Downing et al. (1999) estimated that conversion of native forest to agriculture utilizing high nitrogen fertilizer could result in a 25-fold increase in nitrogen export from the system. Further urbanization of the same system could result in a nearly 50-fold increase in nitrogen export as compared to native forest (Downing et al. 1999). Understanding the role of land use in nutrient and sediment runoff is essential to understanding alterations in aquatic ecosystems in altered regions as well as effective planning, management, and restoration of altered watersheds.

Land use change has resulted in as much as a 20-fold increase in nitrogen (N) and phosphorus (P) concentrations of many rivers worldwide as compared to pre-industrial levels (Downing et al. 1999). Nitrogen and phosphorus enter aquatic ecosystems as a result of atmospheric deposition as well as excess fertilizer application on agricultural plots, industrial and domestic activities such as detergent use, and untreated or incompletely treated human and animal waste (Correll, 1998; Downing et al. 1999; Schmutz and Sendzimir, 2018). N and P from these sources are dissolved in rain or ground water, or transported on sediments and particulate matter, and are deposited in rivers. As either N or P tend to be the limiting nutrient for plant or algal growth in freshwater systems, elevated concentrations of either or both can have a number of deleterious effects including: the proliferation of algae

and cyanobacteria resulting in increased levels of harmful algal toxins, reduction in dissolved oxygen, and alterations to flora and fauna communities (Allan 2004; Canning & Death 2021; Wurtsbaugh et al. 2019). In addition to altering the absolute levels of N and P, anthropogenic nutrient loading in freshwater systems can alter the stoichiometric ratios of dissolved N and P. An altered N:P ratio can shift trophic interactions and biogeochemical cycling in freshwater ecosystems (Wurtsbaugh et al. 2019).

In addition to anthropogenic nutrient enrichment, many rivers are experiencing increased sediment loading as a result of land clearing for new development and agriculture (Bartley et al. 2013). The removal of forest vegetation exposes soil to erosion from precipitation and wind while also reducing the soil holding capacity of the cleared area by reducing vegetation root depth and root mass (Downing et al. 1999). The erosion capacity of a deforested plot of land increases rapidly with increasing slope and regional precipitation. Elevated sediment concentrations in rivers increase turbidity and reduce light availability in addition to altering the geomorphology of riverbeds (Allan, 2004). Furthermore, sediments can carry chemical pollutants which are part of grain structure, or absorbed onto the surface, and are released into the water as sediments are mechanically or biologically eroded (Vidal-Dura, et al. 2018). The results of increased sedimentation are often freshwater ecosystems that are more prone to harmful algal and bacterial blooms, and have less vertebrate and invertebrate diversity (Allan, 2004).

Watersheds located on high volcanic islands are particularly vulnerable to the impacts of land clearing. In tropical zones, these high islands often have high annual rainfall and periodic large storms that can quickly displace fertilizer from agricultural fields. The steep slopes and highly erodible soils on these islands also

mean that rain events can result in large amounts of terrigenous sediments running into freshwater and coastal bodies (Albert et al. 2021, Surchat et al. 2021, Koshiba et al. 2013). In addition to the potential ecological impacts of runoff, people living on these islands are often dependent on rivers for clean water for drinking and bathing. Thus, freshwater bodies with increased nutrient and sediment pollution can reduce human health and well-being (Guernier et al. 2017, Viau & Boehm 2011, Strauch 2017) through exposure to runoff as well as algae and bacteria. Tropical islands are experiencing rapid growth in their populations, tourism, industry, logging, and large-scale agriculture resulting in the clearing of forest for farms and developments (Comeros-Rayna et al. 2021, Albert et al. 2021, Dadhich and Nadaoka, 2012). As a result, it is important to understand the impacts of active development on the nutrient and sediment concentrations in rivers on tropical islands.

Here, we focus on rivers of Moorea, French Polynesia, to examine how nutrient and sediment concentrations relates to human alterations of the landscape. Moorea is a high volcanic island with a rapidly changing landscape due to increased tourism, housing, and industrial development, and increasing agriculture (Loiseau et al. 2021, Duane 2006). Many people on Moorea have raised issues regarding the state of rivers on the island, citing observations of turbid water, algal and bacterial blooms that result in rashes and other health concerns, and reduced abundance of a freshwater shrimp species that is an important traditional food (*personal communications with community members*). Further, Moorea is home to near-shore coral reef ecosystems, and both resident observations and recent academic work suggests that terrestrially derived nutrients are likely having a negative impact on near-shore reefs (Adam et al. 2021, Loiseau et al. 2021), which could compromise the ecosystem services (e.g. fisheries and tourism) provided by these

reefs. However, to date no study assessing river nutrient and sediment loading as it relates to land use has been conducted on Moorea. Understanding the movement of sediment and nutrients from the land to the sea for Moorea is critical for management of the island's natural resources. These challenges are also relevant for many other high tropical island ecosystems (Comeros-Rayna et al. 2021, Albert et al. 2021, Dadhich and Nadaoka, 2012). In response to this community and scientific need, we tested the following hypotheses about the watersheds in Moorea:

Watersheds with higher proportions of cleared land will have higher sediment loading in rivers.

Watersheds with higher proportions of cleared land and higher populations will have high concentrations of nitrogen and phosphorus as compared to those with lower populations and less land clearing.

The watersheds on Moorea with the highest percentages of land use and higher populations will exceed nutrient and sediment thresholds established for human and environmental protection in similar systems.

To test these hypotheses, we collected water samples from eleven watersheds on Moorea across rainy and dry seasons in two years. Water samples were analyzed for nitrate (NO_3^-), nitrite (NO_2^-), and ammonium (NH_4^+), the three nitrogen species that comprise dissolved inorganic nitrogen (DIN), as well as orthophosphate (PO_4^{3-}) and total suspended solids (TSS). We used linear models to evaluate how nutrients and sediment varied over space and time around Moorea. Using 2018 Landsat imagery we calculated the percent area of each watershed that is ei-

ther forested or cleared for agriculture and human settlement. We integrated these data with watershed size and watershed-level population data from local census data and used principal components analysis (PCA) and linear modeling to evaluate how these factors influenced the nutrient and sediment dynamics of rivers across the island. Lastly, we compared nutrient and sediment loading in Moorea to similar systems including Hawaii, American Samoa, Guam, Fiji, and the Solomon Islands using concentration thresholds established in these regions to assess potential concerns regarding human health and alteration to ecosystem functions.

B. Materials and Methods

1. Study Location

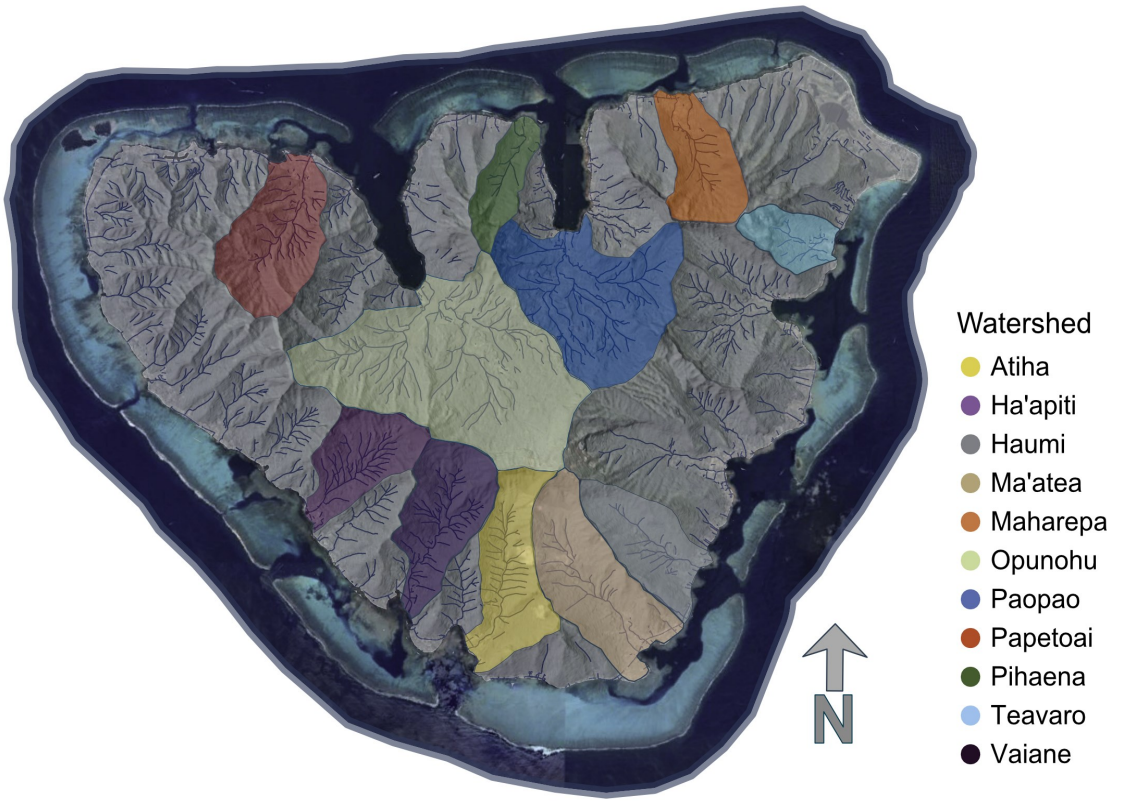

Figure 1. Moorea, French Polynesia mapped with hillshade, stream channels and focal watersheds.

Moorea is a volcanic island located in the Society Archipelago of French Polynesia (17° 29′ S, 149° 50′ W). As the island eroded and subsided, a barrier reef formed separating the open ocean from a 53 km^2 lagoon (Collin et al. 2018). The island has a relatively small area of 134 km^2, but features diverse topography. Since it was formed by a volcanic eruption approximately 1.6 million years ago (Meyer et al. 2015), Moorea has collapsed and eroded into 57 distinct watersheds separated by steep, sharp ridgelines with a highest elevation of 1207 m at Mount Tohiea (Meyer et al., 2015) (Figure 1). A majority of the soils (98.7%) on the island formed from weathering and erosion of volcanic parent material with the remainder being coralline in origin (Jamet, 2000). Of the eight soils of volcanic origin on Moorea, five originate from weathered basalt (Jamet, 2000).

Moorea has been inhabited by humans since around 200 CE when it was settled by the Polynesians (Kirch, 2000) who brought with them a variety of non-native plants and animals for cultivation. A 2015 study of vegetation on Moorea classified 32% of the island as urbanized and cultivated lands, 17% as novel habitat dominated by invasive species, 45% as hybrid habitats featuring a mix of introduced and native species, and 6% as native habitat which is primarily located on extremely steep slopes and at high elevation (Meyer et al., 2015). As of the 2017 census, Moorea is home to 17,357 permanent residents (“Institut de la statistique de la Polynésie Française").

The largest watersheds on Moorea are two adjacent valleys on the north shore, Opunohu (15.7 km^2) and Paopao (11.4 km^2) (Table 1), formed by a collapse of the volcano’s caldera (Meyer et al., 2015). Opunohu is home to a small population (97 people), but hosts a large portion of the island’s commercial agriculture which is principally comprised of pineapple plantations and cattle pasture. Using

Table 1. Watershed parameters including orientation of shore, watershed area, population size, Stahler stream order of the sampled river, and stream length from source to discharge location.

Watershed	*Shore*	*Area (km^2)*	*Population*	*Stream Order*	*Stream Length (km)*
Atiha	W	5	495	2	3.5
Ha'apiti	W	4.2	337	2	2.3
Haumi	E	3.7	421	2	2.5
Ma'atea	E	5.5	582	2	3.5
Maharepa	N	3.5	915	2	2.5
Opunohu	N	15.7	97	4	4.8
Paopao	N	11.4	1557	3	3.3
Papetoai	N	4.8	614	2	3.3
Pihaena	N	3.7	705	2	1.8
Teavaro	E	1.1	248	2	1.3
Vaiane	W	5.8	371	2	2.9

the Stahler method, the Opunohu River is the only 4th order stream on the island (Strahler, 1952). As an example of the steepness of watersheds on Moorea, more than 90% of the Opunohu valley is comprised of slopes greater than 10% (Binet & Gonnot, 2005). Neighboring Paopao is home to the largest population center (1557 people) and small mixed agricultural fields, and features a 3rd order stream. In contrast, the smallest watershed included in this study, Teavaro, is located on the eastern shore of the island and is only 1 km^2, but is home to 248 people. Teavaro and the rest of the rivers in this study are second order streams. The variety of watersheds in close proximity featuring a range of areas, land uses and populations makes Moorea a compelling location to investigate interactions between human activity and riverine nutrients and sediments.

In order to study rivers and land use on Moorea, we first engaged the local community to receive feedback regarding key questions that would be of interest

and value to the people of Moorea. The goals, objectives, and research locations for this study were shaped by meetings with community members organized by the Te Pu Atiti'a Polynesian Cultural Center located directly adjacent to the University of California Gump Research Station, where our research was based. These conversations precipitated a new community science organization on Moorea called Ati Vai ('Water Clan' in Tahitian). Members of Ati Vai contributed to the study design, provided local knowledge and site context, and aided with field data collection throughout this study. The combination of modern scientific tools and techniques with traditional and local knowledge of the island and its rivers was paramount to the success of this research.

2. Focal watershed selection

In the first year, eight watersheds were chosen to represent a range of watershed sizes, land uses and population densities, and are located on all three shores of the island. Specifically, the focal watersheds were: Atiha, Ha'apiti, Maharepa, Opunohu, Paopao, Pihaena, Teavaro, and Vaiane. Three additional watersheds - Haumi, Ma'atea, and Papetoai - were added in the second year of sampling to increase representation of medium-sized, moderately-impacted watersheds (Figure 1,Table 1). All of the rivers included in this study are perennial, with the exception of Pihaena which has low or no flow during the dry season.

3. Water sample collection

We collected water samples during two rainy and two dry seasons between January 2018 and September 2019 (rainy: January - March 2018 and February - March 2019, dry: August - September 2018 and 2019). During the study periods,

water samples were collected as close to the mouths of the rivers as possible (Figure 1), but above brackish mixing zones. Where natural or manmade impediments to access existed, we made every effort to find a suitable sampling location as close to the river mouth as possible. During the above periods, samples were collected at least once a week with attention paid to capturing samples across river stages from low-flow to storm-flow. We collected storm-flow samples during or shortly after rain events to ensure that we captured the nutrient and sediment regimes at high flows.

River samples were collected in approximately 60% water depth (e.g. at 40 cm above the bottom in a 1 m deep river) at the center of flow. Samples were collected in acid washed 1-liter HDPE Cubitainers® and transported on ice to the lab at Gump Station and kept refrigerated until processed. Samples were processed upon return to the lab within no more than 24 hours. Each sample was divided and filtered for nutrients or total suspended solids. Sub-samples were then filtered using a multi-channel peristaltic filtration system.

4. Nutrient analyses

Nutrient sub-samples were filtered through 47 mm 0.15 µm PES filter discs and then divided for separate analytical methods. NH_4^+ analyses were conducted immediately after filtration using the OPA method (Taylor et al. 2007) on a Turner Trilogy fluorometer fitted with an ammonium detection module (Minimum Detection Limit (MDL): 0.05 µM). The remaining samples were frozen at -20°C and transported to the Centre de Recherches Insulaires et Observatoire de l'Environnement (CRIOBE) – Opunohu, Moorea, French Polynesia – where they were analyzed for PO_4^{3-} (MDL: 3 nM), NO_3^- (MDL: 2 nM), and NO_2^- (MDL: 2 nM) on a Seal AA3 Auto-

analyzer (“AutoAnalyzer Multi-test Methods”). Total DIN per sample represents the sum of NO_2^-, NO_3^-, and NH_4^+. The molar N:P ratio was calculated for each sample by dividing DIN by phosphate.

5. Total suspended solids (TSS) analysis

TSS samples were filtered using pre-dried and pre-weighed 47 mm GF/F (0.70 µm) filter discs. Filters were weighed on a Mettler-Toledo XS104 balance with 0.1 mg readability. Samples were filtered to 200 mL, or until the filters were completely clogged preventing more water to pass through, whichever came first. After filtration, the GF/F filters were placed in a drying oven at 95°C for a minimum of 24 hours at which time they were re-weighed. TSS was calculated using the following equation:

$$TSS = \frac{(post-filtering\ and\ drying\ weight)-(pre-filtering\ weight)}{volume\ filtered}$$

.

6. Landsat image classification

The Operational Land Imager (OLI) is a sensor carried by the Landsat 8 satellite (LS8), collecting repeated imagery every 8 days with a multispectral ground resolution of 30 m (“Landsat 8 | U.S. Geological Survey”). We used a LS8 OLI Level 2 image that was collected on March 22nd, 2018, orthorectified and atmospherically corrected to classify land cover on Moorea during the study period (Figure 2). We selected this image because of its low cloud cover (<3%). Water was masked out of the imagery using a digital elevation model, leaving only Landsat pixels above sea level. Land cover classifications were then produced using the supervised classification tool in the image processing software ENVI (version 5.5.2)

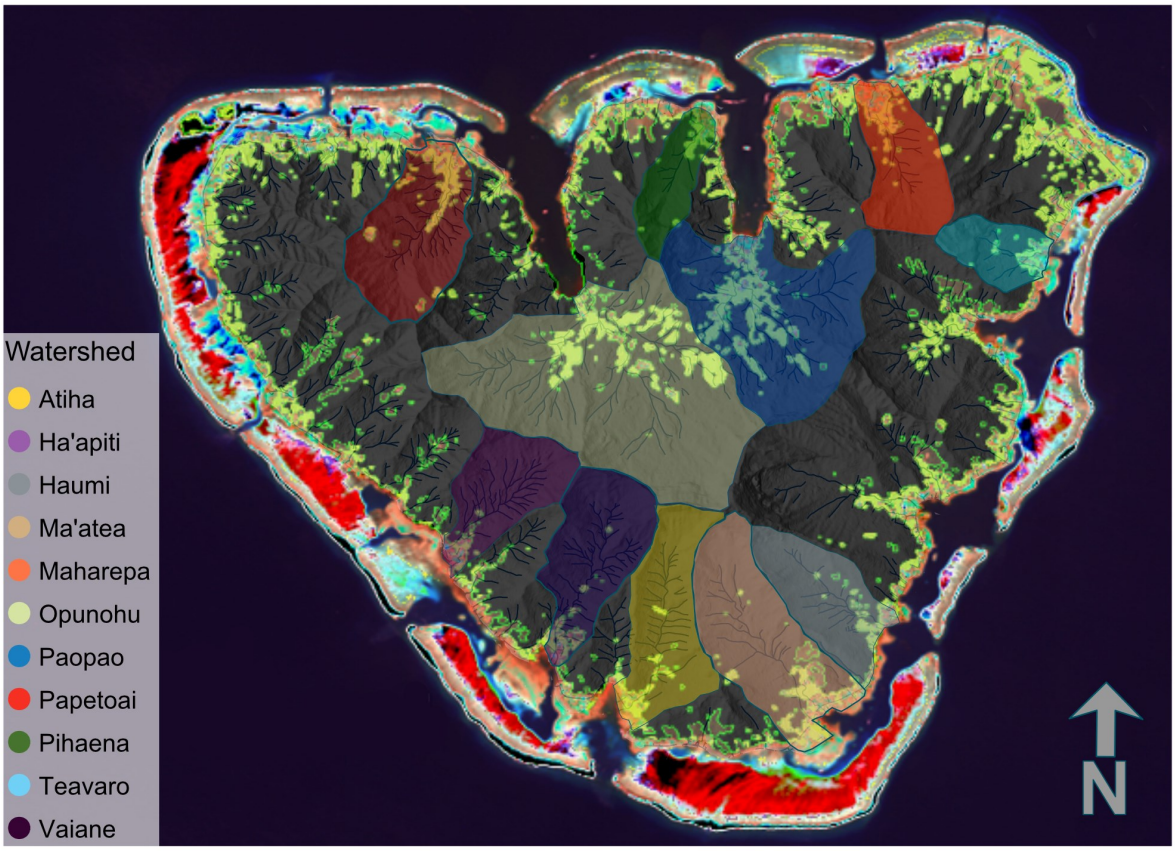

Figure 2 . Classification of a Landsat 8 OLI Level 2 image, collected on March 22nd, 2018. Cleared land including agriculture and development is represented in light green and forest in dark green. Red and magenta are masks for reef, while blue is a mask for water.

("Image Processing & Analysis Software"). Training regions were created for cloud cover, forested areas, and cleared land. The cleared land classification incorporates all land not covered by forest or buildings. This classification captures agricultural land, as well as land cleared for the construction of new homes, businesses, hotels, and industrial buildings. Regions were produced based on photo interpretation and expert knowledge to delineate forested areas from cleared land. Using these training regions, we conducted a supervised classification of the image using the Maximum Likelihood method ("Classification"). In order to reduce noise, we utilized a Majority-Minority Post Classification tool using nearest neighbor analysis to smooth the data and create more uniform classes. We then applied an accuracy

assessment using a confusion matrix with ground truthed regions of interest within the image.

Watersheds were delineated using the Hydrology tool in the Spatial analyst toolbox within ArcGIS (version 10.6.1) (“About ArcGIS | Mapping & Analytics Software and Services”). Using a digital elevation model (DEM) from the Shuttle Radar Topography Mission Version 3 (30 m resolution) (Siemonsma, 2015), we identified the main watersheds on the island using the Flow Accumulation and Flow Direction Tools in ArcGIS. Points along the rivers were identified towards the mouth of rivers of interest using the Snap Pour Point tool. Watersheds of interest for the project were then delineated using the Watershed tool. Watershed boundaries were then used as regions of interest in ENVI, thereby subsetting the land classifications by watershed.

7. Precipitation and Census Data

Hourly precipitation data for Moorea between January 1, 2018 and September 31, 2019 were obtained through a license agreement with Meteo France which operates 7 meteorological stations on the island with tipping bucket rain gauges. Census data for 2017 was obtained via a license agreement between the Gump Research Station and the Institut de Statistiques de la Polynésie Française. The census data were originally collected in 102 districts on the island, often with multiple districts located inside of a watershed. In order to determine the population per watershed, we mapped the districts onto a digital elevation model (DEM) in QGIS and aggregated the populations of districts located within a single watershed.

8. TSS and DIN Concentration Thresholds

A low and a high threshold for both DIN and TSS concentrations were selected from a review of literature from similar systems including Hawaii, Guam, the Solomon Islands and American Samoa. The low threshold for TSS 5 mg/L represents concerns for human consumption and bathing (Wenger et al. 2018; Albert et al. 2021). The high TSS threshold of 50 mg/L is based on water quality standards established in Hawaii ("Amendment and Compilation of Chapter 11-54 Hawaii Administrative Rules," 2021) and is based on the levels at which exposure to suspended sediment become lethal to a majority of fish species (Wenger et al. 2018). According to the Hawaiian standards, TSS in streams should not exceed 50 mg/L for more than 10% of the time in the rainy season. The lower DIN concentration threshold of 0.1 mg/L was selected based on studies of runoff impacts to nearshore reefs in American Samoa (Houk et al. 2020) and Guam (Houk et al. 2022). An exceedance of this threshold in streams for more than 20% of the time was associated with diminished diversity and size of coral communities in both regions. The higher threshold of 0.18 mg/L DIN was based on Hawaiian water quality standards which state that streams should not exceed this threshold more than 10% of the time in the rainy season ("Amendment and Compilation of Chapter 11-54 Hawaii Administrative Rules," 2021). We calculated the percentage of time that samples collected from each watershed on Moorea exceeded these thresholds using the following equation:

$$\%\ exceedance = \left(\frac{\#\ of\ samples\ from\ watershed\ that\ exceed\ threshold}{total\ number\ of\ samples\ from\ watershed}\right) * 100$$

9. Statistical Analyses

All analyses were conducted in R (R core team 2022). Hourly rainfall data from 2018 and 2019 were aggregated by season and then analyzed using a linear model to: 1) assess differences across shores of the island (North, West, and East) and 2) assess between the rainy (December to April) and dry seasons (May to November).

We used linear models to analyze differences by watershed and season, and the interaction of watershed and season for all nutrient and TSS data. When a significant watershed by season interaction existed, or to investigate differences between sites, we used post-hoc Tukey tests with adjusted alpha (p-value) by the number of tests. Data were 1+log transformed prior to analysis to improve model fit, based on inspection of q-q plots and residuals using the 'qqplot', 'qqnorm', and 'resid' functions in R. Only watersheds that had samples from the wet and dry seasons were included in the linear models, so Pihaena was excluded because it only flowed in the wet season.

To assess the significance of watershed variables (area, population, and percent cleared land) in explaining river chemistry in the wet and dry season, we used principal components analyses (PCA). PCA is a form of ordination analysis based on Euclidean distance that is well suited to complex datasets with covarying variables. Differences across watersheds and seasons were assessed based on a correlation matrix of dissolved inorganic nitrogen, phosphate, N:P, and total suspended solids levels at a given sampling event. All data were standardized (mean=0, SD=1) prior to analysis. River chemistry data were 1+log transformed before analysis. We used the 'envfit' function in the R package 'Vegan' to test whether watershed characteristics, namely area, population, percent cleared land in 2018,

watershed, and season could explain the variation in river chemistry (Oksanen et al. 2022). Envfit finds vectors or factor averages of environmental variables, analogous to fitting a linear model, in ordination space.

To further explore relationships between watershed variables and river conditions, we performed a series of linear models testing whether cleared land percentage and population predict nutrient and sediment concentrations. Models were run using the mean concentrations of nutrients and sediment across all seasons and years. Additional models were run using maximum observed nutrient and sediment values to elucidate relationships between land use and high flow runoff events. We also analyzed the relationship between population from the census data and the area of cleared land from the Landsat analyses using linear models.

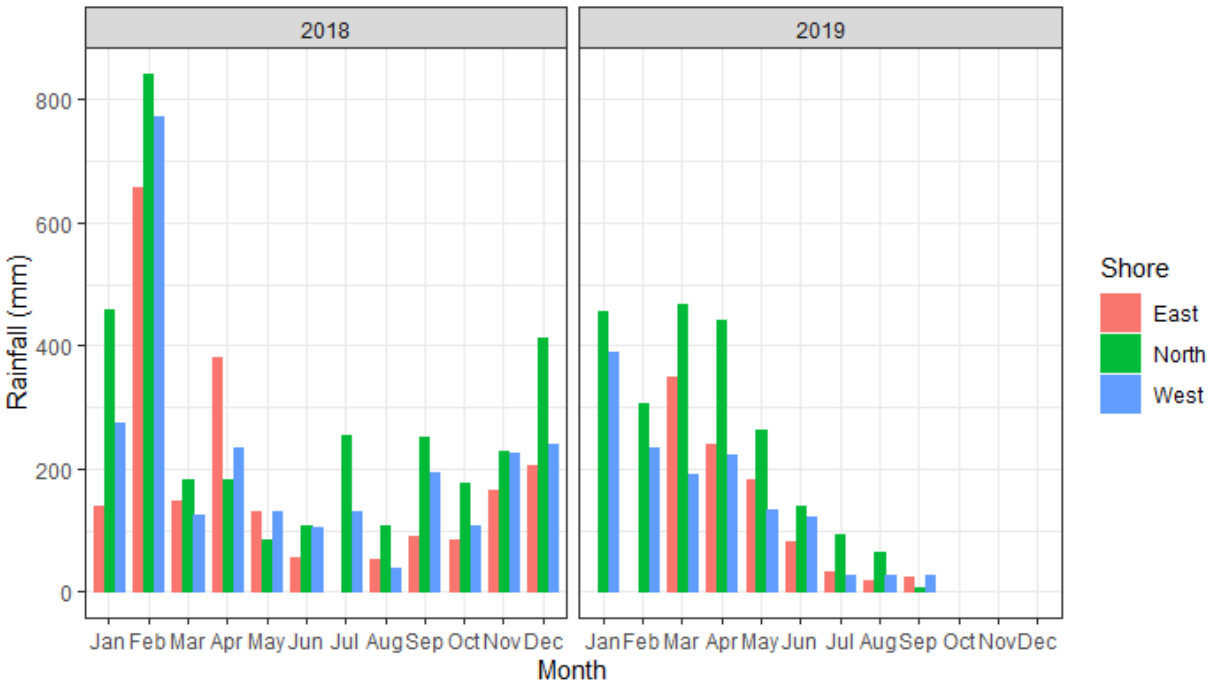

Figure 3. Monthly rainfall by shore orientation during sampling periods. Rainy season sampling was in January - March 2018 and February - March 2019. Dry season sampling was in August September 2018 and 2019. No rainfall data were obtained for October, November and December in 2019.

C. Results

1. Patterns in Rainfall

Within our sampling dates, February of 2018 had the highest monthly average rainfall with 841 mm of precipitation on the North shore, 772 mm on the West shore, and 657 mm on the East shore (Figure 3). August of 2018 had the least amount of precipitation during our sampling that year with 106 mm of precipitation on the North shore, 53 mm on the East shore, and 39 mm on the West. The rainy season in 2019 had lower monthly average precipitation than the previous year with a peak of 466 mm in March on the North shore, 348 mm on the East and 192 mm on the West. In the dry season in 2019 September had only 26 mm of precipitation on the West shore, 23 mm on the East shore, and 7 mm on the North shore.

2. Watershed and Seasonal Differences in Water Chemistry

Water chemistry varied considerably by nutrient, season, and watershed across the sampling period (Table 2). DIN concentrations ranged from a minimum of 0.05 μM measured in samples collected from Vaiane and Papetoai in the dry season, to 37.72 μM measured in a sample collected in Paopao during the rainy season. DIN differed significantly across watersheds ($p < 0.001$), seasons ($p=0.04$) and had a significant interaction with watershed and season ($p = 0.03$) (Figure 4). We found no significant differences between seasons within each watershed in the post-hoc Tukey test, though the fact that the interaction was significant indicates that rainy season DIN concentrations were higher than dry season in some watersheds while the opposite pattern was observed in other watersheds. The watershed with the highest mean DIN concentrations was Paopao (15.63 μM), and the lowest mean concentrations were found in Vaiane (3.87 μM). The nitrogen species com-

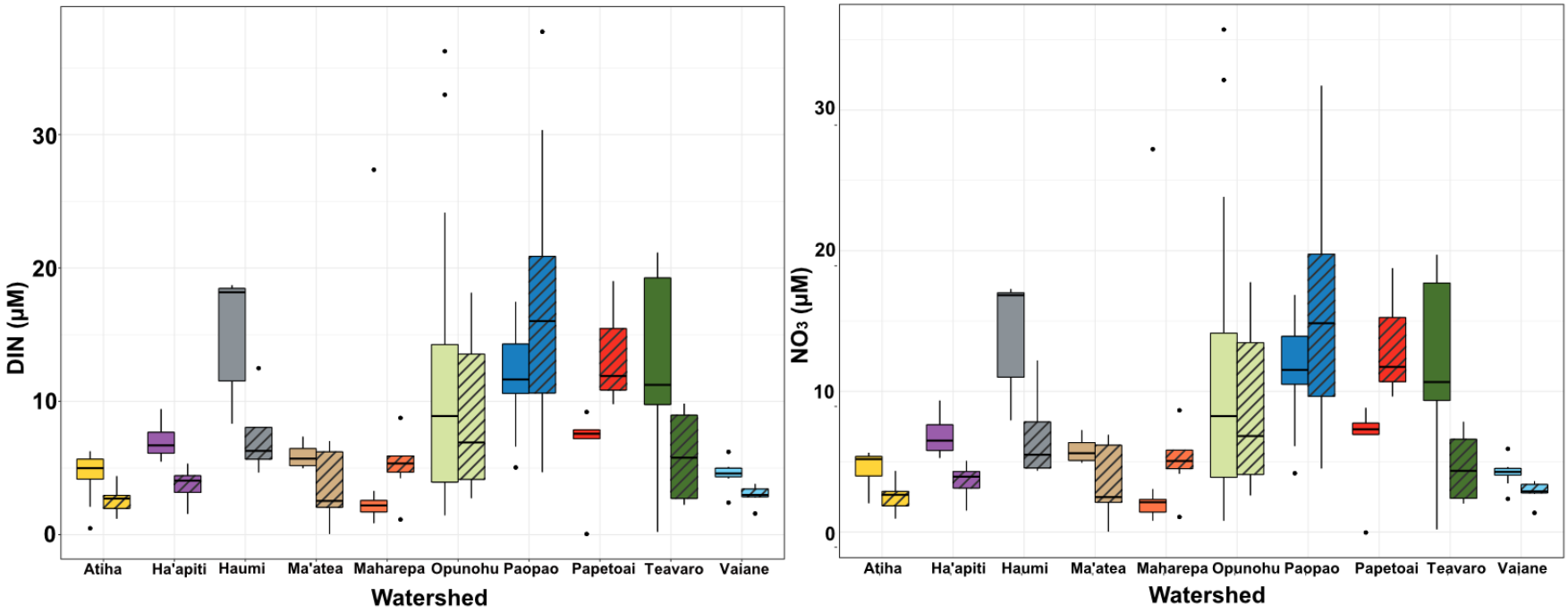

Figure 4a. Nitrogen concentrations as dissolved inorganic nitrogen (DIN) and nitrate across sites and seasons (dry season indicated by an open box and rainy season as a striped box). Boxes indicate the first and third quartiles; the horizontal line represents the median; and the vertical lines extend to the upper and lower 1.5 times the interquartile range.

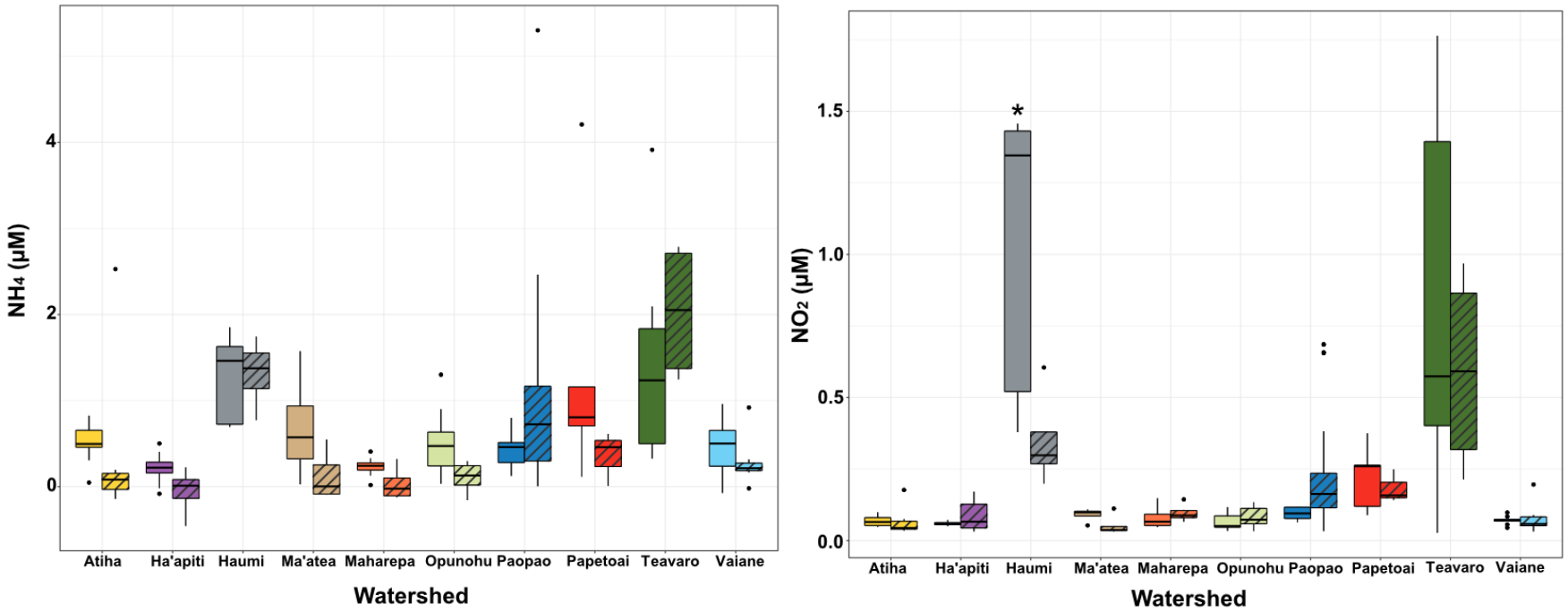

Figure 4b. Nitrogen concentrations as ammonium and nitrite across sites and seasons (dry season indicated by an open box and rainy season as a striped box). Boxes indicate the first and third quartiles; the horizontal line represents the median; and the vertical lines extend to the upper and lower 1.5 times the interquartile range. Stars indicate significance between seasons within a site ($p<0.05$)

prising the majority of DIN was nitrate, followed by ammonium and finally nitrite. Nitrate concentrations differed significantly by watershed ($p < 0.001$) and season ($p = 0.04$), and there was a significant interaction between watershed and season ($p = 0.02$); like DIN, the post-hoc Tukey test found no significant differences in nitrate concentrations between seasons among watersheds (Figure 4). Ammonium concentrations differed significantly by watershed ($p < 0.001$), while the interaction with season was not significant. The watersheds Teavaro followed by Haumi had higher ammonium levels than the other watersheds. Nitrite concentrations differed significantly by watershed ($p < 0.001$) but not by season although there was a significant interaction of watershed and season ($p < 0.001$). The rainy season nitrite concentrations were significantly lower than the dry season concentrations in Haumi. Like ammonium, Teavaro and Haumi had higher nitrite values relative to the other watersheds (Figure 4).

Phosphate concentrations ranged from a minimum of 0.19 μM from a sample collected in Teavaro in the dry season to a maximum of 7.58 μM in a sample collected from Paopao in the rainy season. Phosphate differed significantly among watersheds ($p < 0.001$) and season ($p = 0.01$) and had a significant interaction of watershed and season ($p = 0.007$) (Figure 5). Rainy season concentrations of phosphate were significantly higher than the dry season in the Paopao watershed, based on the post-hoc Tukey analysis. The highest mean phosphate concentrations were observed in Pihaena (3.04 μM) while the lowest were observed in Vaiane (1.01 μM). The N:P ratio ranged between a minimum of 0.03 in Papetoai, and a maximum of 54 in Paopao. A N:P ratio less than one indicates higher phosphate than DIN, a ratio larger than one indicates higher DIN. The mean N:P ratio was highest in Paopao (15) and lowest in Pihaena (1.9). N:P differed significantly

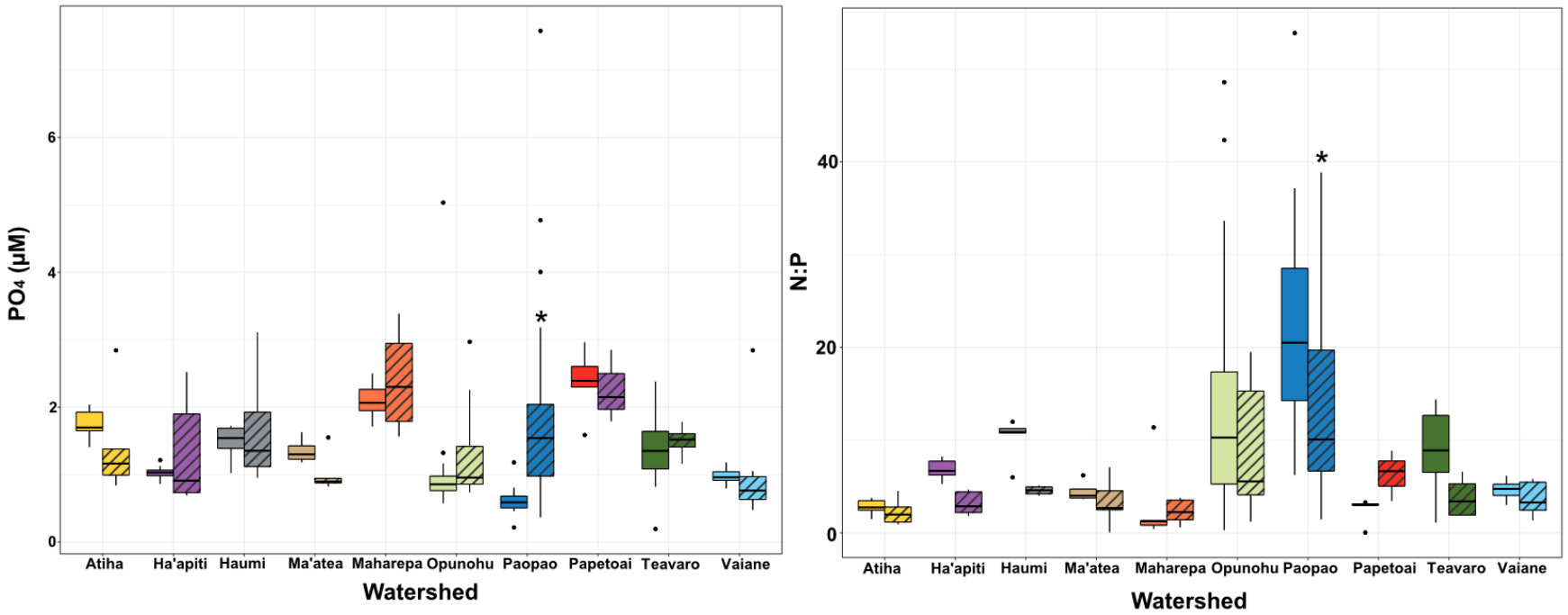

Figure 5. Phosphate concentrations and molar DIN:PO_4^{3-} ratio across seasons and sites. Dry season is indicated by an open box and rainy season as a striped box. Boxes indicate the first and third quartiles; the horizontal line represents the median; and the vertical lines extend to the upper and lower 1.5 times the interquartile range. Stars indicate significance between seasons within a site ($p<0.05$).

across watersheds ($p < 0.001$) and seasons ($p < 0.001$) and had a significant interaction with watershed and season ($p = 0.03$), with Paopao having significantly higher N:P in dry season than the rainy season (Figure 5).

Total suspended solids concentrations ranged from the below detection in Atiha, Ha'apiti, and Maharepa in the dry season to a maximum of 902 mg/L found in a sample collected in Paopao during the rainy season. Differences in TSS among watersheds and seasons were significant ($p = 0.03$ and $p<0.001$, respectively) and the interaction of watershed and season was not significant ($p = 0.09$)

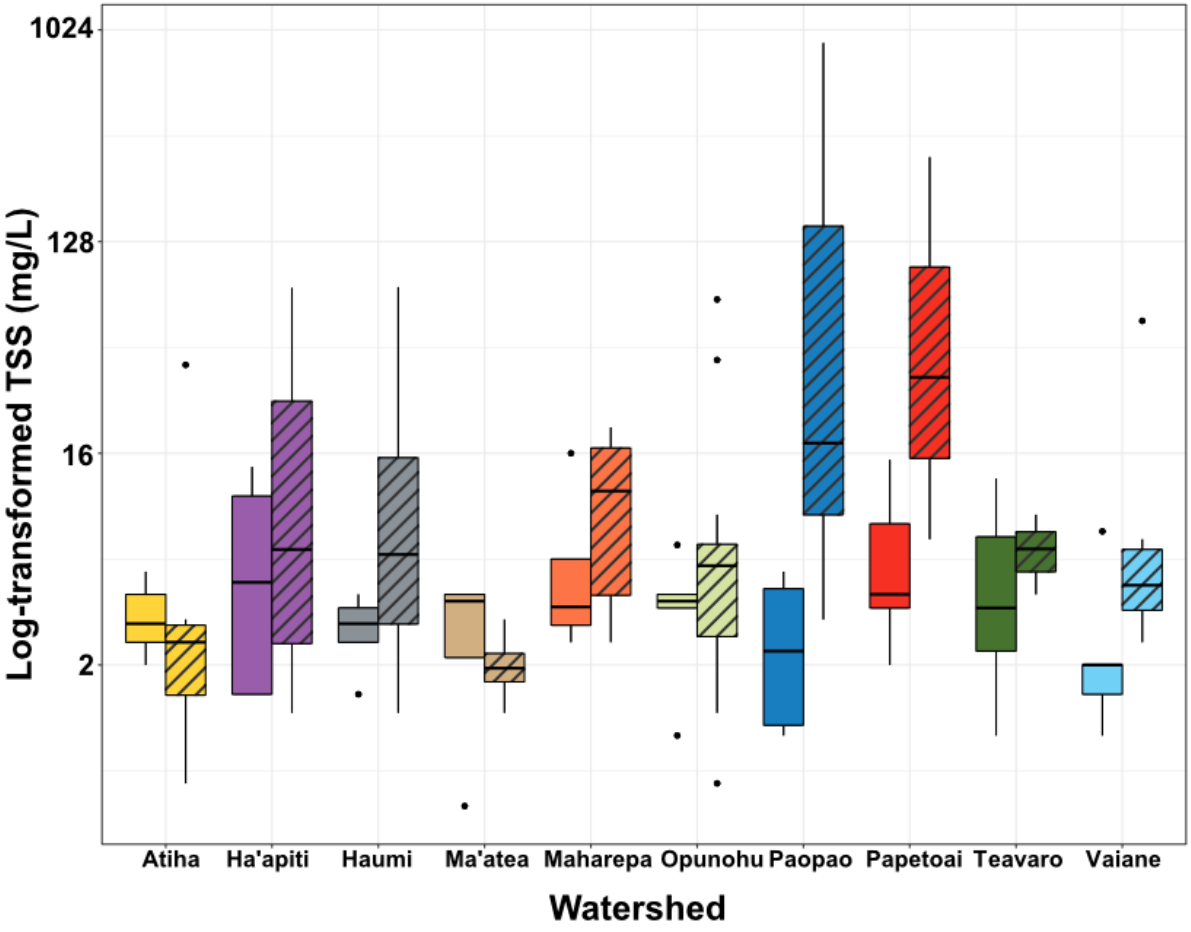

Figure 6. Total suspended solids concentrations (mg/L) across seasons and sites. Dry season is indicated by an open box and rainy season as a striped box. Boxes indicate the first and third quartiles; the horizontal line represents the median; and the vertical lines extend to the upper and lower 1.5 times the interquartile range. Note: the y-axis is on a $\log^{10}$ scale.

Table 2. Summary table of watershed nutrient and sediment concentrations from samples collected at each watershed across two rainy and two dry seasons. Mean, range and standard deviation of dissolved inorganic nitrogen (DIN = NO_3^- + NO_2^- + NH_4^+) phosphate (PO_4^{3-}) concentrations are reported in micromolar (µM). The DIN to PO_4^{3-} (N:P) ratio is unitless, and TSS values are reported in mg/L.

	Dissolved Inorganic Nitrogen (DIN)			Phosphate (PO_4^{3-})			N:P Ratio			Total Suspended Solids (TSS)		
Watershed	*Mean (µM)*	*Range (µM)*	*SD*	*Mean (µM)*	*Range (µM)*	*SD*	*Mean*	*Range*	*SD*	*Mean (mg/L)*	*Range (mg/L)*	*SD*
Atiha	3.67	0.48 - 6.25	1.79	1.58	0.84 – 2.84	0.49	2.5	0.9 – 4.5	1.0	5.39	0.00 – 38.13	10.40
Ha'apiti	5.68	1.56 - 9.42	2.08	1.16	0.69 – 2.52	0.52	5.4	1.8 – 8.2	2.1	14.07	0.00 – 81.25	24.12
Haumi	11.66	4.67 - 18.71	5.67	1.57	0.95 – 3.11	0.64	7.7	4.0 – 12.0	3.4	12.26	1.25 – 81.88	26.20
Ma'atea	4.62	0.06 - 7.07	2.51	1.17	0.82- 1.63	0.30	2.5	0.1 – 7.1	1.3	2.53	0.50 – 4.00	1.31
Maharepa	5.02	0.86 - 27.37	6.35	2.22	1.57 – 3.39	0.54	2.3	0.1 – 11.4	2.7	7.63	0.00 – 20.63	7.57
Opunohu	10.71	1.46 - 36.25	8.97	1.22	0.58 – 5.03	0.92	12.0	0.3 – 48.6	12.1	9.31	0.625 – 72.50	17.02
Paopao	15.63	4.69 - 37.72	7.07	1.53	0.22 – 7.58	1.24	15.5	1.5 – 53.9	10.9	128.45	1.00 – 901.67	287.02
Papetoai	9.07	0.05 - 19.01	5.29	2.33	1.59 – 2.96	0.48	3.9	0.03 – 8.8	2.7	45.86	2.00 – 126.25	100.69
Pihaena	5.54	0.15 - 24.92	6.08	3.04	1.27 – 7.24	1.66	1.9	0.04 – 5.1	1.6	29.58	2.50 – 126.25	41.00
Teavaro	10.39	0.22 - 21.15	7.11	1.40	0.19 – 2.38	0.56	7.1	1.1 – 14.4	4.6	5.55	1.00 – 12.50	3.63
Vaiane	3.87	0.05 - 37.72	1.18	1.01	0.48 – 2.84	0.53	4.3	1.4 – 6.1	1.4	8.24	1.00 – 58.75	16.04

(Figure 6). The lowest mean TSS concentration was recorded in Ma'atea at 2.5 mg/L while the highest was recorded in Paopao at 128.5 mg/L. The next highest mean TSS concentration was recorded in Opunohu at 46 mg/L, 83 mg/L lower than Paopao.

3. Land-use and population across Moorea

Our analysis of land use focused on the percent cleared land in a watershed estimated using the classification of a Landsat image from 2018 (Figure 2). Accuracy assessments indicate that our classifications are accurate for 96% of the image. The watershed with the highest proportion of cleared land in 2018 was Paopao (14%), followed by Opunohu (9%) while the lowest was Atiha (3%) (Table 3). The human population on Moorea was 17,463 residents in 2017, with the largest popu-

Table 3. Land cover/land use classification percentages by watershed from Landsat 8 imagery of Moorea in 2018 (Figure 2). Forested % represents land covered by mostly by trees. Cleared % includes land cleared for agriculture and development. Other % includes buildings, roads and any other pixels not classified in the other categories. Cloud % is the percent cover of clouds in the image.

Watershed	*Forest %*	*Cleared %*	*Buildings %*	*Cloud %*
Atiha	96	3	1	0
Ha'apiti	95	3	2	0
Haumi	91	5	2	2
Ma'atea	93	4	3	0
Maharepa	89	7	4	0
Opunohu	90	8	2	0
Paopao	83	14	3	0
Papetoai	91	8	1	0
Pihaena	88	8	5	0
Teavaro	93	5	3	0
Vaiane	95	3	2	2

lation in the Paopao watershed (1557 residents) and the smallest in Opunohu (97 residents) (Table 1). Percent cleared land in a watershed in 2018 was positively correlated with the population in that watershed in 2017 (Pearson's correlation; r^2 = 0.72, p = 0.01), however there were important exceptions to this relationship (e.g. Opunohu valley had the second highest percentage of land cleared (8.4%), but it

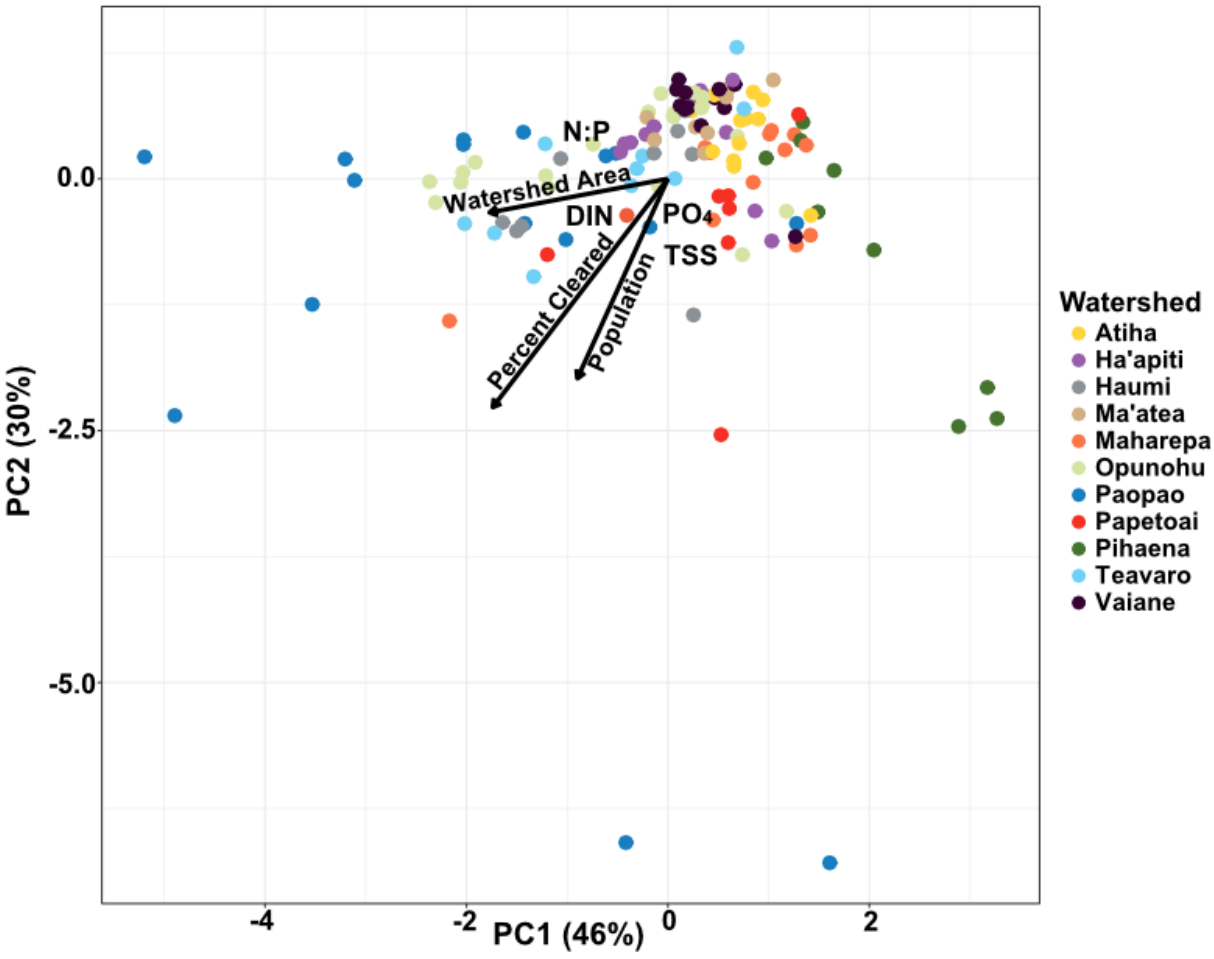

Figure 7. Principal components analysis (PCA) results of stream chemistry (DIN, PO_4, TSS, and N:P) across watersheds. Stream chemistry centroids are labeled in grey with the nutrient name. On the first PC axis, PO_4 loaded strongly positively, and DIN and N:P strongly negatively, with TSS close to zero. On the second PC axis, TSS and PO_4 loaded strongly negatively, DIN moderately negatively, and N:P close to zero. Each point represents one sampling event, and the color of the points indicate the site from which the sample originated. Arrows represent significant ($p<0.05$) correlations between stream chemistry and measures of watershed development; the length of arrow represents the relative strength of the correlation.

has the lowest population (97) as land use in this watershed consists primarily of agriculture).

4. PCA of watershed development and river chemistry

Sample points across the watersheds and seasons were distributed across the ordination space in the PCA (Figure 7). The first PC axis explained 46% of the variability and was strongly negatively correlated with N:P and DIN (PC1 loadings of -0.67 and -0.59, respectively) and had a modest positive correlation with PO_4^{3-} (PC1 loading of 0.44). The second PC axis explained 30% of the variability and was strongly negatively correlated with TSS and modestly negatively correlated with PO_4^{3-} (PC2 loadings of -0.79 and -0.51, respectively) (Table 4). All watershed variables (watershed, season, watershed area, population, and percent cleared land) were significantly related to the ordination axes ($p < 0.01$): watershed most strongly explained the spread of the data in the ordination space (r^2=0.38), followed by percent cleared land in 2018 (r^2=0.33), population (r^2=0.19), watershed area

Table 4. PCA axis loadings of phosphate, dissolved inorganic nitrogen, N:P, and total suspended solids concentrations.

Parameter	*PC1*	*PC2*	*PC3*	*PC4*
PO_4^{3-} µM	0.442	-0.512	-0.686	0.270
DIN µM	-0.597	-0.329	-0.384	-0.623
N:P	-0.668	-0.092	-0.073	0.734
TSS mg/L	0.041	-0.788	0.614	-0.001

(r^2=0.13), and finally season (r^2=0.05). Percent cleared land and population explained more of the variation along the second PC axis (PC2 loadings of -0.92 and -0.81, respectively), the axis that represented the spread of TSS and, less strongly, PO_4^{3-}. Percent cleared land and watershed area explained variation along the first

PC axis (PC1 loading of -0.59 and -0.97, respectively), the axis that represented the spread of N:P and DIN. Percent cleared land and population were closely associated in the PC ordination space and positively associated with TSS and somewhat positively associated with phosphate. Watershed area was strongly positively associated with DIN and N:P, and percent cleared land was also moderately positively associated with DIN.

5. Linear models of mean and maximum nutrient and sediment concentrations

Individually, the percentage of cleared land within a watershed and population living within a watershed were significant predictors of mean TSS ($p=0.002$, $r^2 = 0.70$ and $p=0.002$, $r^2 = 0.69$, respectively) and maximum TSS ($p=0.002$, $r^2 = 0.69$ and $p=0.003$, $r^2 = 0.65$, respectively). A mixed effects model including both the cleared land percentage and population was an even stronger predictor of mean and maximum TSS ($p=0.001$, $r^2 = 0.82$ and $p=0.002$, $r^2 = 0.78$, respectively). Population alone was not a significant predictor of mean or maximum DIN concentrations ($p = 0.30$, $r^2 = 0.12$ and $p=0.20$, $r^2 = 0.17$). However, the percentage of cleared land in a watershed was a significant predictor of mean DIN ($p=0.01$, $r^2=0.54$) and maximum DIN concentrations ($p<0.001$, $r^2 = 0.79$). A mixed effects model including both the cleared land percentage and population was the strongest predictor of mean and maximum DIN ($p=0.02$, $r^2 = 0.61$ and $p<0.001$, $r^2 = 0.89$, respectively). The percentage of cleared land in a watershed was also a significant predictor of maximum phosphate concentrations ($p=0.002$, $r^2 = 0.68$), but not mean concentrations ($p=0.28$, $r^2 = 0.13$). There was not a significant relationship between mean and maximum phosphate and population ($p=0.31$, $r^2 = 0.12$ and $p=0.06$, $r^2 = 0.34$, respectively). There were also no significant relationships between watershed area

and mean or maximum TSS (mean: $r^2 = 0.152$, $p = 0.24$, max: $r^2 = 0.19$, $p = 0.18$), DIN (mean: $r^2 = 0.19$, $p = 0.19$, max: $r^2 = 0.31$, $p = 0.08$), and PO_4^{3-} (mean: $r^2 = 0.08$, $p = 0.39$, max: $r^2 = 0.34$, $p = 0.06$).

6. DIN and TSS Thresholds

Samples from all watersheds, except for Ma'atea, exceeded the lower TSS threshold of 5 mg/L. On average, watersheds on Moorea exceeded this threshold 41% of the time (Table 5). The maximum exceedance percentage was found in Pihaena at 79% of the time. Seven of the eleven watersheds included in this study

Table 5. Exceedance percentages by watershed of low and high TSS and DIN thresholds. **Bold values represent exceedance frequencies of concern.** The low threshold of 5 mg/L TSS represents concerns for human consumption and bathing (Wenger et al. 2018; Albert et al. 2021). The high TSS threshold of 50 mg/L is based on the levels at which exposure to suspended sediment become lethal to a majority of fish species (Wenger et al. 2018). TSS in streams should not exceed 50 mg/L for more than 10% of the time in the rainy season ("Amendment and Compilation of Chapter 11-54 Hawaii Administrative Rules," 2021). The lower DIN concentration threshold of 0.1 mg/L was selected based on studies of runoff impacts to nearshore reefs (Houk et al. 2020; Houk et al. 2022). An exceedance of this threshold in streams for more than 20% of the time was associated with diminished diversity and size of coral communities. The high threshold of 0.18 mg/L DIN was based on Hawaiian water quality standards. Samples should not exceed this threshold more than 10% of the time in the rainy season ("Amendment and Compilation of Chapter 11-54 Hawaii Administrative Rules," 2021).

Watershed	*> 5 mg/L TSS*	*> 50 mg/L TSS*	*> 0.1 mg/L DIN*	*> 0.18 mg/L DIN*
Atiha	**17**	0	**88**	**63**
Ha'apiti	**50**	8	**94**	**88**
Haumi	**22**	**11**	**100**	**100**
Ma'atea	0	0	**89**	**67**
Maharepa	**42**	0	**75**	**50**
Opunohu	**45**	5	**96**	**93**
Paopao	**56**	**19**	**100**	**100**
Papetoai	**63**	**13**	**88**	**88**
Pihaena	**78**	**22**	**61**	**55**
Teavaro	**50**	0	**91**	**82**
Vaiane	**33**	8	**94**	**81**
Overall	**41**	8	**89**	**79**

exceeded the upper TSS threshold of 50 mg/L. Across Moorea, this threshold was exceeded on average 8% of the time. Four watersheds exceeded Hawaiian water quality standards with values of 50 mg/L more than 10% of the time (Haumi: 11%, Paopao: 19%, Papetoai: 12%, and Pihaena: 22%). All watersheds exceeded both the lower and the upper DIN thresholds (Table 5). On average, stream samples across Moorea exceeded 0.1 mg/L DIN 89% of the time and 0.18 mg/L 79% of the time. Haumi and Paopao exceeded both standards 100% of the time.

D. Discussion

Through a combination of island-wide water sampling and remote sensing analyses, we identified strong relationships between land use at the watershed scale and the nutrient and sediment concentrations in rivers on Moorea. Dissolved inorganic nitrogen (DIN), phosphate, total suspended solids (TSS), and the nitrogen to phosphorus (N:P) ratio differed across sampled rivers and between the rainy and dry seasons. We show through PCA mixed effects regression analysis that dissolved inorganic nitrogen concentrations and total suspended solids were strongly related to the percentage of land in a watershed that was cleared of forest and the population levels in that watershed. DIN and TSS concentrations regularly exceed thresholds established in similar systems to identify watersheds of concern where there may be a danger to human health and the health of aquatic biota. Phosphate concentrations, however, were not related to the metrics of land use change we considered, but were related to TSS concentrations, and are likely the result of weathering of the island's phosphate rich geology. N:P was driven primarily by DIN concentrations as nitrogen concentrations were higher on average and had greater variance than phosphate across the sampled watersheds.

1. Dissolved Inorganic Nitrogen

In the PCA and linear models, we observed a strong positive linear relationship between land-clearing and high DIN concentrations. The model fit improved with the addition of watershed population, but not with watershed parameters such as catchment size. Similar relationships between DIN and land-clearing combined with human population were found in studies of rivers in American Samoa (Houk et al. 2020) and Guam (Houk et al. 2022). These results indicate that these two watershed parameters – cleared land and population – may be sufficient to make approximate predictions of river DIN concentrations in steep tropical islands. This could be a valuable tool to remotely approximate DIN concentrations in unstudied steep-island watersheds, using only satellite-derived data on cleared land and census data on human populations. It is important to note that a more data complex runoff model would be required to calculate flux of DIN from watersheds (Aguilera and Melack, 2018). However, estimates of DIN concentrations can be valuable in assessing potential human or environmental health concerns (Houk et al. 2020; Houk et al. 2022) and regulatory thresholds are commonly based on concentrations rather than fluxes (“Amendment and Compilation of Chapter 11-54 Hawaii Administrative Rules,”).

In contrast to the Houk et al. (2020; 2022) studies, our study observed substantially higher DIN concentrations in rivers on Moorea. The highest observed DIN sample in our study, 2.09 mg/L (37.72 μM), was an order of magnitude higher than the maximum measured in the Guam study (0.20 mg/L, Houk et al. 2020), and much higher than the maximum in the American Samoa study (0.75 mg/L, Houk et al. 2022). Likewise, another study in American Samoa recorded a mean of 8.5 μM

DIN in a heavily disturbed watershed (Comeros-Rayna et al. 2021) which is close to the overall mean observed in our study, including data from all watersheds from minimally to highly disturbed. As a result of this difference, DIN concentrations in all watersheds on Moorea exceeded the DIN threshold of 0.1 mg/L established by these studies. DIN values from all watersheds on Moorea also exceeded the 0.18 mg/L threshold from the Hawaii water quality standards, despite values being comparable to watersheds in Hawaii with similar land use (Hoover, 2002; Hoover & Mackenzie, 2009).

Our PCA analysis and linear mixed models indicate that DIN runoff on Moorea is likely primarily a result of agricultural activity as the percent cleared land classification in our satellite image analysis includes agricultural land. One of the primary commercial crops grown on Moorea is pineapples (Surchat et al., 2021). Pineapple farming requires year-round applications of nitrogen fertilizer and has contributed to nitrogen-loading in rivers across the tropics (Hawaii: Ryder and Fares 2008; Philippines: Guinto and Inciong 2012; Australia: Milbank and Nothard 2023). The nitrogen in these fertilizers is usually in the form of urea (CH_4N_2O) which transforms to ammonium and then nitrate via nitrification in the soil due to biological activity (Norton & Ouyang 2019). Nitrate was the most abundant form of nitrogen we observed. Nitrate is highly water soluble and thus is easily transported from terrestrial to aquatic environments via surface runoff. Nitrogen enriched runoff is likely exacerbated on Moorea by the lack of runoff control or riparian buffers preservation requirements between fields and rivers (Feld et al. 2011).

While we did not observe a strong relationship in linear models between DIN concentrations in rivers and population as a single effect, the inclusion of population in a mixed model with land clearing did improve model fit. The DIN signal from

the population metric would likely be the result of sewage. Previous work on Moorea measuring nitrogen isotopes in nearshore macroalgae observed elevated $\delta^{15}N$ in algae tissue sampled near population centers indicating that sewage leaching directly into the nearshore environment via submarine groundwater discharge was likely a large contributor to nitrogen pollution (Adam et al. 2021; Knee et al. 2016; Haβler et al. 2019). Direct measurements of DIN concentrations in groundwater and submarine groundwater seeps in these studies recorded DIN levels as high as 45 μM (Haβler et al. 2019). It is likely that groundwater carrying DIN is also entering streams through hyporheic exchange in the lower reaches of the stream due to the porous nature of the volcanic geology (Boano et al., 2014) and high head pressure from the island's short, steep slopes (Shuler et al., 2020). This exchange may be enhanced in the lower reaches of the rivers as they have been heavily channelized and fortified for flood control (*personal observation*) which has enhanced stream bed erosion and deepening of river channels (Schmutz and Sendzimir, 2018) resulting in an increase in head near the terminus where our samples were collected.

2. Total Suspended Solids

Both the PCA and regression analyses illustrated that TSS concentrations were significantly associated with the percentage of cleared land and population in a given watershed, suggesting that both urbanization and agriculture contribute to the mobilization of sediment. Our linear mixed model using only watershed percent cleared land area and population was highly predictive of mean and maximum TSS concentrations in rivers ($p=0.001$, $r^2 = 0.82$ and $p=0.002$, $r^2 = 0.78$, respectively). Similar models have been applied effectively to predict TSS in other watersheds

including in the western Sierra mountains in California (Ahearn et al. 2005). These models do not predict discharge or sediment flux, but like our DIN model they could be a useful framework for a first order assessment of potential human health or environmental impact concerns in similar regions. TSS thresholds and regulations are often based on concentrations, not flux ("Amendment and Compilation of Chapter 11-54 Hawaii Administrative Rules") In locations where data are lacking, such as many high islands in the South Pacific, this simple linear modeling approach may provide valuable insights where there is insufficient data to inform a more complicated runoff model like the Soil and Water Assessment Tool (SWAT), Revised Universal Soil Loss Equation (RUSLE), Modified Morgan–Morgan–Finney (MMF) model, or others that are commonly paired with remote sensing analysis to assess relationships between land use and TSS (Arnold et al., 2012; Renard et al., 1994; Das et al., 2021).

TSS concentrations in all studied watersheds on Moorea, except for Ma'atea, exceeded the TSS threshold of 5 mg/L for safe drinking, bathing and cleaning ("Amendment and Compilation of Chapter 11-54 Hawaii Administrative Rules," 2021 & Wenger et al. 2018) on average 41% of the time. TSS values from seven out of the eleven watersheds also exceeded the 50 mg/L threshold representing potentially lethal levels for fish species (Wenger et al. 2018) 8% of the time. We also observed high variability in TSS levels between samples, including some outliers (e.g. >900 mg/L compared to mean of 26 mg/L in Paopao) that illustrate how sediment is mobilized in these flashy systems and how difficult it can be to capture differences between watersheds or seasons when much of the sediment that moves from land to river can mobilize during a few major rain events (Wymore et al. 2019). The range of TSS values observed across watersheds experiencing

varying degrees of land clearing and urbanization are within the ranges observed in a study across an urbanization gradient in Hawaii (Augustijin et al. 2010) and a study of a “pristine” rainforest watershed in Fiji that includes samples taken during a cyclone (Ram and Terry, 2016). TSS values observed in the most disturbed watersheds of our study (Paopao and Opunohu) were considerably lower than those observed in a study of urban and developing watersheds on Tahiti which recorded values as high as 33.3 g/L TSS in a watershed that was actively undergoing sizeable earthworks projects (Wotling and Bouvier, 2002).

Much of the existing land suitable for development in Moorea has been utilized, so new residential or industrial development requires considerable earth moving efforts, including forest clearing and terracing to create flat buildable plots. We did not observe use of soil retention measures (e.g. vegetative cover, mulch, silt fences, geotextiles) that have been shown in similar steep tropical systems to reduce erosion (e.g. Sutherland 1999; Sutherland and Ziegler 2007). Furthermore, a majority of the roads in the interior of the island are not paved, tend to follow river channels, and lack any soil retention devices (*pers. observation)* that have been successfully demonstrated in comparable systems (Wemple et al. 2017). As a result of their demonstrated ability to reduce erosion, implementation of erosion control measures such as those listed above are required by law on construction projects in Hawaii (HAR 11-55).

Land clearing associated with agriculture is also likely a large contributor to TSS runoff as pineapple farming is known to contribute to high erosion rates (reviewed in Martinez et al. 2022). In a recent study which scored farming practices in French Polynesia based on soil preservation, pineapple farming scored the lowest for its contributions to soil degradation (Surchat et al., 2021). Across French

Polynesia and in many other tropical climates pineapples are often grown on moderate to steep slopes making it difficult to employ erosion control measures such as cover crop or mulching between rows, which have been shown to be effective in reducing soil erosion in other agricultural systems (Ryder and Fares 2008; Surchat et al. 2021). Further, to maximize yield from a farmed plot, many farms in Moorea extend right up to riverbanks with no riparian zone or other buffer to slow the movement of sediment from the fields to the rivers (*pers. observation*). All of these conditions create high erosion potential, and contribute to the strong relationship between land clearing and TSS in rivers we observed in Moorea.

3. Phosphate

Phosphate concentrations ranged from a 0.19 µM sample collected in Teavaro to a 7.58µM sample collected in Paopao. Phosphate concentrations differed significantly among watersheds ($p < 0.001$) and season ($p = 0.01$) and had a significant interaction of watershed and season ($p = 0.007$). The range of phosphate concentrations recorded in this study are comparable to those found in a study of watersheds on Oahu, Hawaii, across base and stormflow and including watersheds considered to be forested, agricultural and urban (Hoover & Mackenzie, 2009). In both the PCA and linear regression analysis, riverine phosphate on Moorea was decoupled from both land clearing and population, suggesting that agriculture and urbanization were not directly responsible for the differences in phosphate concentrations we observed around the island.

Anthropogenic sources of phosphate often come in the form of agricultural fertilizers, however pineapples need little to no phosphorus fertilizer where soils have a naturally high phosphorus content as they likely do on Moorea

(Bartholomew et al. 2002). Soils on the island are derived from erosion of volcanic basalts which tend to be rich in phosphorus, and the availability of phosphorus in the soil of a given area is additionally dependent on numerous factors including age, weathering, and localized precipitation (Rechberger et al. 2021). Phosphate concentrations in rivers are often tied to sediment concentrations as phosphate can desorb from sediment particles in transit (de Campos et al. 2018). As there are at least eight different volcanic soils on Moorea (Jamet 2000), differences in riverine phosphate between watersheds could be related to erosion, vegetative utilization, or leaching of soils with different phosphate levels depending on which soil types happen to be exposed in a given watershed. Groundwater and submarine groundwater discharge on Moorea is also elevated in phosphate relative to surface water. This is likely due to weathering of phosphate rich basaltic rock in aquifers (Haβler et al. 2019). It is likely that phosphate also enters streams on Moorea via hyporheic exchange. Differences in phosphate in rivers on Moorea may also be the result of differences in bedrock phosphate concentrations, underground mobilization rates, and/or differences in groundwater-surface water hyporheic exchange rates. As anthropogenic sources of DIN increase on the island due to expanded agriculture and urbanization, it is likely that the N:P ratio will also increase as nitrogen enrichment outpaces phosphate mobilization.

E. Conclusion

This study provides the first island-wide assessment of riverine nutrient and sediment concentrations on Moorea, and explores the relationships between these concentrations, land use and populations. Watersheds on Moorea, as well as other small high tropical watersheds worldwide, are developing rapidly with growing pop-

ulations, tourism, logging and large-scale agriculture (Tanaka et al. 2021, Carlson et al. 2019). Our study puts Moorea in context of these other efforts to study land-use and its impacts on rivers. The relationships we observed between land use and river nutrient chemistry on Moorea are comparable to those observed in other developed and developing islands around the world (Comeros-Rayna et al. 2021, Albert et al. 2021, Dadhich and Nadaoka, 2012). In some cases, Moorea may be more susceptible to land-use initiated sediment erosion and runoff as indicated by our comparison with the Wenger et al. (2020) studies in the Solomon Islands with respect to TSS threshold exceedance.

Perhaps most importantly, this study highlights watersheds on Moorea which present risks for human health and/or concerns regarding ecosystem processes based on nutrient and sediment thresholds. All of the watersheds we studied on Moorea exceeded the lower DIN thresholds on average 89% of the time, with Paopao and Haumi exceeding the thresholds 100% of the time. Paopao and Haumi also exceeded the upper DIN threshold 100% of the time, with all watersheds exceeding the threshold on average 79% of the time. If these watersheds were located in Hawaii, the exceedance of the upper threshold more than 10% of the time would have triggered the enactment of an Implementation and Monitoring plan to reduce nitrogen enrichment for all of the rivers (“Amendment and Compilation of Chapter 11-54 Hawaii Administrative Rules,” 2021). No such procedure exists on Moorea however.

Of the watersheds we surveyed, all but Ma’atea exceeded the lower TSS threshold. Rivers on Moorea exceeded this threshold 41% of the time. An exceedance of this threshold more than 10% of the time indicates concern for human interaction with the river including drinking, cleaning and bathing (Wenger et al. 2018;

Albert et al. 2021). Our work indicates that based on TSS concentrations, a majority of the rivers on the island may be unsafe for human consumption and contact without treatment. Fortunately running water sent to households on Moorea is treated, however many households do not have running water and rely on rivers or public taps (*personal communications with community water advocacy groups on Moorea).* TSS values from seven out of the eleven watersheds also exceeded the 50 mg/L threshold representing potentially lethal levels for fish species (Wenger et al. 2018) 8% of the time. Though watersheds on Moorea do not exceed this threshold more than 10% of the time, some watersheds like Paopao and Pihaena exceed the threshold ~20% of the time. It is possible that aquatic communities in these rivers have been altered as a result. This study also serves as a point of comparison against future changes on Moorea as land clearing and population growth continue on the island. As Moorea, and the other high tropical islands, continue to develop, impacts of watershed change are likely to increase with potentially profound consequences for human and ecosystem health.

Support and Funding:

Credit to Benoit Espiau at CRIOBE for his meticulous nutrient analyses. Particular mention to Corinne Fuchs, Kyla Pierce, Maya Gorgas and the members of ‘Ati Vai for their assistance collecting, processing and analyzing samples. Thank you to the staff of the Richard B. Gump station for all of the work solving logistical, administrative and mechanical issues. We could not have done this work without you.

Funding for this research was provided by the NSF GRFP program, NSF Career grant OCE—1547952, NSF grant MCR—1637396, The Schmidt Family Foundation, and The Worster Summer Research Fellowship. Funding for education and outreach related to this work was provided by the ASLO Global Outreach Initiative.

F. Citations

About ArcGIS | Mapping & Analytics Software and Services [WWW Document], URL https://www.esri.com/en-us/arcgis/about-arcgis/overview (accessed 8.25.23).

Adam, T.C., Burkepile, D.E., Holbrook, S.J., Carpenter, R.C., Claudet, J., Loiseau, C., Thiault, L., Brooks, A.J., Washburn, L., Schmitt, R.J., 2021. Landscape-scale patterns of nutrient enrichment in a coral reef ecosystem: implications for coral to algae phase shifts. Ecological Applications 31, e2227. https://doi.org/10.1002/eap.2227

Aguilera, R., Melack, J.M., 2018. Relationships Among Nutrient and Sediment Fluxes, Hydrological Variability, Fire, and Land Cover in Coastal California Catchments. J. Geophys. Res. Biogeosci. 123, 2568–2589. https://doi.org/10.1029/2017JG004119

Albert, S., Deering, N., Tongi, S., Nandy, A., Kisi, A., Sirikolo, M., Maehaka, M., Hutley, N., Kies-Ryan, S., Grinham, A., 2021. Water quality challenges associated with industrial logging of a karst landscape: Guadalcanal, Solomon Islands. Marine Pollution Bulletin 169, 112506. https://doi.org/10.1016/j.marpolbul.2021.112506

Allan, J.D., 2004. Landscapes and Riverscapes: The Influence of Land Use on Stream Ecosystems. Annu. Rev. Ecol. Evol. Syst. 35, 257–284. https://doi.org/10.1146/annurev.ecolsys.35.120202.110122

Arnold, J.G., Moriasi, D.N., Gassman, P. W., Abbaspour, K.C., White, M.J., Srinivasan, R., Santhi, C., Harmel, R.D., Van Griensven, A., Van Liew, M.W., Kannan, N., Jha, M.K., 2012. SWAT: Model Use, Calibration, and Validation. Transactions of the ASABE 55, 1491–1508. https://doi.org/10.13031/2013.42256

AutoAnalyzer Multi-test Methods [WWW Document], URL https://www.seal-analytical.com/Methods/AutoAnalyzer-Methods/AutoAnalyzer-Multi-test-Methods (accessed 6.13.23)

Bartholomew, D., Rohrbach, K., Evans, D., 2002. Pineapple cultivation in Hawaii. Fruits and Nuts. 7, 1-8.

Bartley, R., Bainbridge, Z.T., Lewis, S.E., Kroon, F.J., Wilkinson, S.N., Brodie, J.E., Silburn, D.M., 2014. Relating sediment impacts on coral reefs to watershed sources, processes and management: A review. Science of The Total Environment 468–469, 1138–1153. https://doi.org/10.1016/j.scitotenv.2013.09.030

Boano, F., Harvey, J.W., Marion, A., Packman, A.I., Revelli, R., Ridolfi, L., Wörman, A., 2014. Hyporheic flow and transport processes: Mechanisms, models, and biogeochemical implications. Reviews of Geophysics 52, 603–679. https://doi.org/10.1002/2012RG000417

Canning, A.D., Death, R.G., 2020. The influence of nutrient enrichment on riverine food web function and stability. Ecol Evol 11, 942–954. https://doi.org/10.1002/ece3.7107

Carlson, R.R., Foo, S.A., Asner, G.P., 2019. Land Use Impacts on Coral Reef Health: A Ridge-to-Reef Perspective. Frontiers in Marine Science 6.

CHAPTER 180C] [WWW Document], URL https://www.capitol.hawaii.gov/hrscurrent/vol03_ch0121-0200d/HRS0180C/HRS_0180C-.htm (accessed 6.3.23).

Classification [WWW Document], URL https://www.l3harrisgeospatial.com/docs/Classification.html#ClassSupervised (accessed 7.23.23).

Collin, A., Hench, J.L., Pastol, Y., Planes, S., Thiault, L., Schmitt, R.J., Holbrook, S.J., Davies, N., Troyer, M., 2018. High resolution topobathymetry using a Pleiades-1 triplet: Moorea Island in 3D. Remote Sensing of Environment 208, 109–119. https://doi.org/10.1016/j.rse.2018.02.015

Comeros-Raynal, M.T., Brodie, J., Bainbridge, Z., Choat, J.H., Curtis, M., Lewis, S., Stevens, T., Shuler, C.K., Sudek, M., Hoey, A.S., 2021. Catchment to sea connection: Impacts of terrestrial run-off on benthic ecosystems in American Samoa. Marine Pollution Bulletin 169, 112530. https://doi.org/10.1016/j.marpolbul.2021.112530

Dadhich, A.P., Nadaoka, K., 2012. Analysis of Terrestrial Discharge from Agricultural Watersheds and Its Impact on Nearshore and Offshore Reefs in Fiji. Journal of Coastal Research 28, 1225–1235. https://doi.org/10.2112/JCOASTRES-D-11-00149.1

Das, S., Deb, P., Bora, P.K., Katre, P., 2021. Comparison of RUSLE and MMF Soil Loss Models and Evaluation of Catchment Scale Best Management Practices for a Mountainous Watershed in India. Sustainability 13, 232. https://doi.org/10.3390/su13010232

Downing, J.A., Mcclain, M., Twilley, R., Melack, J.M., Elser, J., Rabalais, N.N., Lewis, W.M., Turner, R.E., Corredor, J., Soto, D., Yanez-Arancibia, A., Kopaska, J.A., Howarth, R.W., 1999. The impact of accelerating land-use change on the N-Cycle of tropical aquatic ecosystems: Current conditions and projected changes. Biogeochemistry 46, 109–148. https://doi.org/10.1007/BF01007576

Duane, T., 2006. Land Use Planning to Promote Marine Conservation of Coral reef Ecosystems in Moorea, French Polynesia.

Feld, C.K., Birk, S., Bradley, D.C., Hering, D., Kail, J., Marzin, A., Melcher, A., Nemitz, D., Pedersen, M.L., Pletterbauer, F., Pont, D., Verdonschot, P.F.M., Friberg, N., 2011. Chapter Three - From Natural to Degraded Rivers and Back Again: A Test of Restoration Ecology Theory and Practice, in: Woodward, G. (Ed.), Advances in Ecological Research. Academic Press, pp. 119–209. https://doi.org/10.1016/B978-0-12-374794-5.00003-1

Green, P.A., Vörösmarty, C.J., Meybeck, M., Galloway, J.N., Peterson, B.J., Boyer, E.W., 2004. Pre-industrial and contemporary fluxes of nitrogen through rivers: a global assessment based on typology. Biogeochemistry 68, 71–105. https://doi.org/10.1023/B:BIOG.0000025742.82155.92

Guernier, V., Richard, V., Nhan, T., Rouault, E., Tessier, A., Musso, D., 2017. Leptospira diversity in animals and humans in Tahiti, French Polynesia. PLOS Neglected Tropical Diseases 11, e0005676. https://doi.org/10.1371/journal.pntd.0005676

Guinto, D., Inciong, M., 2012. Soil quality, soil management practices and sustainability of pineapple farms in Cavite, Philippines: Part 1. Soil quality. Journal of South Pacific Agriculture 16, 30–41.

Hoffmann, T., Thorndycraft, V.R., Brown, A.G., Coulthard, T.J., Damnati, B., Kale, V.S., Middelkoop, H., Notebaert, B., Walling, D.E., 2010. Human impact on fluvial regimes and sediment flux dur-

ing the Holocene: Review and future research agenda. Global and Planetary Change 72, 87–98. https://doi.org/10.1016/j.gloplacha.2010.04.008

Hoover, D.J., 2002. Fluvial nitrogen and phosphorus in Hawaii: Storm runoff, land use, and impacts on coastal waters (Ph.D.). University of Hawai'i at Manoa, United States -- Hawaii.

Houk, P., Castro, F., McInnis, A., Rucinski, M., Starsinic, C., Concepcion, T., Manglona, S., Salas, E., 2022. Nutrient thresholds to protect water quality, coral reefs, and nearshore fisheries. Marine Pollution Bulletin 184, 114144. https://doi.org/10.1016/j.marpolbul.2022.114144

Houk, P., Comeros-Raynal, M., Lawrence, A., Sudek, M., Vaeoso, M., McGuire, K., Regis, J., 2020. Nutrient thresholds to protect water quality and coral reefs. Marine Pollution Bulletin 159, 111451. https://doi.org/10.1016/j.marpolbul.2020.111451

Image Processing & Analysis Software | Geospatial Image Analysis Software | ENVI® [WWW Document], URL https://www.nv5geospatialsoftware.com/Products/ENVI (accessed 8.25.23).

Institut de la statistique de la Polynésie Française [WWW Document], URL https://www.ispf.pf/ (accessed 8.25.23).

Jamet, R., 2000. Les sols de Moorea et des îles Sous-le-Vent [cartographic material] : archipel de la Société, Polynésie Française / par Rémi Jamet. [WWW Document]. Les sols de Moorea et des îles Sous-... | Items | National Library of New Zealand | National Library of New Zealand. URL https://natlib.govt.nz/records/20850230 (accessed 6.7.23).

Kirch, P.V., 2017. On the Road of the Winds: An Archaeological History of the Pacific Islands before European Contact, Revised and Expanded Edition, in: On the Road of the Winds. University of California Press. https://doi.org/10.1525/9780520968899

Knee, K.L., Crook, E.D., Hench, J.L., Leichter, J.J., Paytan, A., 2016. Assessment of Submarine Groundwater Discharge (SGD) as a Source of Dissolved Radium and Nutrients to Moorea (French Polynesia) Coastal Waters. Estuaries and Coasts 39, 1651–1668. https://doi.org/10.1007/s12237-016-0108-y

Koshiba, S., Besebes, M., Soaladaob, K., Isechal, A.L., Victor, S., Golbuu, Y., 2013. Palau's taro fields and mangroves protect the coral reefs by trapping eroded fine sediment. Wetlands Ecol Manage 21, 157–164. https://doi.org/10.1007/s11273-013-9288-4

Kroon, F.J., Kuhnert, P.M., Henderson, B.L., Wilkinson, S.N., Kinsey-Henderson, A., Abbott, B., Brodie, J.E., Turner, R.D.R., 2012. River loads of suspended solids, nitrogen, phosphorus and herbicides delivered to the Great Barrier Reef lagoon. Marine Pollution Bulletin, The Catchment to Reef Continuum: Case studies from the Great Barrier Reef 65, 167–181. https://doi.org/10.1016/j.marpolbul.2011.10.018

Labrière, N., Locatelli, B., Laumonier, Y., Freycon, V., Bernoux, M., 2015. Soil erosion in the humid tropics: A systematic quantitative review. Agriculture, Ecosystems & Environment 203, 127–139. https://doi.org/10.1016/j.agee.2015.01.027

Landsat 8 | U.S. Geological Survey [WWW Document], URL https://www.usgs.gov/landsat-missions/landsat-8 (accessed 8.25.23).

Loiseau, C., Thiault, L., Devillers, R., Claudet, J., 2021. Cumulative impact assessments highlight the benefits of integrating land-based management with marine spatial planning. Science of The Total Environment 787, 147339. https://doi.org/10.1016/j.scitotenv.2021.147339

Marcus, L., 2022. French Polynesia to cap tourist numbers [WWW Document]. CNN. URL https://www.cnn.com/travel/article/french-polynesia-tahiti-tourist-cap/index.html (accessed 8.2.23)

Martinez, C., Menjívar, J.C., Saavedra, R., 2022. Soils erosion in pineapple (Ananas comosus L. Merr) producing areas. Revista de Ciencias Agrícolas 39, 142–154. https://doi.org/10.22267/rcia.223901.176

Meyer, J., Pouteau, R., Spotswood, E., Taputuarai, R., Fourdrigniez, M., 2015. The importance of novel and hybrid habitats for plant conservation on islands: a case study from Moorea (South Pacific). Biodiversity & Conservation 24, 83–101. https://doi.org/10.1007/s10531-014-0791-6

Millbank, H., Nothard, B., 2023. Understanding the economics of horticultural management practices and systems for improving water quality runoff in the Great Barrier Reef catchment areas [WWW Document]. URL http://era.daf.qld.gov.au/id/eprint/9271/ (accessed 6.7.23).

Nessel, M.P., Konnovitch, T., Romero, G.Q., González, A.L., 2021. Nitrogen and phosphorus enrichment cause declines in invertebrate populations: a global meta-analysis. Biological Reviews 96, 2617–2637. https://doi.org/10.1111/brv.12771

Norton, J., Ouyang, Y., 2019. Controls and Adaptive Management of Nitrification in Agricultural Soils. Frontiers in Microbiology 10.

Oksanen, J., Simpson, G., Blanchet, F.G., Kindt, R., Legendre, P., Minchin, P., hara, R., Solymos, P., STEVENS, H., Szöcs, E., Wagner, H., Barbour, M., Bedward, M., Bolker, B., Borcard, D., Carvalho, G., Chirico, M., De Cáceres, M., Durand, S., Weedon, J., 2022. vegan community ecology package version 2.6-2 April 2022.

Piao, S., Friedlingstein, P., Ciais, P., de Noblet-Ducoudré, N., Labat, D., Zaehle, S., 2007. Changes in climate and land use have a larger direct impact than rising CO2 on global river runoff trends. Proceedings of the National Academy of Sciences 104, 15242–15247. https://doi.org/10.1073/pnas.0707213104

Rechberger, M.V., Zehetner, F., Gerzabek, M.H., 2021. Phosphate sorption-desorption properties in volcanic topsoils along a chronosequence and a climatic gradient on the Galápagos Islands. Journal of Plant Nutrition and Soil Science 184, 479–491. https://doi.org/10.1002/jpln.202000488

Renard, K.G., Foster, G.R., Yoder, D.C., McCool, D.K., 1994. RUSLE revisited: Status, questions, answers, and the future. Journal of Soil and Water Conservation 49, 213–220.

Ryder, M. H., Fares, A., 2008. Evaluating Cover Crops (Sudex, Sunn Hemp, Oats) for Use as Vegetative Filters to Control Sediment and Nutrient Loading From Agricultural Runoff in a Hawaiian Watershed1. JAWRA Journal of the American Water Resources Association 44, 640–653. https://doi.org/10.1111/j.1752-1688.2008.00189.x

Schmutz, S., Sendzimir, J. (Eds.), 2018. Riverine Ecosystem Management: Science for Governing Towards a Sustainable Future. Springer International Publishing, Cham. https://doi.org/10.1007/978-3-319-73250-3

Shuler, C.K., Dulai, H., Leta, O.T., Fackrell, J., Welch, E., El-Kadi, A.I., 2020. Understanding surface water–groundwater interaction, submarine groundwater discharge, and associated nutrient loading in a small tropical island watershed. Journal of Hydrology 585, 124342. https://doi.org/10.1016/j.jhydrol.2019.124342

Siemonsma, D., 2015. The Shuttle Radar Topography Mission (SRTM) Collection User Guide.

Strahler, A.N., 1952. Hypsometric (Area-Altitude) Analysis of Erosional Topography. GSA Bulletin 63, 1117–1142. https://doi.org/10.1130/0016-7606(1952)63[1117:HAAOET]2.0.CO;2

Strauch, A.M., 2017. Relative change in stream discharge from a tropical watershed improves predictions of fecal bacteria in near-shore environments. Hydrological Sciences Journal 62, 1381–1393. https://doi.org/10.1080/02626667.2017.1310381

Surchat, M., Wezel, A., Tolon, V., Breland, T.A., Couraud, P., Vian, J.-F., 2021. Soil and Pest Management in French Polynesian Farming Systems and Drivers and Barriers for Implementation of Practices Based on Agroecological Principles. 15. https://doi.org/10.3389/fsufs.2021.708647

Sutherland, R.A., 1998. Rolled erosion control systems for hillslope surface protection: a critical review, synthesis and analysis of available data. I. Background and formative years. Land Degradation & Development 9, 465–486. https://doi.org/10.1002/(SICI)1099-145X(199811/12)9:6<465::AID-LDR311>3.0.CO;2-4

Sutherland, R.A., Ziegler, A.D., 2006. Hillslope runoff and erosion as affected by rolled erosion control systems: a field study. Hydrological Processes 20, 2839–2855. https://doi.org/10.1002/hyp.6078

Tanaka, Y., Minggat, E., Roseli, W., 2021. The impact of tropical land-use change on downstream riverine and estuarine water properties and biogeochemical cycles: a review. Ecological Processes 10, 40. https://doi.org/10.1186/s13717-021-00315-3

Taylor, B.W., Keep, C.F., Hall, R.O., Koch, B.J., Tronstad, L.M., Flecker, A.S., Ulseth, A.J., 2007. Improving the fluorometric ammonium method: matrix effects, background fluorescence, and standard additions. Journal of the North American Benthological Society 26, 167–177. https://doi.org/10.1899/0887-3593(2007)26[167:ITFAMM]2.0.CO;2

Viau, E.J., Boehm, A.B., 2011. Quantitative PCR-based detection of pathogenic Leptospira in Hawai'ian coastal streams. Journal of Water and Health 9, 637–646. https://doi.org/10.2166/wh.2011.064

Vidal-Durà, A., Burke, I.T., Stewart, D.I., Mortimer, R.J.G., 2018. Reoxidation of estuarine sediments during simulated resuspension events: Effects on nutrient and trace metal mobilisation. Estuarine, Coastal and Shelf Science 207, 40–55. https://doi.org/10.1016/j.ecss.2018.03.024

Wemple, B.C., Browning, T., Ziegler, A.D., Celi, J., Chun, K.P. (Sun), Jaramillo, F., Leite, N.K., Ramchunder, S.J., Negishi, J.N., Palomeque, X., Sawyer, D., 2018. Ecohydrological disturbances

associated with roads: Current knowledge, research needs, and management concerns with reference to the tropics. Ecohydrology 11, e1881. https://doi.org/10.1002/eco.1881

Wenger, A., Harris, D., Weber, S., Vaghi, F., Nand, Y., Naisilisili, W., Hughes, A., Delevaux, J., Klein, C., Watson, J., Mumby, P., Jupiter, S., 2020. Best-practice forestry management delivers diminishing returns for coral reefs with increased land-clearing. Journal of Applied Ecology 57. https://doi.org/10.1111/1365-2664.13743

Winkler, K., Fuchs, R., Rounsevell, M., Herold, M., 2021. Global land use changes are four times greater than previously estimated. Nat Commun 12, 2501. https://doi.org/10.1038/s41467-021-22702-2

Wurtsbaugh, W.A., Paerl, H.W., Dodds, W.K., 2019. Nutrients, eutrophication and harmful algal blooms along the freshwater to marine continuum. WIREs Water 6, e1373. https://doi.org/10.1002/wat2.1373

II. Land use and river water chemistry reduce coral cover and homogenize reef community composition in Moorea, French Polynesia

Contributing Authors: *Terava Atger* — Local and traditional ecological knowledge, sample collection and laboratory assistance. *Tauira Punu* — Local and traditional ecological knowledge, sample collection and laboratory assistance. *Christian Green* — Satellite image analysis. *Will Underhill*—Satellite image analysis. *Jordan A. Hollarsmith* — Advising of statistical analyses, editing. *Deron E. Burkepile* — Advising.

A. Introduction

The hydrology of tropical high islands is particularly susceptible to land use change (Albert et al. 2021, Surchat et al. 2021, Koshiba et al. 2013). The removal of island forest vegetation with deep, complex root systems, exposes highly erodible soils to erosion from the heavy and periodic rainfall often found on tropical islands (Godard and Barriot 2022). Soil erosion is exacerbated on steep slopes that comprise much of the topography of high islands (Wenger et al. 2020). If forests on these slopes are replaced by agriculture or pasture for livestock, runoff will also contain excess fertilizer, pesticides, herbicides and manure (Correll, 1998; Downing et al. 1999; Schmutz and Sendzimir, 2018). If forests are replaced by urban environments, runoff can contain minimally-treated human sewage as well as household and industrial chemicals (Ramírez et al. 2012). A key question on many tropical islands is how human development of the landscape impacts the movement of sediments and nutrients through rivers and streams to the coastal environment as well as how these sediments and nutrients impact the ecology of nearshore ecosys-

tems (Risk 2014). On many tropical islands, the coral reefs that are adjacent to shore, often known as ‘fringing reefs’, are especially vulnerable to stressors associated with watershed alterations due to their proximity to land development, agriculture and input from rivers (Rouzé et al. 2015). Freshwater runoff transports terrestrial sediments and nutrients to nearshore reefs, and the volume of transport can be high in watersheds that are deforested or converted to agriculture (Brodie et al. 2012, Bartley et al. 2013). Deposition of terrigenous sediment and exposure to elevated nutrients can impact the physiology of individual corals as well as alter the structure, diversity and function of reef ecosystems (reviewed in Fabricius 2005; Zhao et al 2021). Reefs exposed to even moderate increases in nutrients and sedimentation often have lower coral diversity and higher cover of macroalgae than reefs without these stressors (Houk et al. 2020 & 2022). As growing human populations alter land use and as climate change has increased frequency and intensity of rainfall events, it is necessary to understand how these influences affect the health of tropical rivers and the coral reefs adjacent to them.

Coral reef ecosystems tend to be oligotrophic, often with submicromolar dissolved inorganic nitrogen (DIN) and phosphorus concentrations (Lapointe 1997). As such, corals and other reef organisms adapted to these conditions can be sensitive to changes in nutrient availability. Elevated DIN and dissolved phosphorous often have direct negative impacts on corals by lowering calcification rates, reducing fertility and fecundity, altering coral microbiomes, and increasing susceptibility to disease and bleaching (Shantz and Burkepile, 2014, Vega Thurber et al. 2014, Zaneveld et al. 2016, Nalley et al. 2023). Elevated nutrients can also lead to indirect negative effects on corals via changes in the reef community by giving competitive advantage to faster growing macroalgae and turf algae which are capable of rapidly

utilizing available nutrients (Fabricius, 2005; D'Angelo and Wiedenmann 2014). Increases in algae on reefs can lower coral growth rates and survivorship via competition (Hughes et al. 2007, Box and Mumby 2007, Zaneveld et al. 2016), lower coral fecundity (Foster et al. 2008), as well as reduce the settlement and success of coral larvae (Hughes et al 2007). Because of this wide array of negative direct and indirect effects of nutrients on corals, even relatively modest increases in DIN have been correlated to reduced species diversity in reefs adjacent to rivers (Houk et al. 2020 & 2022).

Exposure to increased sedimentation can affect corals by reducing photosynthetically available radiation (PAR) resulting in lower photosynthesis (Junjie et al. 2014, Browne et al. 2014), reducing coral growth and survivorship through burial (Rice et al. 2021), and reducing available substate for coral recruitment (Babcock and Davies 1991, Wakwella et al. 2020). Sedimentation can also suppress herbivory by fishes and results in increased abundance of filamentous turf algae (Goatley and Bellwood 2012, Goatley et al. 2016), with these algal-trapped sediments significantly suppressing coral recruitment (Speare et al. 2019). Reefs under high levels of sedimentation often have different benthic communities than reefs experiencing low sedimentation (Acevedo et al. 1989, Rogers 1990, McClanahan and Obura 1997). Furthermore, nutrients and other pollution can sorb onto the surface of sediment particles, to be released into the water column once the particles settle to the benthos (Vidal-Durà et al. 2018). On volcanic high islands with soils derived from phosphorus-rich basalt, sedimentation can be a significant source of phosphate enrichment on nearshore reefs (de Campos et al. 2018). Thus, sedimentation and nutrient enrichment may co-occur and work synergistically to compromise coral health and alter benthic reef communities (Risk 2014).

Here, we address the impact of sediments and nutrients in rivers on the ecology of nearshore coral reefs on the high island of Moorea, French Polynesia. The diversity of watersheds in close proximity featuring a range of land uses and populations makes Moorea a compelling location to investigate interactions between human activity, riverine nutrients and sediment, and reef community composition. To address how river water quality may impact nearshore coral reefs, we first quantified coral reef community composition near the outflow of six of the major rivers on Moorea and then measured both the sediment concentrations and water chemistry in these rivers. Then to address how land clearing and urbanization in Moorea is influencing nearshore reef community composition, we analyzed satellite images to quantify land use across the watersheds on Moorea and used census data to assess any role of population density in reef health. Using these datasets we addressed two hypotheses. First, we hypothesized that reefs adjacent to the mouths

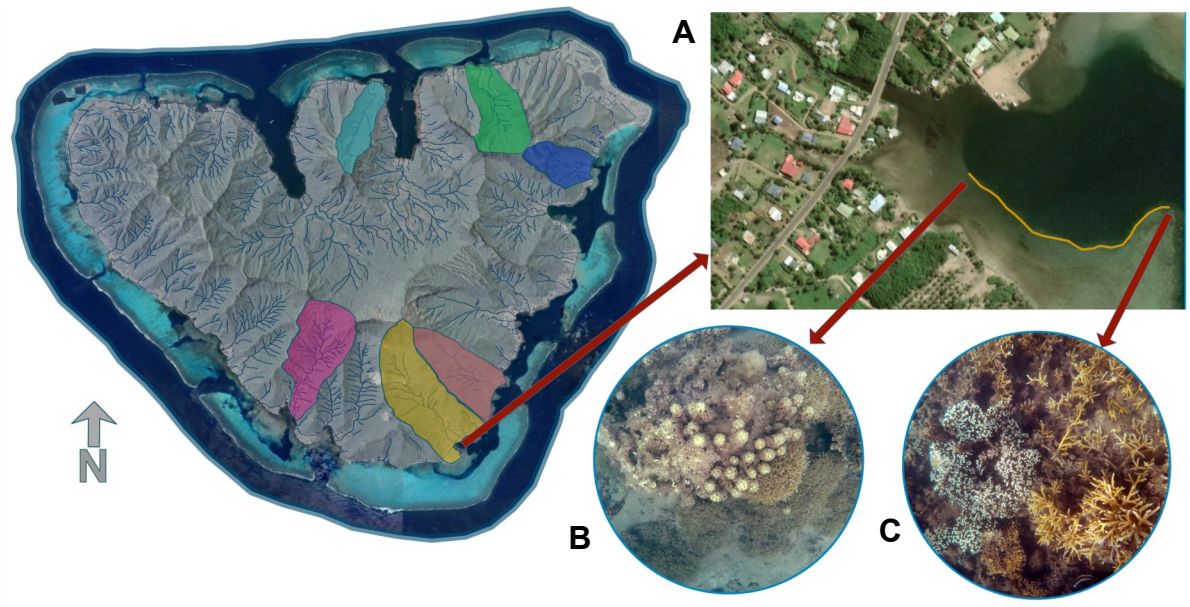

Figure 1. Moorea, French Polynesia mapped with hillshade, stream channels and focal watersheds. Inset A showcases the fringing reef photo transect at Maatea. Inset B demonstrates the benthic composition near the beginning of the transect — dominated by substrate covered in sediment and macroalgae. Inset C demonstrates the benthic composition near the end of the transect — dominated by live coral.

of rivers with more land clearing and higher populations, resulting in elevated nutrient and sediment concentrations, would have lower overall coral cover and higher cover of macroalgae. Second, we hypothesized that the species composition of reef communities experiencing higher anthropogenic stress as a result of land use would be more homogenous even at distances farther from the river mouths than those under lower stress from runoff.

B. Materials and Methods

1. Study location

Moorea is a high island of volcanic origin located in the Society Archipelago of French Polynesia (17° 29′ S, 149° 50′ W; 134 km^2). Since it was formed by a volcanic eruption approximately 1.6 million years ago (Meyer et al. 2015), Moorea has collapsed and eroded into 57 distinct watersheds separated by steep, sharp ridgelines with a highest elevation of 1207 m at Mount Tohiea (Meyer et al. 2015). Over the millennia, as the island eroded and subsided, a barrier reef formed separating the open ocean from a 53 km^2 lagoon (Collin et al. 2018). Moorea has been inhabited by humans since around 200 CE when it was settled by the Polynesians (Kirch, 2000). As of the 2017 census, Moorea was home to 17,357 people (Institut de la statistique de la Polynésie Française).

The largest watersheds on Moorea are two adjacent valleys on the north shore, Opunohu (15.7 km^2) and Paopao (11.4 km^2), formed by a collapse of the volcano's caldera (Meyer et al., 2015). Opunohu is home to a small population (97 people), but hosts a large portion of the island's commercial agriculture which is principally comprised of pineapple plantations and cattle pastures. As an example of the steepness of watersheds on Moorea, more than 90% of the Opunohu valley

is comprised of slopes greater than 10% (Binet & Gonnot, 2005). Neighboring Paopao is home to the largest population (1557 people) and small, mixed-agricultural fields. In contrast, the smallest watershed included in this study, Teavaro, is on the eastern shore of the island and is only 1 km^2, but is home to 248 people. The variety of watersheds in close proximity featuring a range of areas, land uses and populations makes Moorea a compelling location to investigate interactions among human activity, riverine nutrients and sediment as well as how these factors impact coral reef communities.

Moorea is ringed by a barrier reef that separates the open ocean from a lagoon. Within the lagoon, there are two distinct reef habitats, the back reef and the fringing reef (Figure 1). The back reef is located directly inshore of the barrier reef, while the fringing reef grows adjacent to the shore at the land-sea margin. On Moorea, these fringing reef habitats are generally separated by deep-water channels that typically run parallel to shore and connect to passes in the barrier reef that allow water exchange between the lagoon and the open ocean. In this study, we focus on fringing reefs that are adjacent to the mouths of the major rivers on the island (Figure 1).

In order to study rivers and reefs on Moorea, we first engaged the local community to receive feedback on the key questions that would be of interest and value to the people of Moorea. The goals, objectives, and research locations for this study were shaped by meetings with community members, organized by the Te Pu Atiti'a Polynesian Cultural Center located directly adjacent to the University of California Gump Research Station where our research was based. Additional meetings were held with local fishing collectives and clean water advocacy groups. Across groups, concerns raised in these meetings were similar. People on Moorea have

observed a decline in nearshore corals and a proliferation of turf and macroalgae, specifically the brown alga *Turbinaria ornata*. They are also concerned about the safety of rivers for drinking and swimming. In each meeting, we were implored to look at land to sea connections and the potential of development and agriculture to impact both rivers and reefs. These conversations precipitated the formation of a new community science organization on Moorea called Ati Vai ('Water Clan' in Tahitian). This research was co-produced with the members of Ati Vai. The combination of modern scientific tools and techniques with traditional and local knowledge of the island and its rivers was paramount to the success of this initiative.

2. Assessment of coral reef community composition

Focal reefs for this study were Haumi, Ma'atea, Maharepa, Pihaena, Teavaro, and Vaiane (Figure 1). Reefs sites were selected because of their proximity to the outlet of rivers on Moorea that had been studied in an island-wide study of land-use impacts on rivers (Chapter 2). Further site selection criteria included similar reef geomorphology and sites that represented a range of watershed sizes, agricultural development, and population density. Reefs were chosen near river mouths and near natural deepwater channels separating the fringing reef from adjacent fringing or back reef habitat (Figure 1).

In August and September of 2019, we collected data on reef community composition using photographic transects moving away from river mouths. Transects were conducted by a snorkeler that was pushing a float with a downward facing GoPro4 camera and GPS at the surface. (Figure 1). We entered the water at the river mouth and swam perpendicular from shore until we reached approximately 1.5 m of water depth (the depth at which we could effectively swim over the reef on

snorkel while maintaining high photo quality). Offshore of each river mouth there was a shallow sediment deposition zone. The benthos in this zone was primarily composed of soft brown terrigenous sediment, plant matter, and trash with relatively few living organisms. From this sediment deposition zone, we then swam parallel to the deep-water channel along the reef formation that was present at all of the sites. Transects began where we first observed hard substrate (approximately 100 m away from the river mouth) and continued along the 1.5 m depth contour parallel to the deepwater channels resulting in a coverage of approximately 3 m^2 of the benthos per photo. Transects ended when we encountered large natural or manmade features that would change the geomorphological structure and/or water movement on the reef, for example intersection with a deep-water channel that was perpendicular to the reef formation. Transects ranged in length from ~120 m (Maharepa) to ~300 m (Vaiane). Photos were taken every second while swimming.

From the resulting photo transect, we chose one image every ~20 seconds to ensure no overlap in the photos analyzed. Due to differences in swimming rate between transects, this resulted , this resulted in one image analyzed on average every 5.2 ± 1.5m . Images were then uploaded to CoralNet (CoralNet). In CoralNet, a 4 by 4 grid was overlaid to create 16 cells. In each cell 3 random points were generated for a stratified random sampling of 48 points per photo. All points were identified manually. If the point landed on coral or algae, it was identified to the lowest taxonomic classification possible. Identification was generally to genus for algae and coral, with the exception of the corals *Porites rus, Pocillopora acuta,* and *Acropora pulchra*, which were identified to species. Bleached or recently dead corals were classified separately and were also identified to the lowest possible classification. We also created a number of categories for the benthos including: turf al-

gae, crustose coralline algae/hard substrate, unconsolidated rubble, terrigenous sediment, and calciferous sediment. Anthropogenic trash and terrigenous organic matter (leaves, branches, palm fronds, etc) were also classified. We then aggregated categories into the following functional groups: (1) living coral, (2) macroalgae, (3) algal turf, (4) bleached/dead coral, (5) crustose coralline algae (CCA) /hard substrate, (6) terrigenous sediment, (7) calciferous sediment, (8) coral rubble, (9) terrigenous organic matter, (10) trash, and (11) “other” which includes rare categories like cyanobacterial mats. Observations in each photo were converted to percent cover by dividing each observation by 48 (due to the 48 random points for identification). We aggregated six photos into sections representing 120 seconds of the transect and then averaged the percent cover for the different taxonomic/functional groups for each section of the transect.

3. Assessment of river water quality

One objective was to understand the relationships between sediment and nutrient concentrations in rivers adjacent to fringing reef sites, and reef community composition at those sites. To do this, we collected water samples from rivers associated with reef transects. See chapter 2 methods sections 3, 4 and 5 for sample collection and analytical methods.

4. Quantifying population and land use in watersheds

To assess statistical relations between land use within a watershed and coral reef communities adjacent to rivers, land use was estimated using a Landsat 8 image of the island taken on March 22nd, 2018. See chapter 2 methods section 6 for methods used to analyze the image.

To assess statistical relations between human population density and reefs, population of permanent residents in the different watersheds was obtained from census data for 2017 via a license agreement between the Gump Research Station and the Institut de Statistiques de la Polynésie Française. See chapter 2 methods section 7 for analytical methods of the census data.

5. Statistical analyses

We first examined the how reef communities at the functional group level differed across reef sites and associated watersheds as well as how coral cover varied with different river water quality parameters. First, we hypothesized that cover of key functional groups (e.g. coral, macroalgae, turf algae) would be significantly different across reef sites. To test this idea, we used linear model to test for differences among sites where the replicates were the 120 second sections of each transect followed by Tukey post-hoc tests. Next, we hypothesized that water quality parameters would be significantly different across the different watersheds. To test this idea, we used linear models to test for differences among sites in the different water quality parameters (e.g. DIN, TSS, etc) followed by Tukey-post hoc tests. Only rainy season data were used in these analyses to allow for the inclusion of Pihaena which has low or no flow in the dry season. All analyses were conducted in R (R core team 2022). All stream chemistry data were 1+log transformed prior to analysis to improve normality prior to analysis based on inspection of q-q plots and residuals using the ‘qqplot’, ’qqnorm’, and ‘resid’ functions in R.

Next, we tested the hypothesis that coral and macroalgal algal cover at the site scale would be negatively and positively correlated, respectively, with adjacent river water quality and factors that reduced water quality (e.g., percent cleared

land). To do this we used Kendall's Tau tests to examine correlations between mean coral cover and algal cover, and rainy season mean river DIN, PO_4^{3-}, and TSS concentrations, and mean riverine N:P ratios. We also examined correlations between coral and algal cover and the watershed parameters percent cleared land and population. We chose Kendall's Tau due to the low number of sites used in this study as it is more conservative than the Pearson or Spearman correlation tests (Puka, 2011).

In addition to relationships between watershed parameters and coral and algal cover, we hypothesized that river water quality would explain a significant amount of variation in benthic community composition across sites. To test this hypothesis, we first conducted a PERMANOVA to test for differences in community composition across sites where different distances along each transect represented replicates within sites. Then we visualized the differences in community composition across sites using Nonmetric Multidimensional Scaling (NMDS), which is a form of non-parametric unconstrained ordination method based on Bray-Curtis dissimilarity. We evaluated the fit of the model using the stress of the model output. To determine the extent to which riverine water quality (DIN, TSS, PO_4^{3-}, N:P), watershed parameters (population and percent cleared land), and distance from the start of the transect partitioned the variance in the ordination, we conducted analysis of variance permutation tests (envfit function, vegan package). We then projected the explanatory variables as vectors onto the NMDS. Lastly, we hypothesized that reefs adjacent to streams with lower water quality would show stronger homogenization of the benthic community with less change in community composition with increasing distance from the river mouth. In order to test this hypothesis, we used the betadisper function in the vegan in order to quantify heterogeneity within a site by cal-

culating the non-euclidean distance between each point on a transect and the centroid of the site. We then used a linear model to determine whether there were significant differences in the dispersion of points across reef sites.

C. Results

1. Differences in coral and algal cover across sites

Coral cover differed significantly between sites (ANOVA: $f = 36.15$, $p < 0.001$). Teavaro with 22% and Vaiane with 38% had significantly higher coral cover than the other sites (Tukey test: $p<0.001$). Mean coral cover was 16% across sites (Table 1, Figure 2) while Pihaena had the lowest coral cover at 3% (Table 2, Figure 2). *Porites rus* was the most frequently observed coral with an average of 5% of the benthos across sites. Corals in the genera *Pavona* and *Montipora* were relatively rare (< 1%) across all our transects with the exception of Vaiane which had 10% and 9% cover of these genera, respectively. Similarly, *Acropora pulchra* was relatively rare across sites with the exception Teavaro at which cover of *A. pulchra* was 15%.

There were significant differences between sites in the percent cover of macroalgae (ANOVA: $f = 19.78$, $p < 0.001$) (Table 1, Figure 2). Mean macroalgal cover was 21% across sites (Table 3, Figure 3). Haumi and Ma'atea had the highest macroalgal cover (29% for both) while Teavaro at 18% and Vaiane at 2% had significantly lower algal cover than the other sites (Tukey: $p<0.001$; Table 3, Figure 3c). The most observed genus of macroalgae observed was *Turbinaria,* observed as on average 12.4% of the overall cover. Haumi had the highest percentage of overall coverage of *Turbinaria* at 25%, while no *Turbinaria* was observed at Vaiane. Turf algae was observed with the highest frequency of all functional groups with a

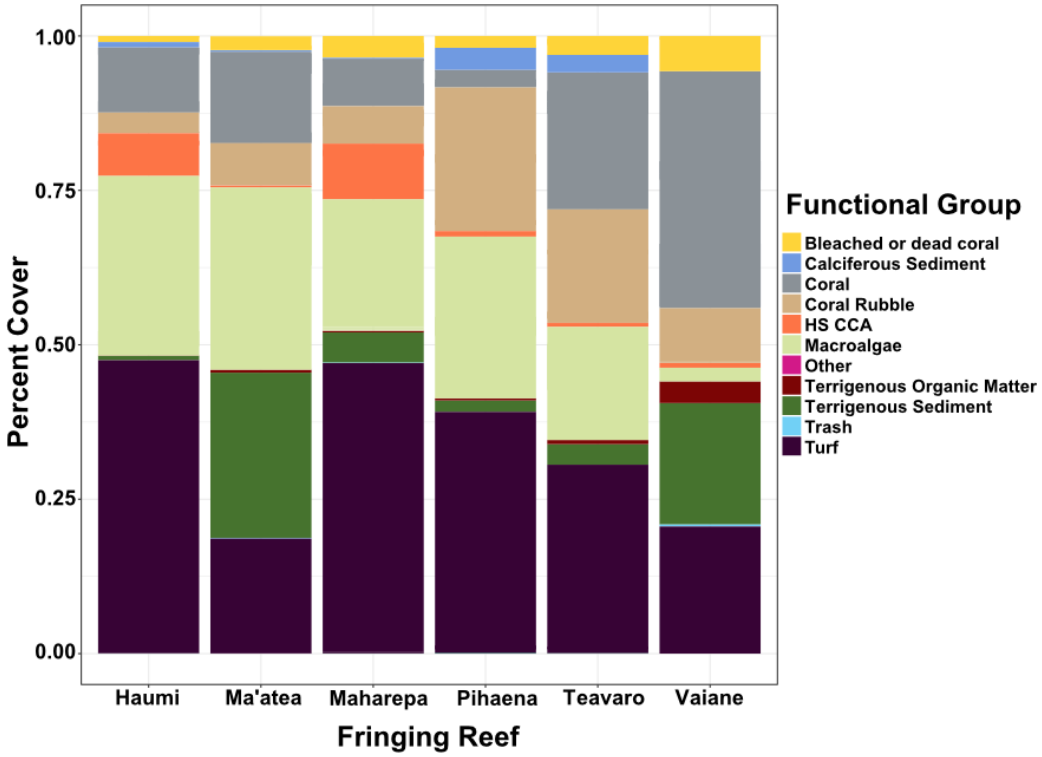

Figure 2. Stacked bar chart of the benthic cover of biotic and abiotic functional groups across fringing reef transects.

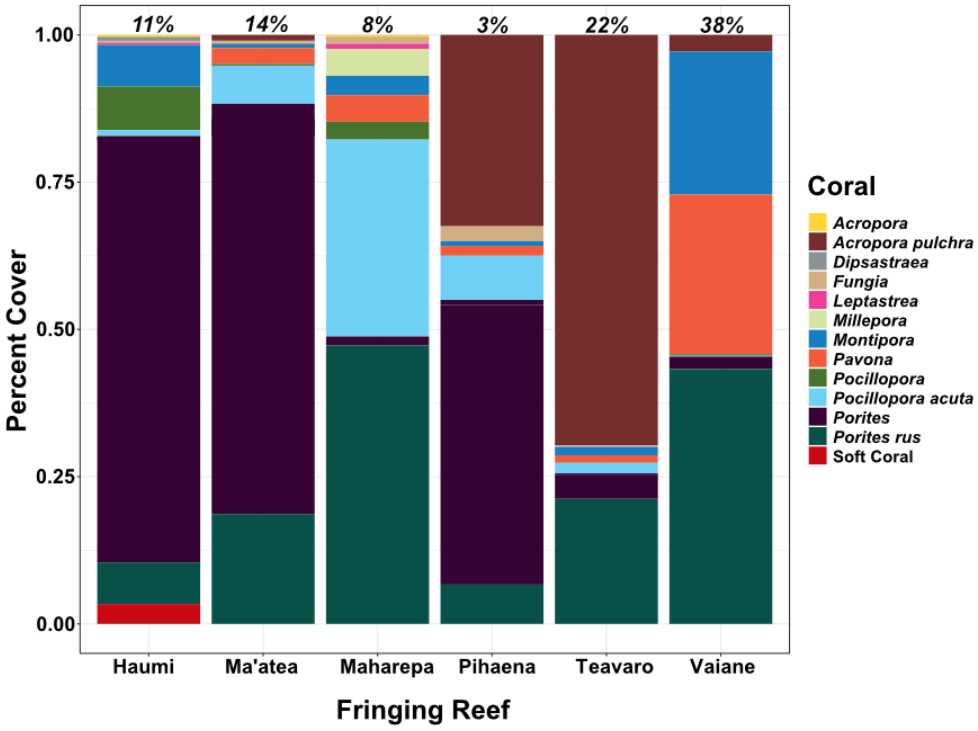

Figure 3. Stacked bar chart of the makeup of coral communities across fringing reef transects by genus or species, when possible. Percent cover on the y-axis is the mean across the entire transect at that site. Percentages at the top of the bars represent total mean cover of all corals at a given site.

Table 1. Summary table of the mean percent cover of primary biotic and abiotic categories across fringing reef transects. The "overall" row is a mean of the category.

	Turf	Macroalgae	Coral	Terrigenous Sediment	Bleached or Dead Coral	CCA/ Hard Substrate	Calciferous Sediment	Other
Haumi	50	29	11	1	1	7	1	1
Ma'atea	25	29	14	26	2	0	0	3
Maharepa	50	21	8	5	6	9	0	1
Pihaena	60	26	3	2	5	1	4	1
Teavaro	46	18	22	3	5	1	3	3
Vaiane	29	2	38	20	6	1	0	5
Overall	43	21	16	9	4	3	1	2

Table 2. Summary table of the mean percent cover of macroalgae genera or category across fringing reef transects. The "overall" row is a mean of the genus or category.

	Porites rus	*Porites*	*Acropora pulchra*	*Pavona*	*Montipora*	*Pocillopora damicornis*	Pocillopora	*Millepora*	Soft Coral	*Fungia*	*Acropora*	*Dipsastrea*
Haumi	1	8	0	0	1	<1	1	0	<1	<1	<1	<1
Ma'atea	3	10	<1	<1	<1	1	<1	0	0	<1	0	0
Maharepa	4	<1	0	<1	<1	3	<1	<1	0	<1	<1	0
Pihaena	<1	1	1	<1	<1	<1	0	0	0	<1	0	0
Teavaro	5	1	15	<1	<1	<1	0	0	0	<1	0	0
Vaiane	17	1	1	10	9	<1	<1	0	0	0	0	0
Overall	5	3	3	2	2	1	<1	<1	<1	<1	<1	<1

Table 3. Summary table of the mean percent cover of coral genera or species across fringing reef transects. The “overall” row is a mean of the genus or species.

	Turbinaria	*Dictyota*	*Padina*	*Halimeda*	Filamentous Green	*Sargassum*	Other Green	Encrusting Red
Haumi	25	0	0	3	1	0	0	<1
Ma’atea	7	17	4	<1	<1	<1	0	0
Maharepa	20	<1	0	<1	<1	0	<1	<1
Pihaena	13	11	<1	1	<1	<1	0	0
Teavaro	9	8	<1	1	<1	<1	0	0
Vaiane	0	2	0	<1	0	0	0	0
Overall	12	6	1	1	<1	<1	<1	<1

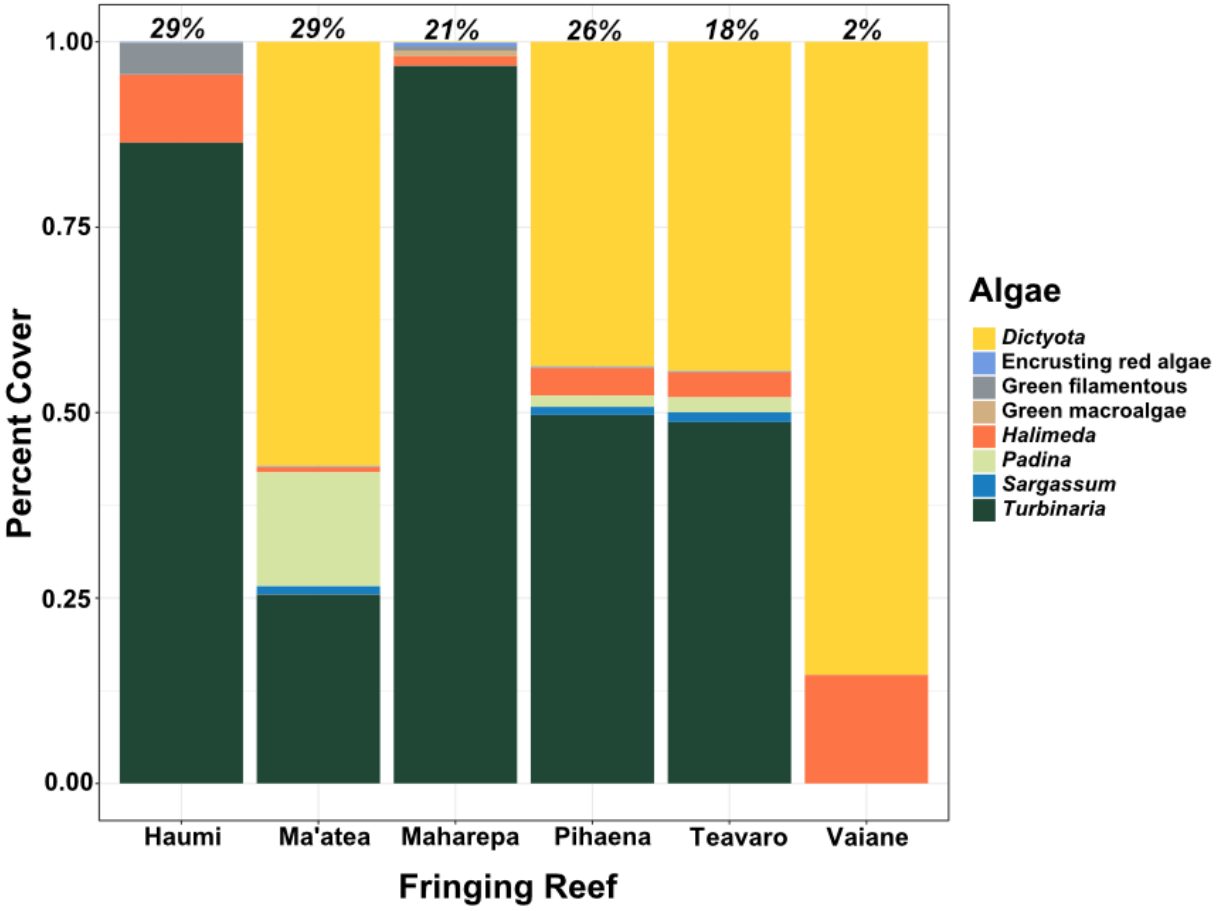

Figure 4. Stacked bar chart of the makeup of macroalgal communities across fringing reef transects by genus. Percent cover on the y-axis is the mean across the entire transect at that site. Percentages at the top of the bars represent total mean cover of all macroalgae at a given site.

mean of 43% (Table 1, Figure 3). There were significant differences in the percent cover of turf between site (ANOVA: f= 11.68, p < 0.001). Ma'atea at 25% and Vaiane at 29% had lower turf cover than the rest of the sites (Tukey: p<0.05), while Pihaena had the highest cover at 60%.

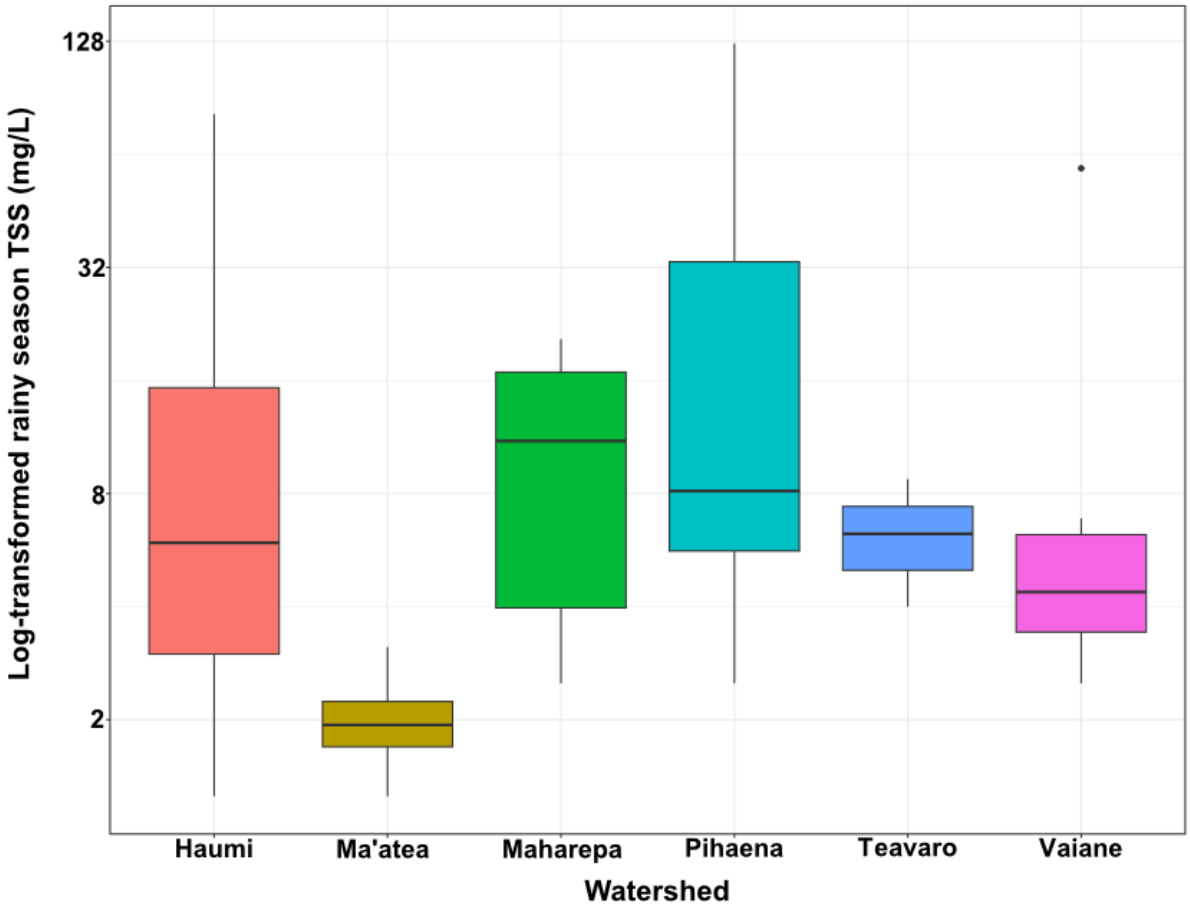

Figure 5. Total suspended solids (TSS) concentrations (mg/L) across sites. Boxes indicate the first and third quartiles; the horizontal line represents the median; and the vertical lines extend to the upper and lower 1.5 times the interquartile range. Note: the y-axis is on a $\log^{10}$ scale.

2. Differences in stream water chemistry across sites

There were no significant differences in TSS among sites (f = 1.31, p = 0.29) (Figure 5) likely as result of the large range in TSS concentrations from a minimum below detection to a maximum of 126 mg/L. Similarly, due to high variability (range

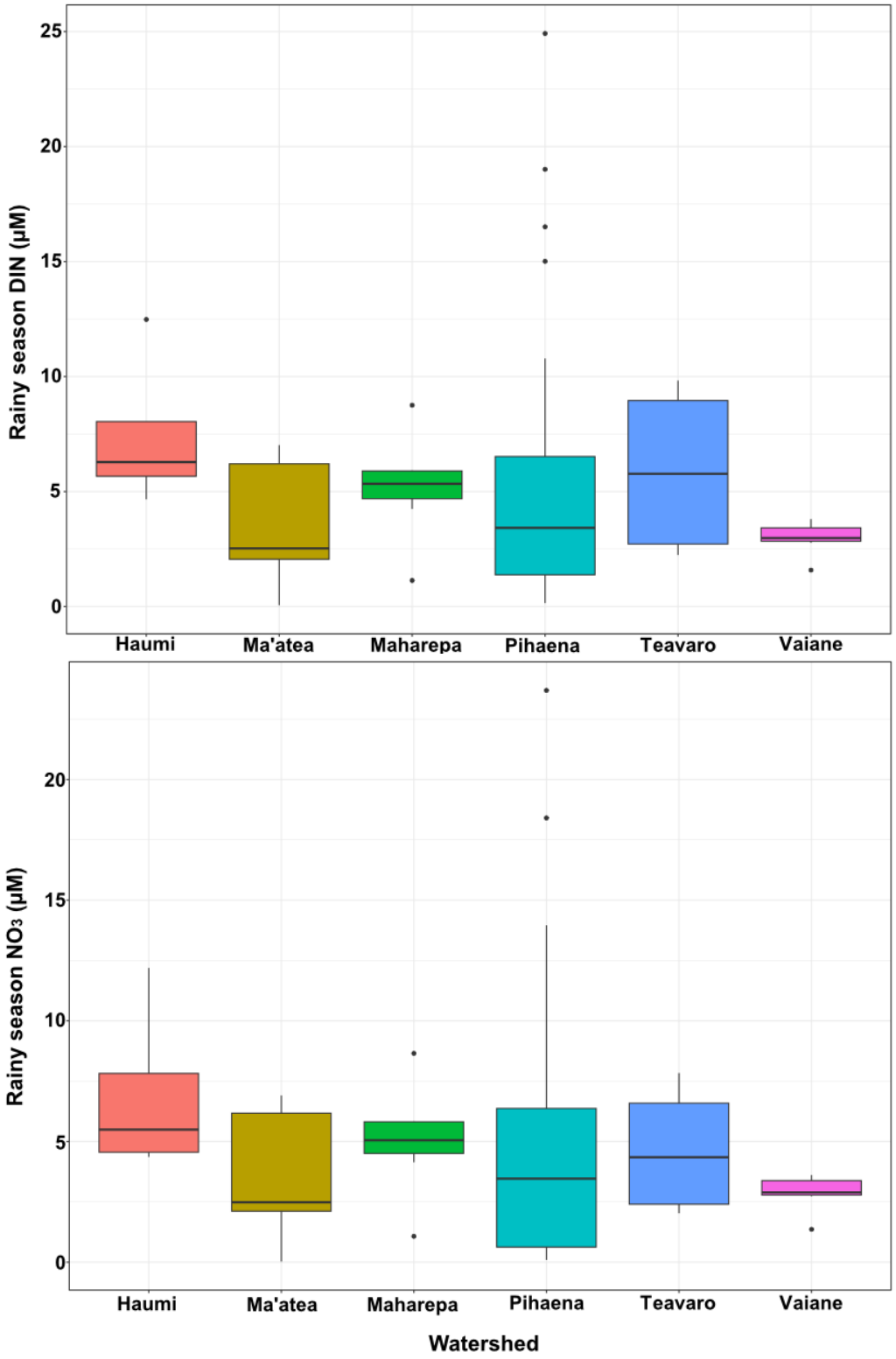

Figure 6. Nitrogen concentrations as total (DIN) and nitrate (NO_3) in micromolar (µM) across sites. Boxes indicate the first and third quartiles; the horizontal line represents the median; and the vertical lines extend to the upper and lower 1.5 times the interquartile range.

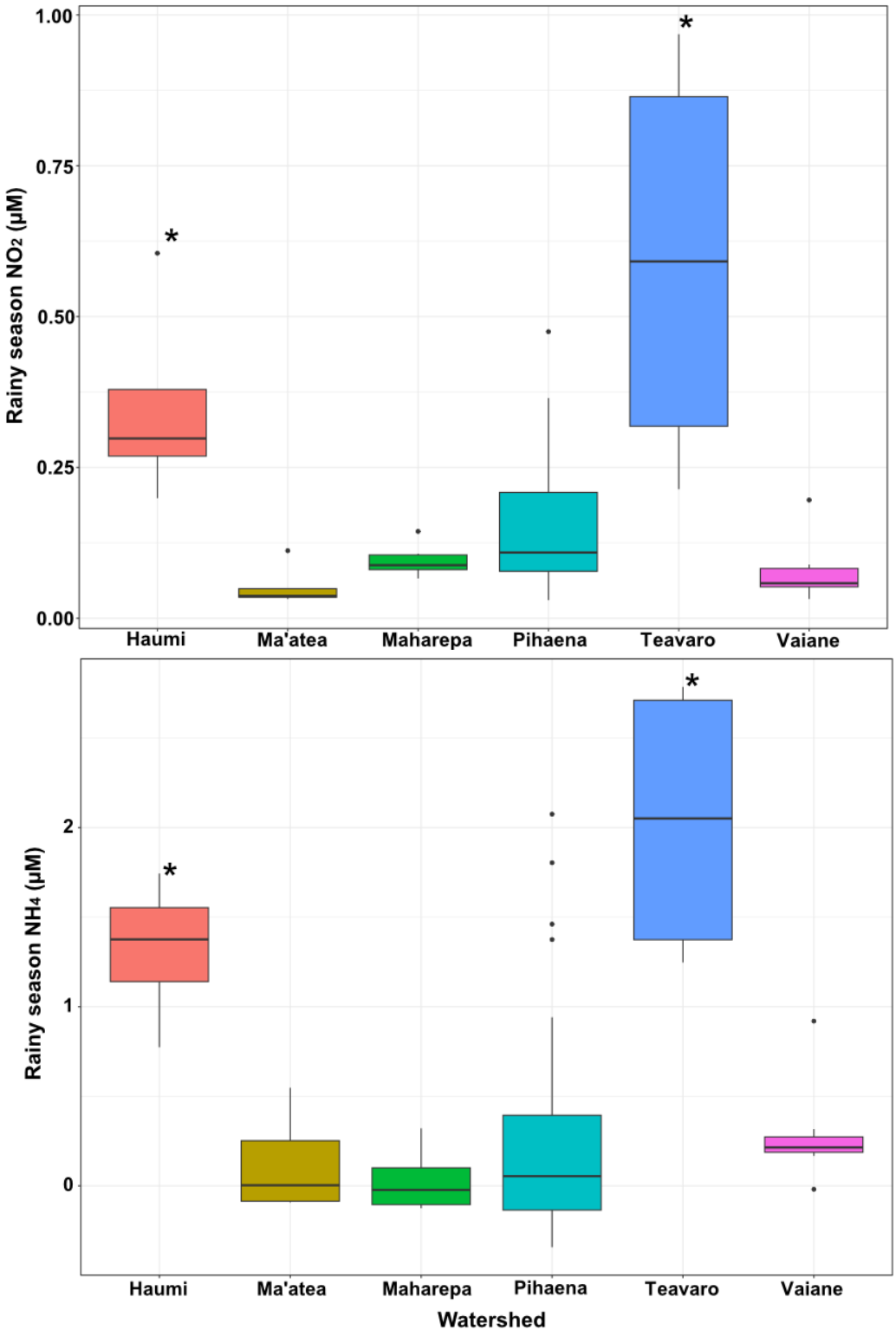

Figure 7. Nitrogen concentrations as nitrate (NO_2) and ammonium (NH_4) in micromolar (µM) across sites. Boxes indicate the first and third quartiles; the horizontal line represents the median; and the vertical lines extend to the upper and lower 1.5 times the interquartile range. Stars indicate sites with significantly higher concentrations ($p<0.05$).

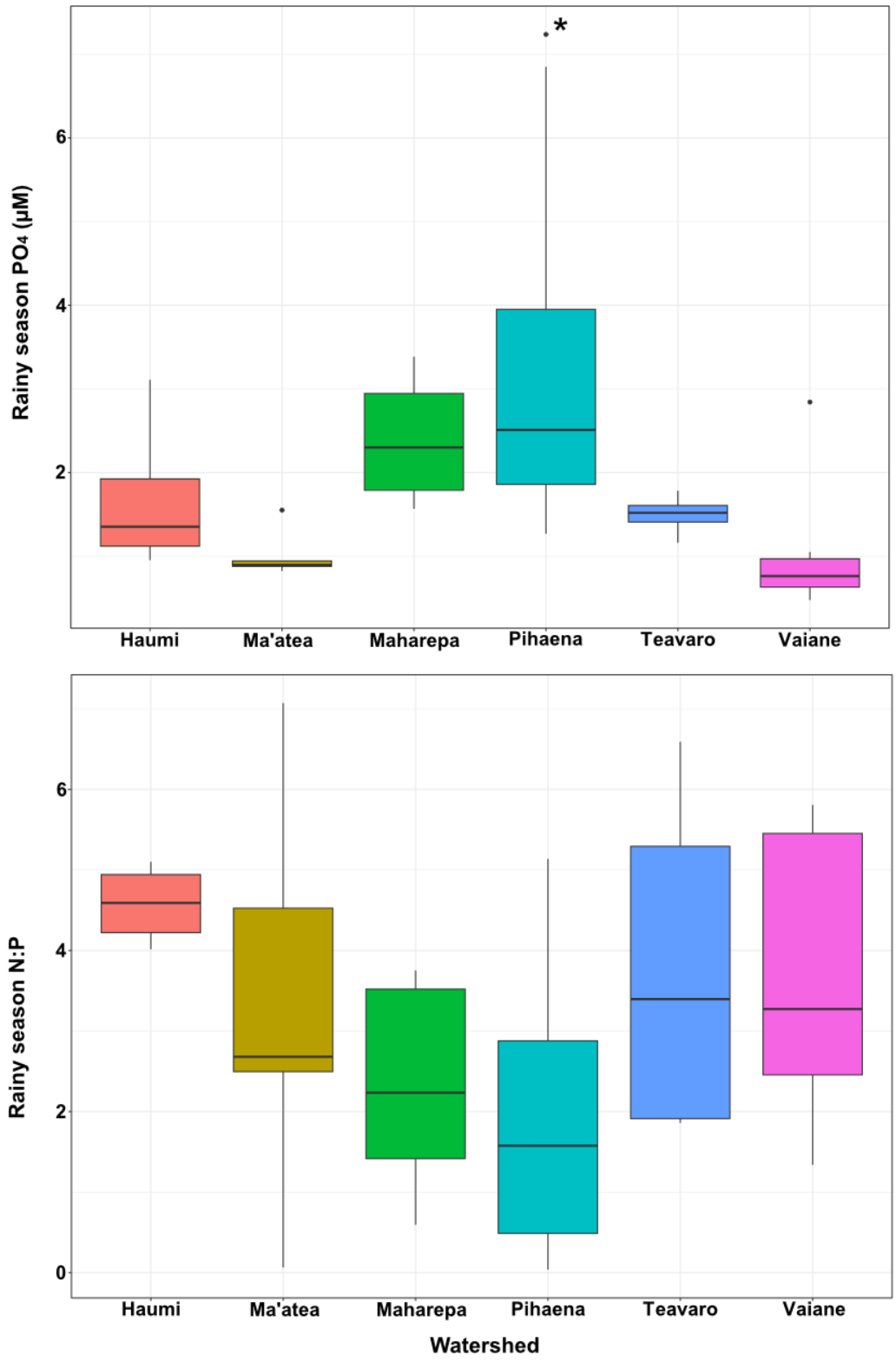

Figure 8. Phosphate (PO_4) concentrations in micromolar (µM) and molar DIN:P ratio across sites. Boxes indicate the first and third quartiles; the horizontal line represents the median; and the vertical lines extend to the upper and lower 1.5 times the interquartile range. Stars indicate sites with significantly higher concentrations ($p<0.05$).

Table 4. Summary table of watershed nutrient and sediment concentrations from bottle samples collected at each watershed across two rainy and two dry seasons. Mean, range and standard deviation of Dissolved Inorganic Nitrogen (DIN = NO_3^- + NO_2^- + NH_4^+) Phosphate (PO_4^{3-}) concentrations are reported in micromolar (µM). The DIN to PO_4^{3-} (N:P) molar ratio is unitless and TSS values are reported in mg/L.

	Dissolved Inorganic Nitrogen (DIN)			Phosphate (PO_4)			N:P Ratio			Total Suspended Solids (TSS)		
Watershed	Mean (µM)	Range (µM)	SD	Mean (µM)	Range (µM)	SD	Mean	Range	SD	Mean (mg/L)	Range (mg/L)	SD
Haumi	11.66	4.67 - 18.71	5.67	1.57	0.95 – 3.11	0.64	7.68	4.02 – 11.97	3.41	12.26	1.25 – 81.88	26.20
Ma'atea	4.62	0.06 - 7.07	2.51	1.17	0.82- 1.63	0.30	2.53	0.07 – 7.07	1.31	2.53	0.50 – 4.00	1.31
Maharepa	5.02	0.86 - 27.37	6.35	2.22	1.57 – 3.39	0.54	2.25	0.41 – 11.37	2.66	7.63	0.00 – 20.63	7.57
Pihaena	5.54	0.15 - 24.92	6.08	3.04	1.27 – 7.24	1.66	1.91	0.04 – 5.14	1.55	29.58	2.50 – 126.25	41.00
Teavaro	10.39	0.22 - 21.15	7.11	1.40	0.19 – 2.38	0.56	7.09	1.11 – 14.37	4.63	5.55	1.00 – 12.50	3.63
Vaiane	3.87	0.05 - 37.72	1.18	1.01	0.48 – 2.84	0.53	4.25	1.34 – 6.14	1.41	8.24	1.00 – 58.75	16.04

of 0.05-37.72 μM) there were no statistically significant differences in DIN across sites (lm: f = 0.81, p = 0.55) (Figure 6). DIN in rivers on Moorea is primarily composed of NO_3- (93% of DIN on average). As such, there were also no significant differences in NO_3- between rivers (lm: f = 0.69, p = 0.63) (Figure 5a). There were differences across sites in NO_2- and NH_4+ as Teavaro and Haumi both had significantly higher NO_2- (f = 12.17, p < 0.001) and NH_4+ (f = 8.8, p < 0.001) than other sites (Figure 5b). Pihaena had significantly higher PO_4^{3-} than other sites (f = 7.75, p = 0.03) (Figure 6). As a result of the high PO_4^{3-} concentrations, Pihaena also had significantly lower N:P ratios than other sites (f = 3.0, p = 0.007) (Figure 6).

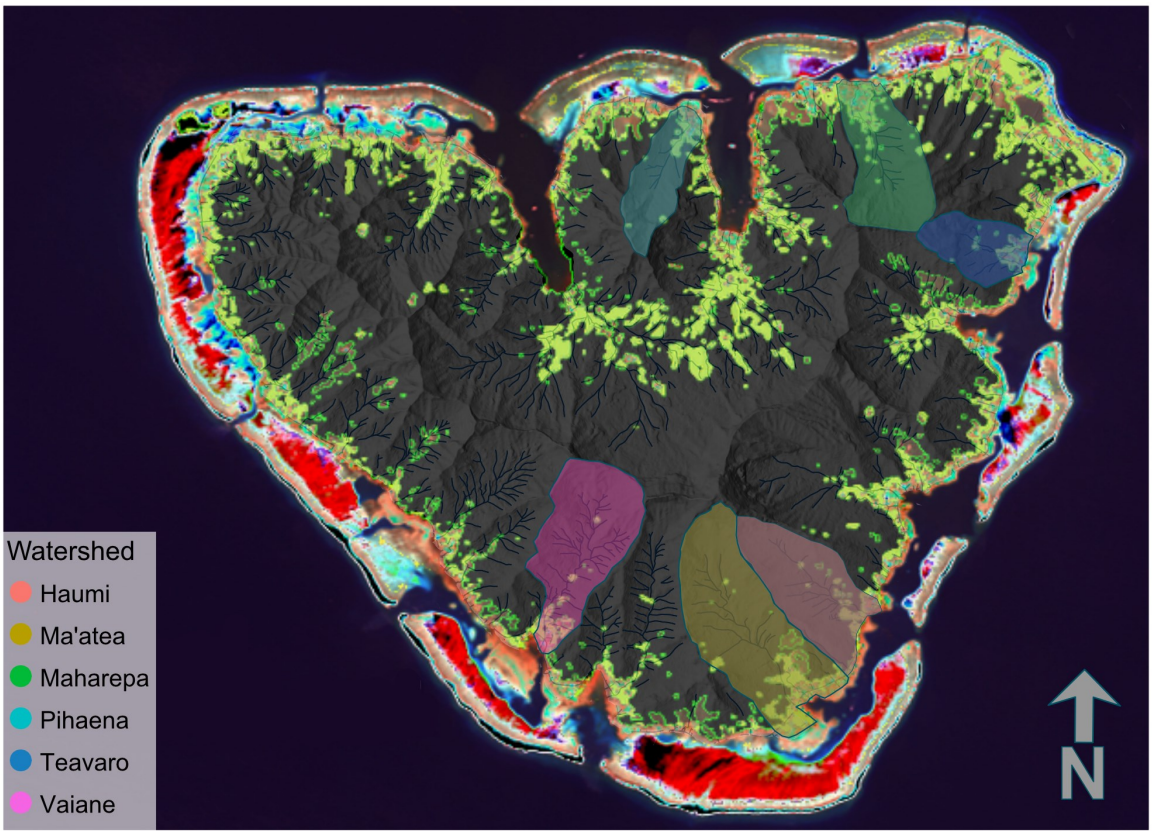

Figure 9. Classification of a Landsat 8 OLI Level 2 image, collected on March 22nd, 2018. Cleared land including agriculture and development is represented in light green and forest in dark green. Red and magenta are masks for reef, while blue is a mask for water.

3. Land-use and population patterns across Moorea

Our analysis of land use focused on the percent cleared land in a watershed estimated using the classification of a Landsat image taken in 2018 (Figure 9). Accuracy assessments indicate that our classifications are accurate for 96% of the image. Of the watersheds adjacent to reefs included in this study, Pihaena had the highest percentage of cleared land (8%) while the lowest percentage was observed in Vaiane (3%) (Table 4). The human population on Moorea was 17,463 residents in 2017. Within the watersheds included in this study, the largest population was located in Maharepa (915 residents) and the smallest in Teavaro (248 residents) (Table 5).

Table 5. Watershed parameters including shore of the island, watershed area and population. Land cover/land use classification percentages by watershed from Landsat 8 imagery of Moorea in 2018 (figure 9). Forested % represents land covered by a majority of trees. Cleared % includes land cleared for agriculture and development.

Watershed	Shore	Area (km^2)	Population	Forest %	Cleared %
Haumi	E	3.7	421	91	5
Ma'atea	E	5.5	582	93	4
Maharepa	N	3.5	915	89	7
Pihaena	N	3.7	705	88	8
Teavaro	E	1.1	248	93	5
Vaiane	W	5.8	371	95	3

4. Relationships between benthic cover and river and watershed characteristics

Mean coral cover on a reef was negatively correlated with the percentage area of cleared land in the adjacent watershed ($p = 0.02$, tau = -0.87) (Figure 10). Coral cover was not significantly correlated to population within a watershed ($p = 0.14$, tau = -0.6) or riverine DIN ($p = 0.47$, tau = -0.33), TSS ($p = 0.47$, tau = -.033), or N:P ($p = 0.27$, tau = 0.47). There was non-significant negative relationship be-

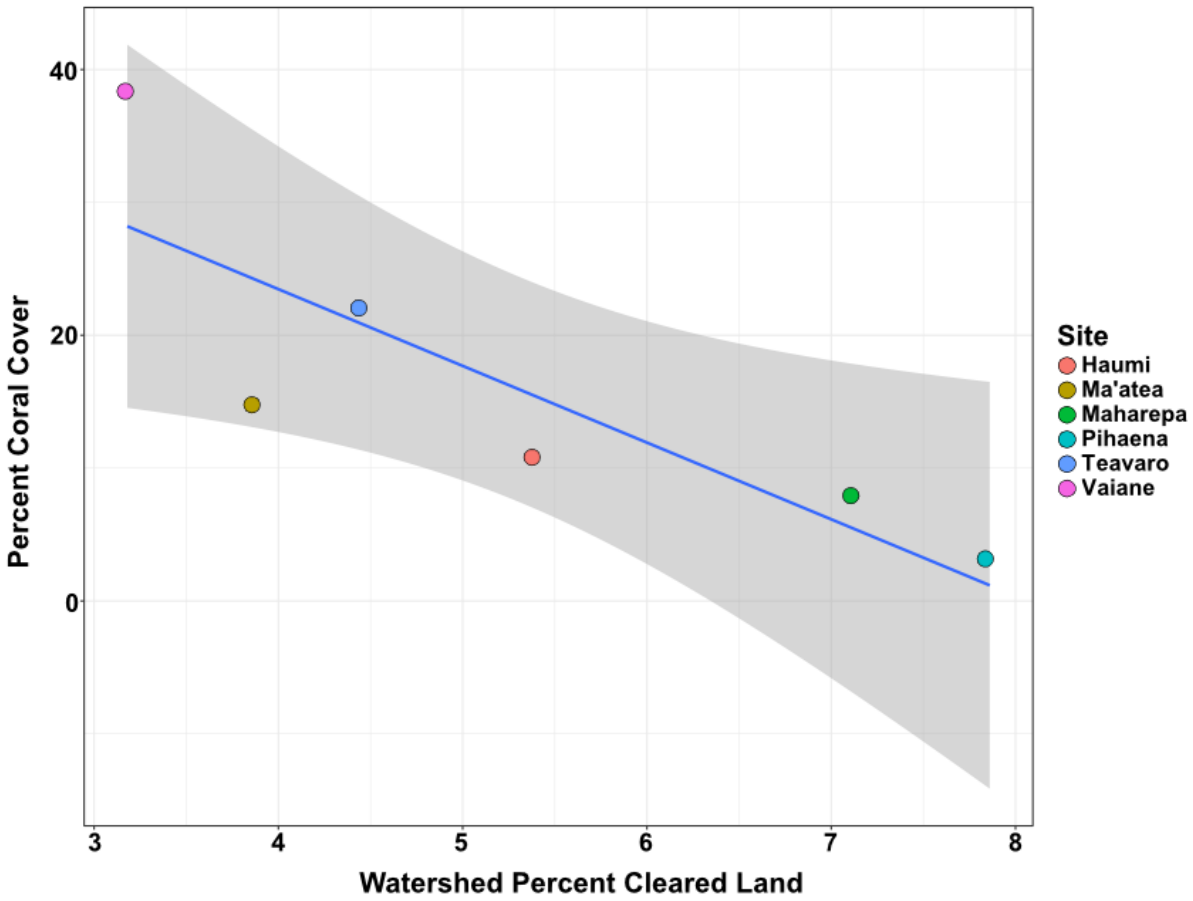

Figure 10. Linear model examining the relationship between the percent of a watershed that has been cleared of trees for agriculture or development and the percent cover of coral on the adjacent fringing reef. Grey shading represents the 95% confidence interval. Multiple $r^2 = 0.72$, adjusted $r^2 = 0.65$, $p = 0.03$.

tween coral cover and riverine phosphate concentrations (p = 0.056, tau = 0.73). At the reef scale, there were no correlations between macroalgal cover and watershed population (p = 1, tau = 0.07), cleared land percentage (p = 0.47, tau = 0.33), or riverine DIN (p = 0.47, tau = 0.33), PO4 (p = 0.72, tau = 0.2), N:P (p = 1, tau = 0.07), or sediment concentrations (p = 1, tau = 0.07).

5. Relationships between benthic community composition and river and watershed characteristics

There were significant differences in benthic community composition across

sites (PERMANOVA: f = 11.57, p = 0.001). The NMDS stress was 0.14, below the 0.2 threshold commonly used in ecological studies to test model fit (Zuur et al., 2007). The non-metric fit of the ordination was r^2= 0.98 and the linear fit was r^2 = 0.91. To evaluate reef community loadings in the NMDS, we divided the ordination plot into four quadrants (Figure 11). The top-left quadrant (1) is largely empty with algae genera *Turbinaria* and *Halimeda* loading close to the MDS2 axis, and the coral genera *Porites* loading close to the MDS1 axis. The top-right quadrant (2) includes terrigenous sediment, coral buried by sediment, and algae in the genus *Dictyota*. The bottom-right quadrant (3) contains *Porites rus*, and corals only observed in high percentages at select sites including *Montipora sp., Pavona sp.,* and at in the bottom right corner *Acropora pulchra*. The bottom left quadrant (4) is characterized primarily by turf algae and CCA/hard substrate, with numerous lesser observed corals such as *Pocillopora acuta* recorded as living bleached and dead. Points from the Haumi and Maharepa transects cluster in quadrants 1 and 4, around where *Turbinaria*, CCA/hard substrate and turf have loaded (figure 11). Pihaena's points are more dispersed, but also loaded primarily in quadrants 1 and 4. The points representing Ma'atea loaded across quandrants 4, 1 and 2, with the bulk of the points from farther along the transect loading in quadrant 2 where *Dictyota* and terrigenous sediment are loaded. Vaiane was dispersed primarily across quadrant 3 where *Monitpora, Pavona,* dead coral, and coral rubble loaded. Teavaro's point were concentrated in the bottom right corner of quadrant three where *Acopora pulchra* loaded, demonstrating how this site stands alone in its association with this coral.

Of the river chemistry variables tested in the analysis, all but N:P (r^2=0.01, p=0.7), were significantly correlated with the distribution of sites in the ordination

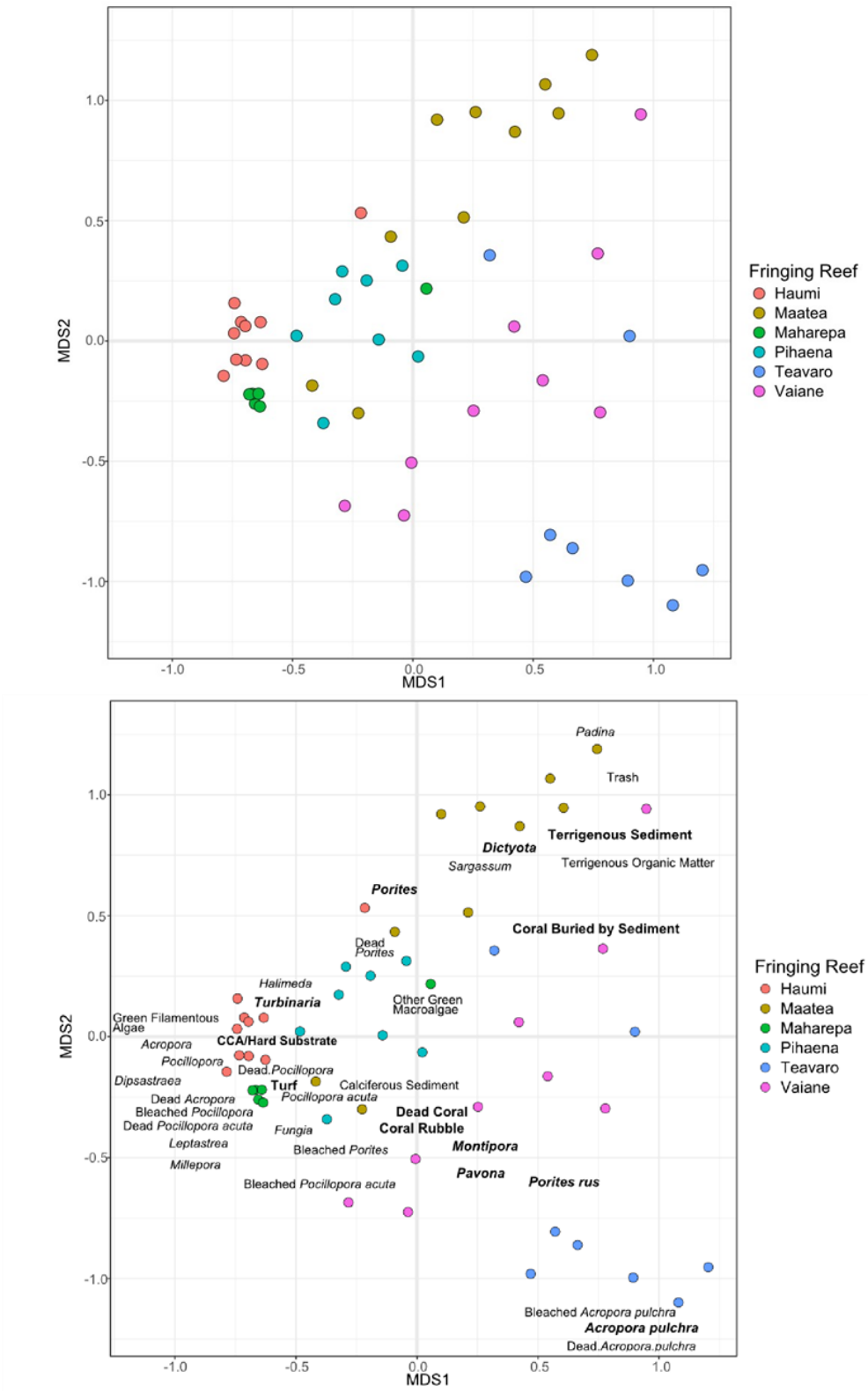

Figure 11. Nonmetric multidimensional scaling (NMDS) results of benthic community surveys. Each point represents the combined benthic community from six photoquadrats. The color of the point indicates the site. The benthic categories are written and the location of the word signifies the centroid for that category. Bold labels indicate categories that represent > 5% benthic cover of at least one site

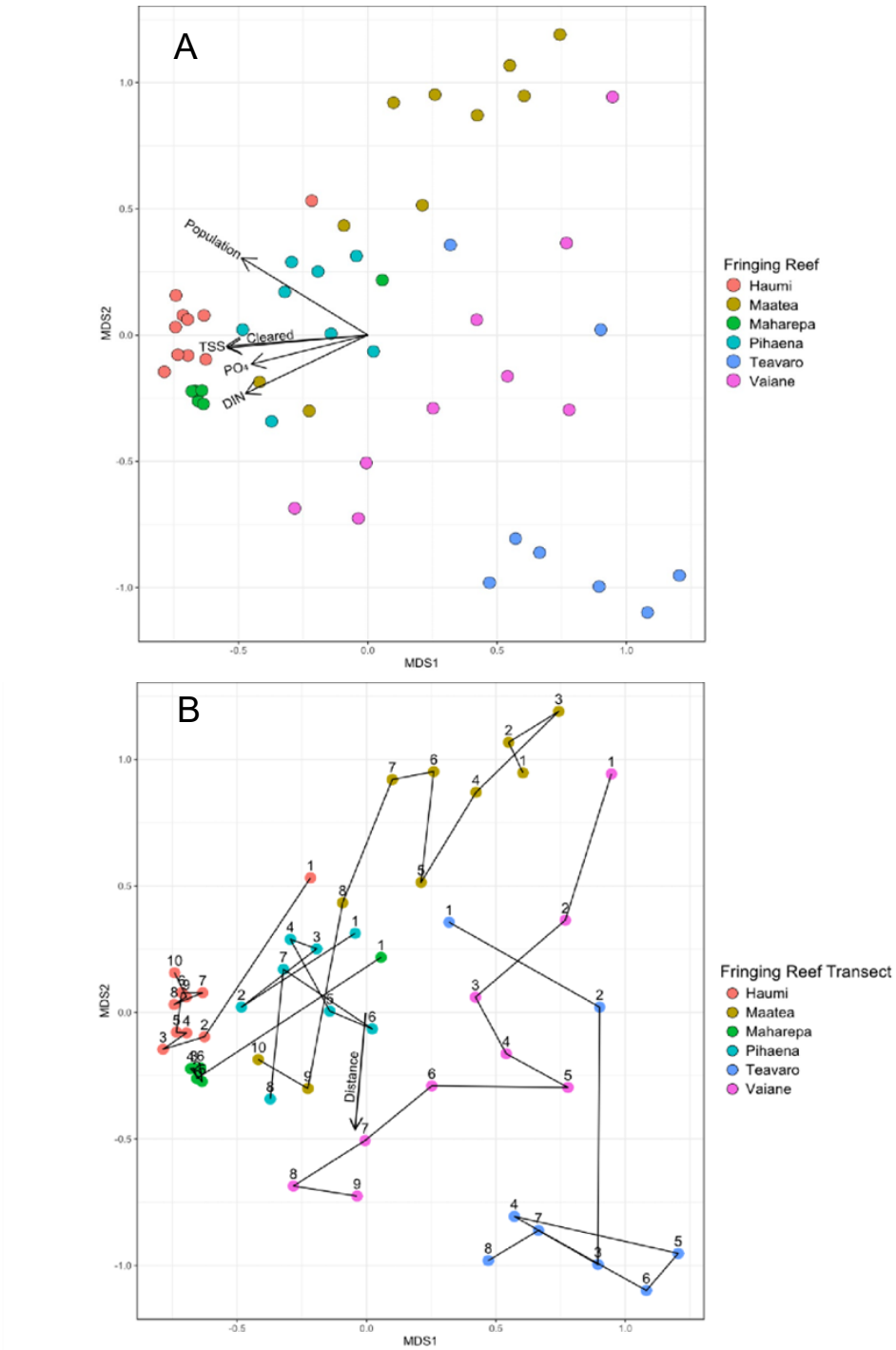

Figure 12. Nonmetric multidimensional scaling (NMDS) results of benthic community surveys. Each point represents the combined benthic community from six photos while the color of the point indicates the site. Arrows in (A) represent significant ($p<0.05$) correlations between benthic community composition and stream chemistry and watershed parameters; the length of arrow represents the relative strength of the correlation. The numbers at each point in (B) show the order of the points along the transect with 1 indicating the closest to the river mouth. The arrows in (B) represents a significant ($p<0.05$) correlation between benthic community composition and distance from the beginning of the transect. The length of arrow represents the relative strength of the correlation.

(Figure 12a). TSS was most strongly correlated with the benthic communities in ordination space (r^2=0.30, p=0.001), followed by DIN (r^2=0.28, p=0.001), and PO_4^{3-} (r^2=0.22, p=0.001). The watershed variables population and percent cleared land were also significantly correlated with the partitioning of the benthic communities in the ordination (r^2=0.33, p=0.001 and r^2=0.30 p=0.001, respectively), as was distance from the start of the transect (r^2=0.21, p=0.004). River chemistry and watershed vectors tend to point along the MDS 1 axis, while distance tends to point along the MDS2 axis. This indicates that the spread of points along the first axis is more related to river and watershed parameters, while spread along the second ax-

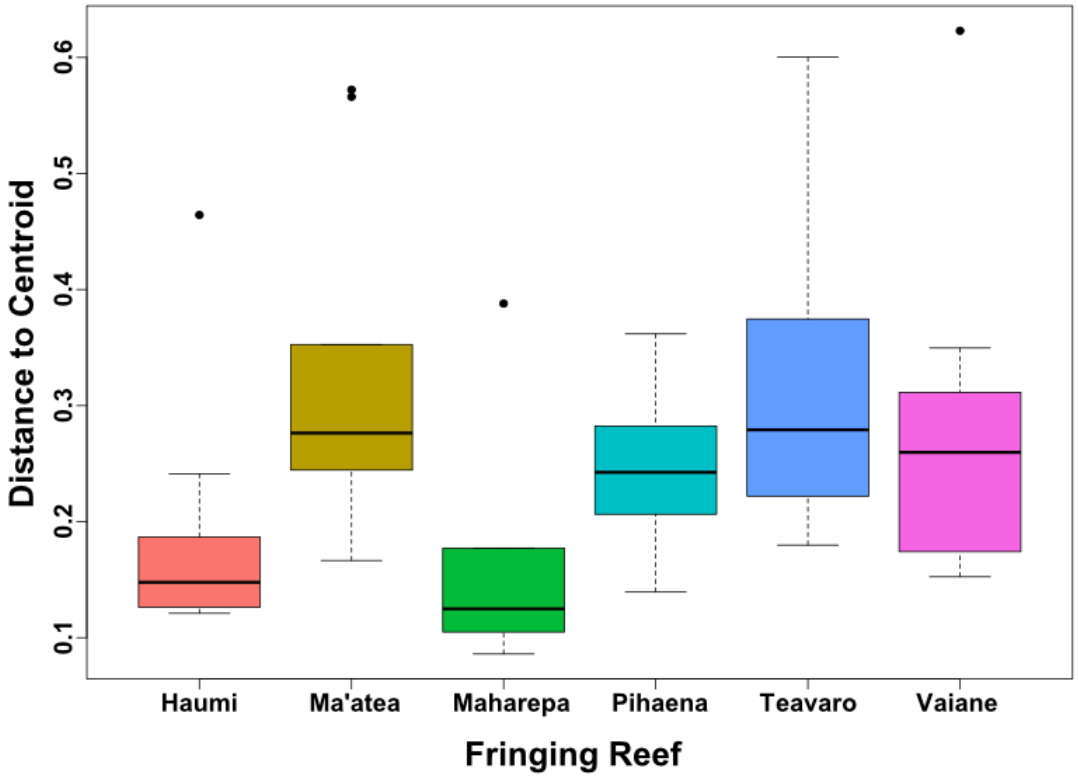

is ***Figure 13.*** Box plot of the non-euclidean distance calculated between each point of a fringing reef transect to the centroid of the site in the NMDS ordination space (figures 11 & 12). is Boxes indicate the first and third quartiles; the horizontal line represents the median; and the vertical lines extend to the upper and lower 1.5 times the interquartile range. Larger distances between points and the centroid on a transect indicate greater dispersion of points and greater heterogeneity in the community at that site. ANOVA: f = 2.46, p = 0.05

more related to distance from the river mouth. The distribution of the vectors of the river and watershed characteristics suggests that higher DIN, PO_4^{3-}, and TSS in streams, and higher watershed populations land clearing, are associated with reef communities like those found in Haumi and Maharepa which are characterized by turf, CCA/hard substrate, and *Turbinaria*. Conversely, lower runoff exposure and lower watershed population is associated a wider range of algae genera and more coral cover, such as the communities featuring abundant corals such as *Pavona* and *Acropora pulchra* found in Vaiane and Teavaro.

In addition to river and watershed characteristics correlating with benthic community composition, there was also a significant correlation between distance away from the river mouth and benthic communities (Figure 12b). Increasing distance away from the river appeared to correlate with increasing coral cover, though the coral genera at more distant points was quite variable across sites. Further, there appeared to be strong differences across sites in terms of how much change there was in the benthic communities with increasing distance away from the river mouths. For example, benthic communities appeared to change substantially across distance at sites such as Teavaro and Vaiane while sites such as Haumi and Maatea showed little change (Figure 13). When we tested for these differences quantitatively, an ANOVA indicated that there were significant differences between sites ($f = 2.46$, $p = 0.05$). Sites such as Teavaro, Vaiane, and Ma'atea had higher dispersion of communities across increasing distance from the river mouth resulting in more heterogeneity across the transect while sites such as Haumi, Maharepa, and Pihaena showed lower levels of dispersion among distances suggesting that the benthic communities at these sites were much more homogeneous even at increasing distances from the river mouths.

D. Discussion:

By integrating data from water quality monitoring in rivers, surveys of coral reef communities, and remote sensing, we show that coral cover and community structure on fringing reefs around Moorea are negatively impacted by human activity in adjacent watersheds. We found that coral cover has a significant negative relationship with the percent area of land cleared for development or agriculture in nearby watersheds (figure 10). Using ordination analysis, we found that land use, watershed population, as well as riverine nutrient and sediment concentrations influence the structure of reefs communities both between and within sites (figures 11 and 12). Reefs experiencing lower anthropogenic stress from land use and runoff were characterized by corals in the genera *Montipora* and *Pavona*, as well as the species *Porites rus and Acropora pulchra* (figure 11). These sites were also more heterogeneous with considerably different communities at the beginning and end of the transects, often with more coral-dominated areas at increasing distance from the river mouth (figure 12b). In contrast, reefs adjacent to watersheds with more land clearing, higher populations and elevated riverine sediment and nutrient concentrations were characterized by benthic communities dominated by the macroalga *Turbinaria ornata*, turf algae, and dead branching corals (figure 11). Reef communities at these sites were also more homogenous along the transect with less turnover in the benthic community and often less coral even in areas the most distant from the river mouth (figure 12b).

Our findings in Moorea are similar to others from high tropical islands demonstrating that watershed development can negatively impact nearshore coral reefs (reviewed in Tanaka et al. 2021). In a larger survey of most of the major rivers

on Moorea, rivers in watersheds with more cleared land had significantly higher nutrient and sediment concentrations than rivers associated with less land clearing (Neumann chp 2). Studies from Guam and American Samoa found that DIN concentrations in rivers above 0.1 μM in 20% of samples were associated with altered reef communities (Houk et al. 2020 & 2022). All of the rivers on Moorea sampled in this study were consistently above those levels, suggesting that the negative impacts of riverine nutrients and sediments on fringing reefs are likely widespread across the island. In fact, an island-wide study of nutrient enrichment patterns across Moorea showed that fringing reefs are consistently enriched in nitrogen around the island and that these patterns have likely existed for a decade or more (Adam et al., 2021). Time series data from Moorea have shown that some reefs in the lagoon have seen declines in coral and increases in algae (Moritz et al. 2021, Adam et al. 2021), with reefs exposed to higher nutrient levels being especially vulnerable to the loss of corals (Adam et al. 2021).

We also found that multiple stressors may influence reef communities, resulting in more homogeneous community composition even at significant distances away from the river mouths, based on the ordination analyses. Though we did not find significant individual relationships between overall coral cover and riverine DIN or TSS concentrations, our ordination analyses suggested cumulative effects of these multiple stressors on benthic community composition. For example, both DIN and TSS were correlated with benthic communities at sites that were associated with more macroalgae, more dead coral, and less live coral. In addition, the sites that were strongly correlated with DIN and TSS, such as Maharepa and Haumi, showed increased homogeneity in community composition even at distances farther from the river mouth, suggesting that the impacts of riverine output spread a

farther distance than at sites with less harmful riverine input such as Teavaro and Vaiane. This finding aligns with those of other studies that found reduced coral cover and reduced reef diversity in areas exposed to elevated nutrient and sediment concentrations (Darling et al. 2019). Although both sediment and nutrients can have harmful direct effects on corals in isolation (reviewed in Nalley 2023, D'Angelo and Wiedenmann 2014, Donovan et al. 2020, Junjie et al. 2014), they may act as synergistic rather than additive stressors, meaning the presence of both has a greater impact that would be predicted based on the effect of each alone (Ban et al. 2013, Fabricius 2010). Cumulative effects of these multiple stressors may be complex, and impacts are likely driven by both exposure concentrations, as well as the duration of exposure (Darling and Coté 2008). Combined nutrient enrichment and sedimentation can catalyze new or reinforce existing shifts in reefs from a coral-dominated to macroalgae- and turf-dominated state (Fabricius 2010, Darling et al. 2019).

In addition to lower overall coral cover at sites in watersheds with higher levels of land clearing, we found a shift in the community composition at these sites. At reefs with higher runoff, we found a higher abundance of macroalgae and massive *Porites* spp. Massive *Porites* spp. may be the most abundant corals at these reefs as they are often some of the more tolerant species to elevated turbidity (Fabricius, 2010) as well as being less impacted by nutrient pollution (Burkepile et al., 2020). Further, massive *Porites* spp. appear minimally affected even when subjected to combined sedimentation and nutrient enrichment (Rice et al. 2021). In contrast, *Pavona* and *Montipora*, which other studies have shown to be more susceptible to sedimentation and/or nutrient pollution (McClanahan and Obura,1997, Fabricius et al. 2013, Golbuu et al. 2008) were generally rare (< 1% cover) across all reef sites.

The one exception was Vaiane which had ~10% cover of each these genera while also having the lowest amount of land clearing and the second lowest population as well as the lowest mean DIN and TSS concentrations.

Another important finding was that some sites with high DIN also had high coral cover and coral taxa not observed at other sites. The reef at Teavaro was an important example as it had one of the highest levels of overall coral cover and the coral community was dominated by the fast-growing coral *Acropora pulchra*, which was rare at all other sites. However, approximately a third of the DIN at Teavaro was ammonium. This distinction is meaningful because corals enriched with ammonium often have increased coral growth (Szmant, 2002, Shantz and Burkepile 2014) and calcification (Ezzat et al. 2016) as well as reduced susceptibility to thermal stress (Fernandes de Barros Marangoni, et al., 2020). This effect of ammonium on corals is in contrast to recent experiments showing that corals experiencing high levels nitrogen in the form of nitrate can show impaired physiological performance (Ezzat et al. 2015), reduced growth rates (Shantz and Burkepile 2014), and increased bleaching susceptibility and mortality (Burkepile et al. 2020). This negative impact of nitrate on corals is likely one reason that most reef sites with high values of nitrate, which represented the majority of DIN, had low coral cover, especially at distances closer to river mouths.

Surprisingly, we did not find positive relationships between high nutrient values in riverine input and macroalgal abundance, despite considerable literature indicating that nutrient enrichment enhances macroalgal growth (Schaffelke and Klumpp 1998, Larned 1998) and leads to negative effects of macroalgal competition on corals (Zaneveld et al. 2016). However, sites with higher levels of nutrients also likely had higher levels of TSS, and sedimentation often has negative impacts

on the growth, survival, and recruitment of macroalgae (Umar et al. 1998, Eriksson and Johansson 2005, Cannon et al. 2023). We did find a positive relationship between nitrate concentrations and turf algal cover. The negative effects of sedimentation on both corals and macroalgae can mean that, filamentous turf algae, rather than corals or macroalgae, often dominate turbid, inshore reefs (Santana et al. 2023). In fact, as anthropogenic stressors such as nutrient pollution and sedimentation increasingly impact reefs, the degraded ecosystem state may be represented by a transition away from dominance by corals to dominance by turf algae rather than dominance by macroalgae (Tebbett et al. 2021).

One limitation of this study is that we did not measure discharge or mass flux of nutrients and sediment from watersheds. It is possible that larger watersheds with lower concentrations of DIN or TSS are exporting more total nitrogen or sediment due to a higher discharge rate relative to a smaller watershed with higher DIN or TSS concentrations. For example, Teavaro is the smallest watershed included in this study at 1.1 km^2, but has the second highest mean DIN concentration (10.4 µM). Yet, Teavaro had some of the highest coral cover at 22% as opposed to Ma'atea which had a mean coral cover of 14% but had DIN values that were nearly half that of Teavaro. Importantly, the Ma'atea watershed is 5x larger at 5.5 km^2 and as larger watersheds tend to have higher river discharge (Zhou et al. 2012), it is likely that Ma'atea has a higher mass flux of nitrogen and TSS per year than Teavaro. It may be that the flux of nutrients and sediment is a more accurate predictor of coral cover on benthic communities than are concentrations of nutrients and sediment. Future work in Moorea and other tropical rivers should focus on the development of watershed models to quantify the extent and timing of nutrient and sediment fluxes to nearshore coral reefs in order to better predict the impact of land use

on these nearshore ecosystems.

Examining the linkages between land and sea is critical to understanding the functioning and future of nearshore coral reefs in the Anthropocene. Here, we have shown that anthropogenic impacts to land use and the resulting impacts on riverine water quality is related to reduced coral cover and altered benthic communities on fringing reefs in Moorea, French Polynesia. Although human development of island resources is a critical component to growing tropical economies (Darling et al. 2019, Wenger et al. 2020), our work joins a growing body of literature showing that the economic benefits may come at a cost to ecological functions and services of nearshore coral reefs (Loiseau et al. 2021, Wenger et al. 2020). Importantly, we show that data from Landsat imagery may be as useful as intensive, *in situ* sampling of river water quality in terms of correlating with the benthic community composition of nearshore coral reefs. Thus, relying on estimates of land use and land clearing from satellite imagery may be useful for predicting impacts to nearshore coral reefs in areas where collecting *in situ* data in watersheds are logistically challenging. Ultimately, helping to ameliorate impacts of current land use on river runoff and ensuring new development is planned around minimizing impacts to rivers will help ensure the health and function of nearshore coral reefs.

Support and Funding:

Credit to Benoit Espiau at CRIOBE for his meticulous nutrient analyses. Particular mention to Corinne Fuchs, Kyla Pierce, Maya Gorgas and the members of ‘Ati Vai for their assistance collecting, processing and analyzing samples. Thank you to the staff of the Richard B. Gump station for all of the work solving logistical, administrative and mechanical issues. We could not have done this work without you.

Funding for this research was provided by the NSF GRFP program, NSF Career grant OCE—1547952, NSF grant MCR—1637396, The Schmidt Family Foundation, and The Worster Summer Research Fellowship. Funding for education and outreach related to this work was provided by the ASLO Global Outreach Initiative.

F. Citations

About ArcGIS | Mapping & Analytics Software and Services [WWW Document], n.d. URL https://www.esri.com/en-us/arcgis/about-arcgis/overview (accessed 8.25.23).

Acevedo, R., Morelock, J., Olivieri, R.A., 1989. Modification of Coral Reef Zonation by Terrigenous Sediment Stress. PALAIOS 4, 92–100. https://doi.org/10.2307/3514736

Adam, T.C., Burkepile, D.E., Holbrook, S.J., Carpenter, R.C., Claudet, J., Loiseau, C., Thiault, L., Brooks, A.J., Washburn, L., Schmitt, R.J., 2021. Landscape-scale patterns of nutrient enrichment in a coral reef ecosystem: implications for coral to algae phase shifts. Ecological Applications 31, e2227. https://doi.org/10.1002/eap.2227

Albert, S., Deering, N., Tongi, S., Nandy, A., Kisi, A., Sirikolo, M., Maehaka, M., Hutley, N., Kies-Ryan, S., Grinham, A., 2021. Water quality challenges associated with industrial logging of a karst landscape: Guadalcanal, Solomon Islands. Marine Pollution Bulletin 169, 112506. https://doi.org/10.1016/j.marpolbul.2021.112506

Babcock, R., Davies, P., 1991. Effects of sedimentation on settlement of Acropora millepora. Coral Reefs 9, 205–208. https://doi.org/10.1007/BF00290423

Ban, S.S., Graham, N.A.J., Connolly, S.R., 2014. Evidence for multiple stressor interactions and effects on coral reefs. Global Change Biology 20, 681–697. https://doi.org/10.1111/gcb.12453

Bartley, R., Bainbridge, Z.T., Lewis, S.E., Kroon, F.J., Wilkinson, S.N., Brodie, J.E., Silburn, D.M., 2014. Relating sediment impacts on coral reefs to watershed sources, processes and management: A review. Science of The Total Environment 468–469, 1138–1153. https://doi.org/10.1016/j.scitotenv.2013.09.030

Binet, T., Gonnot, C., 2005. Etude de l'érosion sur des plantations d'ananas à Moorea (Polynésie française). https://doi.org/10.13140/RG.2.1.4944.2806

Box, S.J., Mumby, P.J., 2007. Effect of macroalgal competition on growth and survival of juvenile Caribbean corals. Marine Ecology Progress Series 342, 139–149. https://doi.org/10.3354/meps342139

Brodie, J., Wolanski, E., Lewis, S., Bainbridge, Z., 2012. An assessment of residence times of land-sourced contaminants in the Great Barrier Reef lagoon and the implications for management and reef recovery. Marine Pollution Bulletin, The Catchment to Reef Continuum: Case studies from the Great Barrier Reef 65, 267–279. https://doi.org/10.1016/j.marpolbul.2011.12.011

Browne, N.K., Precht, E., Last, K.S., Todd, P.A., 2014. Photo-physiological costs associated with acute sediment stress events in three near-shore turbid water corals. Marine Ecology Progress Series 502, 129–143. https://doi.org/10.3354/meps10714

Burkepile, D.E., Link to external site, this link will open in a new window, Shantz, A.A., Adam, T.C., Munsterman, K.S., Speare, K.E., Ladd, M.C., Rice, M.M., Leïla, E., Shelby, M., Y, W.J.C., Baker, D.M., Brooks, A.J., Schmitt, R.J., Holbrook, S.J., 2020. Nitrogen Identity Drives Differential Impacts of Nutrients on Coral Bleaching and Mortality. Ecosystems 23, 798–811. https://

doi.org/10.1007/s10021-019-00433-2

Cannon, S.E., Donner, S.D., Liu, A., González Espinosa, P.C., Baird, A.H., Baum, J.K., Bauman, A.G., Beger, M., Benkwitt, C.E., Birt, M.J., Chancerelle, Y., Cinner, J.E., Crane, N.L., Denis, V., Depczynski, M., Fadli, N., Fenner, D., Fulton, C.J., Golbuu, Y., Graham, N.A.J., Guest, J., Harrison, H.B., Hobbs, J.-P.A., Hoey, A.S., Holmes, T.H., Houk, P., Januchowski-Hartley, F.A., Jompa, J., Kuo, C.-Y., Limmon, G.V., Lin, Y.V., McClanahan, T.R., Muenzel, D., Paddack, M.J., Planes, S., Pratchett, M.S., Radford, B., Reimer, J.D., Richards, Z.T., Ross, C.L., Rulmal Jr., J., Sommer, B., Williams, G.J., Wilson, S.K., 2023. Macroalgae exhibit diverse responses to human disturbances on coral reefs. Global Change Biology 29, 3318–3330. https://doi.org/10.1111/gcb.16694

Classification [WWW Document], n.d. URL https://www.l3harrisgeospatial.com/docs/Classification.html#ClassSupervised (accessed 7.23.23).

Collin, A., Hench, J.L., Pastol, Y., Planes, S., Thiault, L., Schmitt, R.J., Holbrook, S.J., Davies, N., Troyer, M., 2018. High resolution topobathymetry using a Pleiades-1 triplet: Moorea Island in 3D. Remote Sensing of Environment 208, 109–119. https://doi.org/10.1016/j.rse.2018.02.015

Correll, D.L., 1998. The Role of Phosphorus in the Eutrophication of Receiving Waters: A Review. Journal of Environmental Quality 27, 261–266. https://doi.org/10.2134/jeq1998.00472425002700020004x

D'Angelo, C., Wiedenmann, J., 2014. Impacts of nutrient enrichment on coral reefs: new perspectives and implications for coastal management and reef survival. Current Opinion in Environmental Sustainability, Environmental change issues 7, 82–93. https://doi.org/10.1016/j.cosust.2013.11.029

Darling, E.S., Côté, I.M., 2008. Quantifying the evidence for ecological synergies. Ecology Letters 11, 1278–1286. https://doi.org/10.1111/j.1461-0248.2008.01243.x

Darling, E.S., McClanahan, T.R., Maina, J., Gurney, G.G., Graham, N.A.J., Januchowski-Hartley, F., Cinner, J.E., Mora, C., Hicks, C.C., Maire, E., Puotinen, M., Skirving, W.J., Adjeroud, M., Ahmadia, G., Arthur, R., Bauman, A.G., Beger, M., Berumen, M.L., Bigot, L., Bouwmeester, J., Brenier, A., Bridge, T.C.L., Brown, E., Campbell, S.J., Cannon, S., Cauvin, B., Chen, C.A., Claudet, J., Denis, V., Donner, S., Estradivari, Fadli, N., Feary, D.A., Fenner, D., Fox, H., Franklin, E.C., Friedlander, A., Gilmour, J., Goiran, C., Guest, J., Hobbs, J.-P.A., Hoey, A.S., Houk, P., Johnson, S., Jupiter, S.D., Kayal, M., Kuo, C., Lamb, J., Lee, M.A.C., Low, J., Muthiga, N., Muttaqin, E., Nand, Y., Nash, K.L., Nedlic, O., Pandolfi, J.M., Pardede, S., Patankar, V., Penin, L., Ribas-Deulofeu, L., Richards, Z., Roberts, T.E., Rodgers, K.S., Safuan, C.D.M., Sala, E., Shedrawi, G., Sin, T.M., Smallhorn-West, P., Smith, J.E., Sommer, B., Steinberg, P.D., Sutthacheep, M., Tan, C.H.J., Williams, G.J., Wilson, S., Yeemin, T., Bruno, J.F., Fortin, M.-J., Krkosek, M., Mouillot, D., 2019b. Social–environmental drivers inform strategic management of coral reefs in the Anthropocene. Nat Ecol Evol 3, 1341–1350. https://doi.org/10.1038/s41559-019-0953-8

de Campos, M., Antonangelo, J.A., van der Zee, S.E.A.T.M., Alleoni, L.R.F., 2018. Degree of phos-

phate saturation in highly weathered tropical soils. Agricultural Water Management 206, 135–146. https://doi.org/10.1016/j.agwat.2018.05.001

Donovan, M.K., Adam, T.C., Shantz, A.A., Speare, K.E., Munsterman, K.S., Rice, M.M., Schmitt, R.J., Holbrook, S.J., Burkepile, D.E., 2020. Nitrogen pollution interacts with heat stress to increase coral bleaching across the seascape. Proceedings of the National Academy of Sciences 117, 5351–5357. https://doi.org/10.1073/pnas.1915395117

Downing, J.A., Mcclain, M., Twilley, R., Melack, J.M., Elser, J., Rabalais, N.N., Lewis, W.M., Turner, R.E., Corredor, J., Soto, D., Yanez-Arancibia, A., Kopaska, J.A., Howarth, R.W., 1999. The impact of accelerating land-use change on the N-Cycle of tropical aquatic ecosystems: Current conditions and projected changes. Biogeochemistry 46, 109–148. https://doi.org/10.1007/BF01007576

Eriksson, B.K., Johansson, G., 2005. Effects of sedimentation on macroalgae: species-specific responses are related to reproductive traits. Oecologia 143, 438–448. https://doi.org/10.1007/s00442-004-1810-1

Ezzat, L., Maguer, J.-F., Grover, R., Ferrier-Pagès, C., 2016. Limited phosphorus availability is the Achilles heel of tropical reef corals in a warming ocean. Sci Rep 6, 31768. https://doi.org/10.1038/srep31768

Ezzat, L., Maguer, J.-F., Grover, R., Ferrier-Pagès, C., 2015. New insights into carbon acquisition and exchanges within the coral–dinoflagellate symbiosis under NH4+ and NO3− supply. Proceedings of the Royal Society B: Biological Sciences 282, 20150610. https://doi.org/10.1098/rspb.2015.0610

Fabricius, K.E., 2005. Effects of terrestrial runoff on the ecology of corals and coral reefs: review and synthesis. Marine Pollution Bulletin 50, 125–146. https://doi.org/10.1016/j.marpolbul.2004.11.028

Foster, N.L., Box, S.J., Mumby, P.J., 2008. Competitive effects of macroalgae on the fecundity of the reef-building coral Montastraea annularis. Marine Ecology Progress Series 367, 143–152. https://doi.org/10.3354/meps07594

Goatley, C.H.R., Bellwood, D.R., 2012. Sediment suppresses herbivory across a coral reef depth gradient. Biology Letters 8, 1016–1018. https://doi.org/10.1098/rsbl.2012.0770

Goatley, C.H.R., Bonaldo, R.M., Fox, R.J., Bellwood, D.R., 2016. Sediments and herbivory as sensitive indicators of coral reef degradation. Ecology and Society 21.

Golbuu, Y., Fabricius, K., Victor, S., Richmond, R.H., 2008. Gradients in coral reef communities exposed to muddy river discharge in Pohnpei, Micronesia. Estuarine, Coastal and Shelf Science 76, 14–20. https://doi.org/10.1016/j.ecss.2007.06.005

Green, P.A., Vörösmarty, C.J., Meybeck, M., Galloway, J.N., Peterson, B.J., Boyer, E.W., 2004. Pre-industrial and contemporary fluxes of nitrogen through rivers: a global assessment based on typology. Biogeochemistry 68, 71–105. https://doi.org/10.1023/B:BIOG.0000025742.82155.92

Hoffmann, T., Thorndycraft, V.R., Brown, A.G., Coulthard, T.J., Damnati, B., Kale, V.S., Middelkoop, H., Notebaert, B., Walling, D.E., 2010. Human impact on fluvial regimes and sediment flux during the Holocene: Review and future research agenda. Global and Planetary Change 72, 87–98. https://doi.org/10.1016/j.gloplacha.2010.04.008

Houk, P., Castro, F., McInnis, A., Rucinski, M., Starsinic, C., Concepcion, T., Manglona, S., Salas, E., 2022. Nutrient thresholds to protect water quality, coral reefs, and nearshore fisheries. Marine Pollution Bulletin 184, 114144. https://doi.org/10.1016/j.marpolbul.2022.114144

Houk, P., Comeros-Raynal, M., Lawrence, A., Sudek, M., Vaeoso, M., McGuire, K., Regis, J., 2020. Nutrient thresholds to protect water quality and coral reefs. Marine Pollution Bulletin 159, 111451. https://doi.org/10.1016/j.marpolbul.2020.111451

Hughes, T.P., Rodrigues, M.J., Bellwood, D.R., Ceccarelli, D., Hoegh-Guldberg, O., McCook, L., Moltschaniwskyj, N., Pratchett, M.S., Steneck, R.S., Willis, B., 2007. Phase Shifts, Herbivory, and the Resilience of Coral Reefs to Climate Change. Current Biology 17, 360–365. https://doi.org/10.1016/j.cub.2006.12.049

Image Processing & Analysis Software | Geospatial Image Analysis Software | ENVI® [WWW Document], n.d. URL https://www.nv5geospatialsoftware.com/Products/ENVI (accessed 8.25.23).

Institut de la statistique de la Polynésie Française [WWW Document], n.d. URL https://www.ispf.pf/ (accessed 8.25.23).

Junjie, R.K., Browne, N.K., Erftemeijer, P.L.A., Todd, P.A., 2014. Impacts of Sediments on Coral Energetics: Partitioning the Effects of Turbidity and Settling Particles. PLOS ONE 9, e107195. https://doi.org/10.1371/journal.pone.0107195

Kirch, P.V., 2017. On the Road of the Winds: An Archaeological History of the Pacific Islands before European Contact, Revised and Expanded Edition, in: On the Road of the Winds. University of California Press. https://doi.org/10.1525/9780520968899

Koshiba, S., Besebes, M., Soaladaob, K., Isechal, A.L., Victor, S., Golbuu, Y., 2013. Palau's taro fields and mangroves protect the coral reefs by trapping eroded fine sediment. Wetlands Ecol Manage 21, 157–164. https://doi.org/10.1007/s11273-013-9288-4

Kroon, F.J., Kuhnert, P.M., Henderson, B.L., Wilkinson, S.N., Kinsey-Henderson, A., Abbott, B., Brodie, J.E., Turner, R.D.R., 2012. River loads of suspended solids, nitrogen, phosphorus and herbicides delivered to the Great Barrier Reef lagoon. Marine Pollution Bulletin, The Catchment to Reef Continuum: Case studies from the Great Barrier Reef 65, 167–181. https://doi.org/10.1016/j.marpolbul.2011.10.018

Labrière, N., Locatelli, B., Laumonier, Y., Freycon, V., Bernoux, M., 2015. Soil erosion in the humid tropics: A systematic quantitative review. Agriculture, Ecosystems & Environment 203, 127–139. https://doi.org/10.1016/j.agee.2015.01.027

Lapointe, B.E., 1997. Nutrient thresholds for bottom-up control of macroalgal blooms on coral reefs in Jamaica and southeast Florida. Limnology and Oceanography 42, 1119–1131. https://

doi.org/10.4319/lo.1997.42.5_part_2.1119

Larned, S.T., 1998. Nitrogen- versus phosphorus-limited growth and sources of nutrients for coral reef macroalgae. Marine Biology 132, 409–421. https://doi.org/10.1007/s002270050407

Loiseau, C., Thiault, L., Devillers, R., Claudet, J., 2021. Cumulative impact assessments highlight the benefits of integrating land-based management with marine spatial planning. Science of The Total Environment 787, 147339. https://doi.org/10.1016/j.scitotenv.2021.147339

McClanahan, T.R., Obura, D., 1997. Sedimentation effects on shallow coral communities in Kenya. Journal of Experimental Marine Biology and Ecology 209, 103–122. https://doi.org/10.1016/S0022-0981(96)02663-9

Meyer, J.-Y., Pouteau, R., Spotswood, E., Taputuarai, R., Fourdrigniez, M., 2015. The importance of novel and hybrid habitats for plant conservation on islands: a case study from Moorea (South Pacific). Biodivers Conserv 24, 83–101. https://doi.org/10.1007/s10531-014-0791-6

Moritz, C., Brandl, S.J., Rouzé, H., Vii, J., Pérez-Rosales, G., Bosserelle, P., Chancerelle, Y., Galzin, R., Liao, V., Siu, G., Taiarui, M., Nugues, M.M., Hédouin, L., 2021. Long-term monitoring of benthic communities reveals spatial determinants of disturbance and recovery dynamics on coral reefs. Marine Ecology Progress Series 672, 141–152. https://doi.org/10.3354/meps13807

Nalley, E.M., Tuttle, L.J., Conklin, E.E., Barkman, A.L., Wulstein, D.M., Schmidbauer, M.C., Donahue, M.J., 2023. A systematic review and meta-analysis of the direct effects of nutrients on corals. Science of The Total Environment 856, 159093. https://doi.org/10.1016/j.scitotenv.2022.159093

Puka, L., 2011. Kendall's Tau, in: Lovric, M. (Ed.), International Encyclopedia of Statistical Science. Springer, Berlin, Heidelberg, pp. 713–715. https://doi.org/10.1007/978-3-642-04898-2_324

Ramírez, A., Engman, A., Rosas, K.G., Perez-Reyes, O., Martinó-Cardona, D.M., 2012. Urban impacts on tropical island streams: Some key aspects influencing ecosystem response. Urban Ecosyst 15, 315–325. https://doi.org/10.1007/s11252-011-0214-3

Rice, M.M., Baldwin, D.G., Fischer, J.N., Fuchs, C., Burkepile, D.E., 2021. Complex interactions with nutrients and sediment alter the effects of predation on a reef-building coral. Marine Ecology 42, e12670. https://doi.org/10.1111/maec.12670

Risk, M.J., 2014. Assessing the effects of sediments and nutrients on coral reefs. Current Opinion in Environmental Sustainability, Environmental change issues 7, 108–117. https://doi.org/10.1016/j.cosust.2014.01.003

Rogers, C., 1990. Responses of coral reefs and reef organisms to sedimentation. Mar. Ecol. Prog. Ser. 62, 185–202. https://doi.org/10.3354/meps062185

Rouzé, H., Lecellier, G., Langlade, M.J., Planes, S., Berteaux-Lecellier, V., 2015. Fringing reefs exposed to different levels of eutrophication and sedimentation can support similar benthic communities. Marine Pollution Bulletin 92, 212–221. https://doi.org/10.1016/

j.marpolbul.2014.12.016

Santana, E.F.C., Mies, M., Longo, G.O., Menezes, R., Aued, A.W., Luza, A.L., Bender, M.G., Segal, B., Floeter, S.R., Francini-Filho, R.B., 2023. Turbidity shapes shallow Southwestern Atlantic benthic reef communities. Marine Environmental Research 183, 105807. https://doi.org/10.1016/j.marenvres.2022.105807

Schaffelke, B., Klumpp, D.W., 1998. Nutrient-limited growth of the coral reef macroalga Sargassum baccularia and experimental growth enhancement by nutrient addition in continuous flow culture. Marine Ecology Progress Series 164, 199–211. https://doi.org/10.3354/meps164199

Schmutz, S., Sendzimir, J. (Eds.), 2018. Riverine Ecosystem Management: Science for Governing Towards a Sustainable Future. Springer International Publishing, Cham. https://doi.org/10.1007/978-3-319-73250-3

Shantz, A.A., Burkepile, D.E., 2014. Context-dependent effects of nutrient loading on the coral–algal mutualism. Ecology 95, 1995–2005. https://doi.org/10.1890/13-1407.1

Siemonsma, D., 2015. The Shuttle Radar Topography Mission (SRTM) Collection User Guide.

Surchat, M., Wezel, A., Tolon, V., Breland, T.A., Couraud, P., Vian, J.-F., 2021. Soil and Pest Management in French Polynesian Farming Systems and Drivers and Barriers for Implementation of Practices Based on Agroecological Principles. 15. https://doi.org/10.3389/fsufs.2021.708647

Szmant, A.M., 2002. Nutrient enrichment on coral reefs: Is it a major cause of coral reef decline? Estuaries 25, 743–766. https://doi.org/10.1007/BF02804903

Tanaka, Y., Minggat, E., Roseli, W., 2021. The impact of tropical land-use change on downstream riverine and estuarine water properties and biogeochemical cycles: a review. Ecological Processes 10, 40. https://doi.org/10.1186/s13717-021-00315-3

Tebbett, S.B., Bellwood, D.R., 2021. Algal turf productivity on coral reefs: A meta-analysis. Marine Environmental Research 168, 105311. https://doi.org/10.1016/j.marenvres.2021.105311

Umar, M.J., McCook, L.J., Price, I.R., 1998. Effects of sediment deposition on the seaweed Sargassum on a fringing coral reef. Coral Reefs 17, 169–177. https://doi.org/10.1007/s003380050111

Vega Thurber, R.L., Burkepile, D.E., Fuchs, C., Shantz, A.A., McMinds, R., Zaneveld, J.R., 2014. Chronic nutrient enrichment increases prevalence and severity of coral disease and bleaching. Global Change Biology 20, 544–554. https://doi.org/10.1111/gcb.12450

Vidal-Durà, A., Burke, I.T., Stewart, D.I., Mortimer, R.J.G., 2018. Reoxidation of estuarine sediments during simulated resuspension events: Effects on nutrient and trace metal mobilisation. Estuarine, Coastal and Shelf Science 207, 40–55. https://doi.org/10.1016/j.ecss.2018.03.024

Wakwella, A., Mumby, P.J., Roff, G., 2020. Sedimentation and overfishing drive changes in early succession and coral recruitment. Proceedings of the Royal Society B: Biological Sciences 287, 20202575. https://doi.org/10.1098/rspb.2020.2575

Wenger, A., Harris, D., Weber, S., Vaghi, F., Nand, Y., Naisilisili, W., Hughes, A., Delevaux, J.,

Klein, C., Watson, J., Mumby, P., Jupiter, S., 2020. Best-practice forestry management delivers diminishing returns for coral reefs with increased land-clearing. Journal of Applied Ecology 57. https://doi.org/10.1111/1365-2664.13743

Wenger, A.S., Harris, D., Weber, S., Vaghi, F., Nand, Y., Naisilisili, W., Hughes, A., Delevaux, J., Klein, C.J., Watson, J., Mumby, P.J., Jupiter, S.D., 2020. Best-practice forestry management delivers diminishing returns for coral reefs with increased land-clearing. Journal of Applied Ecology 57, 2381–2392. https://doi.org/10.1111/1365-2664.13743

Zaneveld, J.R., Burkepile, D.E., Shantz, A.A., Pritchard, C.E., McMinds, R., Payet, J.P., Welsh, R., Correa, A.M.S., Lemoine, N.P., Rosales, S., Fuchs, C., Maynard, J.A., Thurber, R.V., 2016. Overfishing and nutrient pollution interact with temperature to disrupt coral reefs down to microbial scales. Nat Commun 7, 11833. https://doi.org/10.1038/ncomms11833

Zhao, H., Yuan, M., Strokal, M., Wu, H.C., Liu, X., Murk, A., Kroeze, C., Osinga, R., 2021. Impacts of nitrogen pollution on corals in the context of global climate change and potential strategies to conserve coral reefs. Science of The Total Environment 774, 145017. https://doi.org/10.1016/j.scitotenv.2021.145017

Zhou, S., Lei, T., Warrington, D.N., Lei, Q., Zhang, M., 2012. Does watershed size affect simple mathematical relationships between flow velocity and discharge rate at watershed outlets on the Loess Plateau of China. Journal of Hydrology 444–445, 1–9. https://doi.org/10.1016/j.jhydrol.2012.03.007

Zuur, A.F., Ieno, E.N., Smith, G.M. (Eds.), 2007. Principal coordinate analysis and non-metric multidimensional scaling, in: Analysing Ecological Data, Statistics for Biology and Health. Springer, New York, NY, pp. 259–264. https://doi.org/10.1007/978-0-387-45972-1_15

III. Programmable Autonomous Water Samplers (PAWS): An inexpensive, adaptable and robust submersible system for time-integrated water sampling in freshwater and marine ecosystems

Contributing Authors: *Daniel La* — Mechanical engineering assistance. *Hyemin Yoo* — Electrical engineering and coding assistance. *Deron E. Burkepile* — Advising.

A. Introduction

Modern human activity is responsible for numerous unprecedented chemical inputs into freshwater and marine ecosystems, including, but not limited to, heavy metals, pesticides, herbicides, petroleum products, industrial waste, emerging contaminants (e.g. pharmaceuticals, personal care products, legal and illegal drugs), plastics, and nutrients (e.g. nitrogen and phosphorus from fertilizer, agricultural runoff and sewage) (Borgwardt et al. 2019, Li and Migliaccio 2010, Lewis et al. 2009, Schulz 2004, Carpenter et al. 1998, Woodward et al. 2012, Naidu et al. 2016, Windsor et al. 2019). Each of these pollutants have their own effects and impacts on aquatic systems, and therefore deserve close study. The shared protocol used in studying and understanding these diverse parameters in aquatic ecosystems is the collection and analysis of water samples. In this paper, we present a novel method of collecting water samples through the use of a low-cost, open-source Programmable Autonomous Water Sampler (PAWS).

Water chemistry and environmental conditions in aquatic ecosystems can be highly variable in both space and time, with conditions changing rapidly in response to even small changes in factors such as precipitation, depth, tides, currents, wave action and animal behavior (Borgwardt et al. 2019). One of the primary challenges

associated with monitoring the health of freshwater and marine aquatic systems, is the resource-intensive nature of collecting data at high enough spatial and temporal resolutions to capture these changes (Cassidy and Jordan 2011). The three most common methods of collecting water chemistry data are: 1) bottle sampling at discrete timepoints (grab sampling) followed by laboratory analysis, 2) automated water sampling followed by laboratory analysis, or 3) in-situ analyzers which are deployed in the environment and perform analyses autonomously. These methods support the collection of data with either high spatial or temporal resolution, but due to cost and/or logistical challenges, often cannot feasibly provide both (Cassidy and Jordan 2011, Robertson and Roerish 1999, Chapin 2015). Because of their low cost, ease of use, and adaptability, PAWS aims to allow for the collection of water quality data from highly dynamic aquatic systems with high spatial and temporal resolution (Table 1).

Historically the most widely used method to collect water quality data is through periodic manual sampling in bottles, or similar containers. Collecting a single water sample is relatively simple and allows for a variety of highly accurate lab-based analyses to be conducted on the same sample. Though collection of bottle samples has a relatively low-cost and low effort per sample, it only provides data regarding the single moment in time the sample was taken. Filling in data gaps by increasing the spatial or temporal resolution of bottle sampling requires both large sampling efforts and potentially large budgets depending on the sampling locations (Robertson and Roerish 1999, Chapin 2015) Once collected, samples will need to be transported to and analyzed in a lab. This can escalate costs rapidly depending on the location (in-house vs external lab) and method of analysis. As a result, many long-term, multi-year, water sampling regimes only collect samples on weekly to

Table 1. PAWS compared to other sampling options. PAWS provides a sampling tool that can be appropriate in situations, such as high energy environments, where other options are not available.

	Bottle Sampling	**Commercial Samplers**	**SAS**	**PAWS**
Initial Cost	**Low to Medium,** basic equip inexpensive, but manual samplers can be **>$500**	**Medium to High**, $2.5k - $50k per unit	**Low**, $220 per unit	**Low**, $300 per unit
Sampling Effort	**Low to High** single sample low, increases rapidly with additional samples/sites	**Low**, autonomous collection	**Low**, autonomous collection	**Low**, autonomous collection
Number of Samples	**Variable**, depending on sampling effort	**≤ 24** discrete samples per unit	**2** discrete samples per unit	**1** integrated sample per unit
Sample Volume	**Variable**, depending on sampling equip	**375ml to 9500ml / sample**	**≤ 900 ml / sample**	**60 ml / sample**
Cost per sample	**Low**, depending on sampling effort	**$104 to >$2000**	**$110**	**$300** for an integrated sample
Cost per 24 hours of sampling	**Increasingly higher** effort/cost to add additional timepoints	**$104 to >$2000** (1 sample per hour)	**$2640** (1 sample per hour)	**$300** for an integrated sample
Spatial Resolution	**Low**, increasingly higher effort/cost to add additional sites	**Low**, high cost to add additional sites	**High**, low cost to add additional sites	**High**, low cost to add additional sites

monthly intervals. Relying on this small number of samples to determine the flux of chemical contaminants can result in vast over, or under, estimates (Robertson and Roerish 1999, Chapin 2015). As bottle sampling is limited to collection times with human compatible working conditions including weather, river or sea state and site access, sampling efforts may miss important episodic events like short period, high intensity storms. Manual sampling at depth can be accomplished using Niskin or Van Dorn style samplers, though this type of sampling is also dependent on human safe working conditions. An additional limitation of bottle sampling is the inability to easily collect samples from multiple location simultaneously, making it difficult to capture the same short episodic events across research sites.

In freshwater studies one solution to this limitation has been the deployment of ISCO-style samplers, large sampling systems which use an electric pump to collect water into a sequential rosette of a fixed number of sample bottles over a user-programmable interval (“Portable Samplers”). While these samplers do offer autonomous collection of a limited number of discrete samples, they are large (dia: 69 cm x height: 51 cm), heavy (~15 kgs), and expensive (~$2.5k to $5k) for the most basic and compact versions. Furthermore, these systems, as well as existing lower-cost open-source alternatives (Carvalho 2020) are not waterproof, limiting their use to studies where they can be deployed on land adjacent to the water they are sampling. As such, they often need to be deployed inside of locked enclosures to improve resistance to both weather and tampering. Though ISCO samplers have become a standard in freshwater science for good reason, depending on the study integrated sampling using a submersible system like PAWS may offer a durable, cost-effective alternative.

To address the needs of marine scientists, numerous submersible autono-

mous sample collection systems are commercially available, or have been developed by researchers. As with many depth capable oceanographic instruments, commercial submersible systems are quite expensive ($35k - $45k) (Mucciarone et al. 2021). There is a high coast associated with depth rating and for many freshwater or coastal studies, these systems are essentially over capable as these studies are often conducted in <30 meters. Recent open-source, researcher developed sampling systems are considerably less expensive than their commercial counterparts (Mucciarone et al. 2021, Albright and Langdon 2013, Enochs et al. 2020) and are more appropriate for shallow deployments. However, these systems often employ multiple housings, exposed moving pump components, and/or external sample collection bags or bottles. Though this increases the sample possible sample volume and aids in reducing the system cost, it also increases the footprint, complexity, vulnerability to damage and tampering, and potential failure points of the systems. As such, these systems may not be capable of sampling in high energy (e.g. fast flowing rivers, or in a subtidal area with wave action) or debris laden environments (e.g. a river during a storm surge, or a wastewater channel) without sustaining damage (Mucciarone et al. 2021, Enochs et al. 2020). Of these sampler projects, PAWS is closest in terms of cost and capability is the Subsurface Automated Sampler (SAS) for ocean acidification research (Enochs et al. 2020). The SAS is capable of collecting two separate samples in bags up to 900 mL using one of two sampling regimes 1) At a set time and date, or 2) once daily. SAS would be appropriate if larger sample volumes or more discrete samples were needed, whereas PAWS would be more suited to collect a much smaller time integrated sample in a high energy environment.

In the last few decades, the deployment of in-situ analyzers, waterproof elec-

tronic packages deployed in the environment that measure, record, and often transmit data in real time, have become an alternative to physical collection of samples for lab-based analyses (Anderson et al. 2021). In many cases, this has revolutionized aquatic research. In-situ analyzers can collect data with high temporal resolution in both freshwater and marine ecosystems. As no lab analysis is required, data is collected in near real time and is often transmitted wirelessly. There are however instances where sampling and lab analysis are still preferable. In-situ analyzers have a high upfront cost. For example, a single basic SUNA nitrate sensor for shallow freshwater deployments costs >$32k (“SUNA V2 Nitrate Sensor”). Though the cost per data point of these systems decreases rapidly over time, the upfront cost, as well as maintenance costs, might still be too much for some research programs. The upfront costs are even higher if the goal is to study multiple parameters as each parameter requires its own probe. Additionally, in-situ analyzers are not available for every parameter (Enochs et al. 2020) or are not sensitive enough for a given system. For example, high quality ammonium probes have a detection limit of 0.2 mg/L (“Low cost ISE ammonium probe”) whereas ammonium concentrations in tropical waters are often < 0.02 mg/L (Fernandes de Barros Marangoni et al. 2020). Finally, in-situ analyzers often rely on hardware, firmware, and software that is proprietary, making instruments difficult to repair, troubleshoot and modify in the field. Many analyzers must be sent back to the manufacturer for maintenance and calibration, something that may not be feasible while operating in remote areas.

Generally autonomous water sampling systems and in-situ analyzers are designed with either fresh water, or marine environments in mind. As scientists studying the interface of freshwater and marine ecosystems in remote locations, we saw a need for a device that combined the autonomous nature of in-situ analyzers with

Figure 1. PAWS on a pier ready for deployment. The black bands are SCUBA diving ankle weights. The dive weight attached to the green rope hits the seafloor before the sampler does allowing PAWS to be anchored above the bottom reducing the possibility of particulate matter blocking the sampler's inlet.

the simplicity and adaptability of manual water sampling. In response to this need we developed PAWS, a low-cost, user-friendly, and highly adaptable autonomous water sampler. This device is open source making it easy to construct and repair. In addition, its compact size (11 cm x 61 cm), inconspicuous, durable, and stream-lined housing, and depth rating of 40m allows it to be deployed in a wide range of aquatic environments including high energy or heavily trafficked areas as well as small cryptic spaces (figure 1).

The PAWS system is designed around the concept of time-integrated sampling. This technique is regularly used in ecotoxicology studies using chemically absorptive materials, membranes or devices such as Chemcatchers® (Jaša et al. 2019, "Chemcatcher"). In passive sampling, the chemical structure of the sampler allows molecules or compounds of interest, such as trace metals, PCBs, herbicides and pharmaceuticals to sorb onto the surface of the sampler. Upon retrieval, the compounds are washed off the surface and analyzed in a lab. Using this method,

concentrations of pollutants in aquatic environments are calculated by assessing the amount of a given compound retrieved from a sampler over the period of time it was deployed. As sampling efficacy is determined by the chemical compatibility between the sampler and the compound of interest, many compounds are not suitable for passive sampling (Vrana et al. 2005). PAWS shares the time-integrated strategy with passive sampling, but rather than relying on absorption properties PAWS collects a single, continuous water sample over the deployment period. In this way PAWS is not selective, any dissolved compound, small suspended particles, or microbiota can be sampled.

To accomplish time integrated water sampling, PAWS uses a syringe pump-like mechanism programmed to collect water at a continuous rate. When it is recovered, the sample collection chamber contains an integrated water sample over a period of a few minutes to > 100 hours (even longer deployments are possible with a larger battery). Continuous sample collection in this way offers several benefits over bottle sampling or other manual sampling techniques (Table 1). Integrated sampling captures an overall average of water chemistry over a given time period. This includes large chemical fluxes from short period, high intensity rainstorms that may fall between bottle sampling intervals. The tradeoff with integrated sampling however is the loss of the fine scale temporal resolution offered by high frequency manual or automatic sampling or in-situ analysis. The integrated sample includes an averaged picture of water chemistry including short period high or low intensity events, but it will not indicate the timing and absolute concentrations associated with them. If a study is only concerned with longer term averages of water chemistry PAWS can provide a significant reduction in sample collection cost as compared to bottle sampling by reducing effort and person-hours. Additionally, PAWS can al-

so provide a reduction in analytical cost as compared to bottle sampling, or autonomous rosette sampling, as a single PAWS sample represents an integration over a period that way require multiple spot samples. Less overall number of samples results in lower analytical costs per study.

B. Hardware description

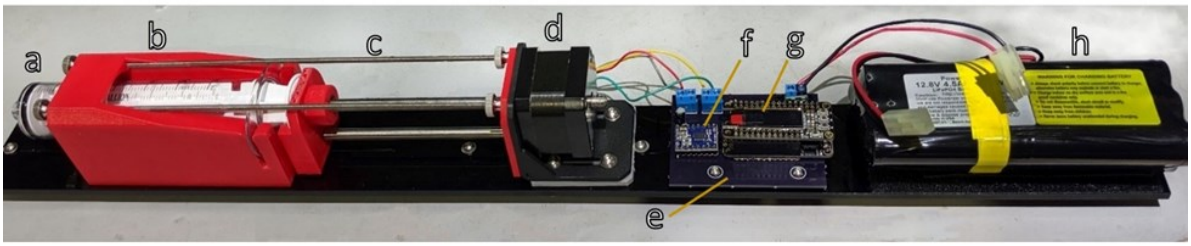

Figure 2. PAWS sampling mechanism, and power and control system out of its housing. a) 60 ml polycarbonate syringe. b) 3D printed syringe cradle. c) Stainless steel threaded rods lock the syringe in place and provide additional bracing. d) NEMA 17 non-captive linear stepper motor actuator. e) PAWS printed circuit board. f) Pololu DRV8880 stepper motor driver carrier. g) Adafruit Feather M0 Express microcontroller with an OLED screen shield. h) Powerizer 12.8v 4.5Ah LiFEPO4 Rechargeable Battery Pack.

One important goal for these samplers was to make them as easy and inexpensive to construct as possible. To achieve this, we designed the system using mostly components that are readily available off the shelf. The few mechanical pieces that are custom made are designed to be fabricated using a laser cutter and a 3D printer, as opposed to machine tools such as a mill or a lathe as is commonly the case for underwater housings. This reduces the cost and ease of production as 3D printers and laser cutters require little training to operate and are increasingly becoming available in many libraries, maker spaces and research labs. Laser cut parts could be cut out carefully using a bandsaw or jigsaw, and a drill. Any of the custom parts could also be made inexpensively by one of the many local or web-based services that have these tools, as opposed to traditional machine shops

which generally have a high overhead due to expensive tooling and a highly trained workforce. Furthermore, all the firmware is open-source and written in Arduino, one of the most accessible and widely used programming languages for hardware control, making it easy to adapt the samplers to new use cases.

PAWS is comprised of three principal component blocks: 1) the sampling mechanism, 2) the power and control system, and 3) the pressure housing.

1. The sampling mechanism

Syringe pumps are a well-established tool for precise dosing or sampling in laboratory settings. Recently, there have been several published open-source syringe pump projects for a variety of lab applications (Iannone et a. 2022, Garcia et al. 2018, Wijnen et al. 2014). To our knowledge however, PAWS is the first environmental water sampler built around a syringe pump-like architecture (figure 2). Previous water sampler designs have used a rosette of spring actuated syringes to col-

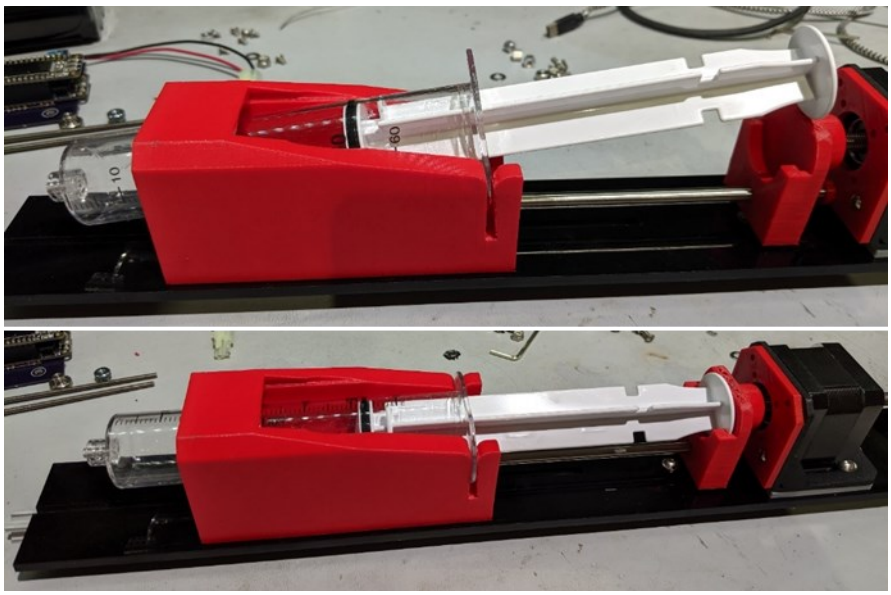

Figure 3. The syringe slides into the syringe cradle and locks into place with a quarter turn.

lect a series of discrete samples (Bird and Ryan 2007, Martin et al. 2004). In contrast, syringe pumps allow for precise control of the sample collection rate in a single syringe. Designing PAWS using this architecture allows for precise collection of an integrated water sample over an extended period of time in a relatively small and inexpensive package. There are numerous additional benefits to building a sampler around a syringe. Syringes are readily available, inexpensive and can

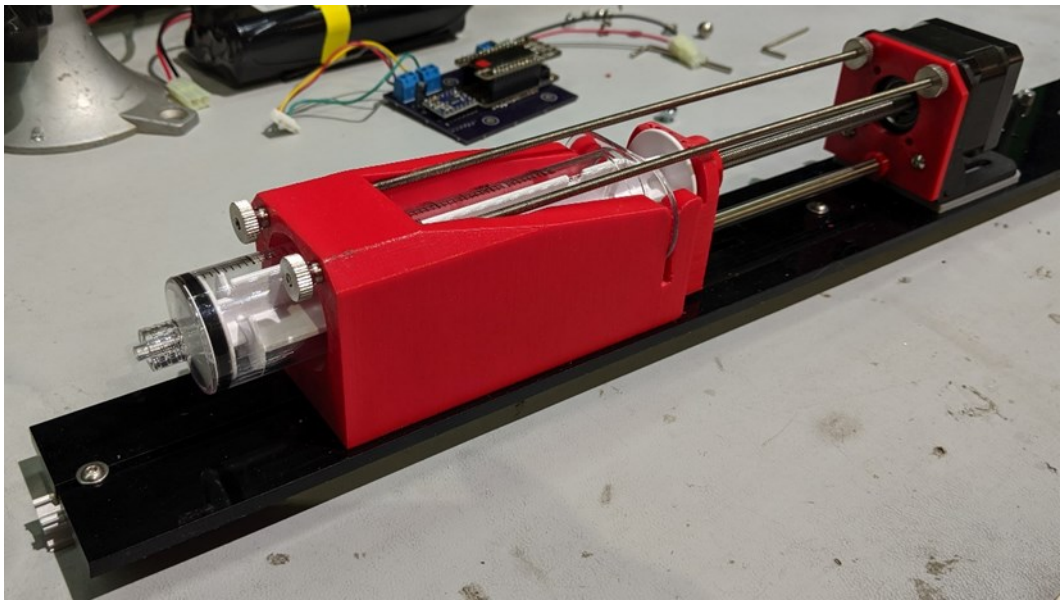

Figure 4. PAWS sampling mechanism built around a 60 ml polycarbonate syringe and a NEMA 17 non-captive stepper motor. The red and grey components were 3D printed on a PRUSA i3 MK3S filament printer using ABS filament. The black tray is made from laser cut acrylic and mounted on an extruded aluminum rail.

come pre-cleaned and sterilized. Though slightly more expensive than the common disposable polypropylene syringe, PAWS utilizes 60 ml polycarbonate syringes which have a longer lifespan, higher pressure rating, lower moisture and gas permeability, and a high thermal tolerance which allows them to be repeatedly steam, gamma, and/or EO sterilized.

After experimenting, and breaking, a handful of established syringe pump designs, we decided to develop our own system for securing the syringe. When in-

serted into the sampler, the syringe slides into a 3D-printed carriage and locks into place with a quarter turn (figure 3). We designed this carriage to hold the syringe securely while the sampler is under high pressure while also allowing the syringe to be easily removed without the use of any tools. The height of the carriage and its angled outside corners are also designed to secure the sampling system inside the housing. The syringe plunger sits into a 3D printed flange that attaches to the sampler motor shaft and rides on a stainless steel rod running between the syringe carriage and the motor mount. Once the syringe is in place, two threaded rods slide into the front of the syringe carriage, over the syringe tabs, and into the motor mount (figure 4). These serve a dual purpose, 1) as extra locks to keep the syringe in place and 2) as tensile rods to stabilize the forces exhibited on the system when under pressure.

The sampling mechanism is driven by a non-captive NEMA 17 hybrid stepper motor linear actuator. With this type of actuator, the motor turns an internal nut which drives a threaded shaft forward or backwards, depending on the direction of rotation (figure 4). Generally, these actuators are very durable and precisely controllable. The additional benefit of the non-captive style motor in this application is that it allows the force of the differential between the housing's internal pressure and the outside water pressure to be directly centered on the motor shaft. This reduces the shear stress on the shaft and motor and allows the motor to run at a lower current. Once the pressure differential is greater than the friction of the o-ring in the syringe, the pressure differential is driving the sample collection with the motor acting like a finely controlled brake. At even shallow depths, PAWS is not drawing in a water sample, but rather letting more water into the syringe in a slow, controlled manner.

2. The power and control system

PAWS is controlled using a microcontroller and a stepper motor driver mounted on a custom printed circuit board (PCB) (figure 5). The Adafruit feather M0 Express was selected for this project because it is a low power and highly versatile microcontroller in a very small package. The Feather has a plethora of configurable analog and digital I/O pins, can be programmed in Arduino or Circuit Python, and Adafruit offers numerous compatible modules ("wings"), such as the screen (OLED) we incorporated into PAWS, which easily stack on top of the Feather. The OLED wing allows the user to access the PAWS menu and program a sampler without connecting it to an external device (figure 5). Once the microcontroller is programmed it communicates with the stepper motor driver to wake up and trigger the motor to step to its next position based on the user defined parameters. We also appreciate the extensive and detailed documentation, user guides, sample code, and support Adafruit provides online for all of their products.

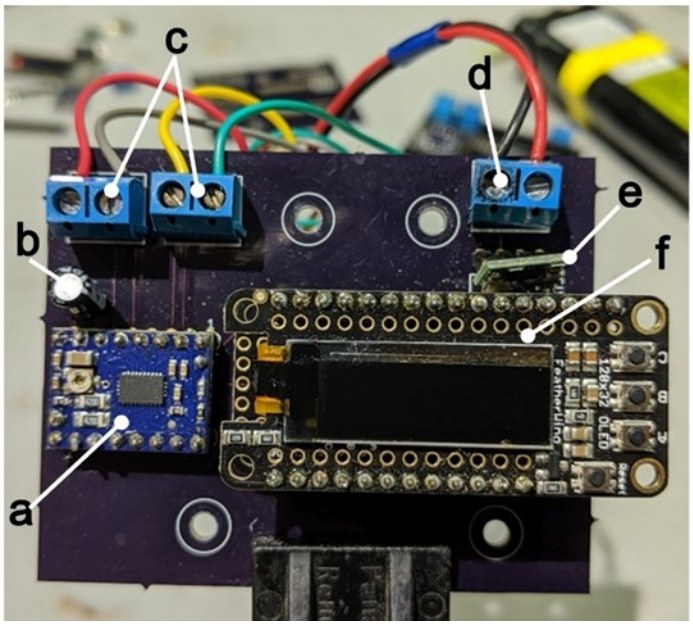

Figure 5. PAWS printed circuit board. a) Pololu DRV8880 stepper motor driver. b) 100 uF capacitor. c) Stepper motor control wire connectors. d) Battery power connector. e) Pololu 3.3v step down voltage regulator. f) Adafruit Feather M0 Express with OLED screen "Featherwing" shield

Power is provided by a 12.8V, 4.5 Ah $LiFePO_4$ rechargeable battery pack. From the battery power is sent to the Feather through a step-down voltage regulator (Pololu D36V6F3) which takes any battery voltage above 4V and outputs 3.3V

to the microcontroller and screen. Full battery power is sent to the stepper motor driver through the PCB and finally to the stepper motor via a bank of screw terminals. The Pololu DRV8880 was selected as the stepper motor driver for its dynamic current scaling capability. Because stepper motors draw current whether they are stepping or not, the dynamic current scaling function allows for PAWS to reduce the power consumption of the motor between steps by more than 90%. While stepping the system can draw up to 455 mA, but in between steps, the system draws only 40 mA. For each step, we energize the motor at full power for 10 milliseconds. Each step rotates the internal nut 1.8 degrees and it takes 10,000 steps to collect 60 ml of water in the syringe. The time it takes to fill the syringe is controlled by varying the delay between steps. Regardless of the duration of sample collection, the system is only running at full power for a total of 0.03 hours (1.7 minutes) consuming just 0.014 Ah of battery capacity. This leaves 112 hours of battery capacity for an initial start delay and/or sampling. In other words, if set to sample immediately after setup, PAWS could collect 60ml over 112 hours (4.7 days), or it could wait in the field for up to 112 hours and then collect 60 ml over one minute, or any combination in between. Longer deployments are possible with larger battery packs. This would likely require lengthening the housing by cutting a longer length of PVC tube.

Unless the user has access to PCB fabrication equipment, the custom PAWS PCB is the only part of the system which will have to be ordered from a fabrication house such as OSH Park. That said, the role of the PCB is to provide location to securely mount the electrical components, as well as a way to streamline and organize connections between components (figure 5). A careful and motivated user could assemble the PAWS control circuitry on a perfboard.

Figure 6. PAWS housing with PVC union threaded endcaps and collars. The front and rear doors (left and right respectively) are made from laser cut clear acrylic. The pass through in the front door is an IV valve epoxied into a laser cut, or drilled, hole through the center of the disc.

3. The pressure housing

The housing for the samplers is constructed from 3-inch schedule 40 PVC pipe capped at each end by PVC unions, components which are readily found at most local hardware stores (figure 6). PVC unions, with one of the flanges replaced by an acrylic disk, make for an excellent housing door as they are already equipped with a face type o-ring seal (Haddock and Dunn 2015). One of the PAWS acrylic doors has a hole into which an IV valve is epoxied. This acts as a connection between the tubing and filters on the outside of the housing, and the syringe on the inside. The other door is made of a solid piece of acrylic. The overall cost of the housing could be reduced by ~$40 if this solid door and its union were replaced by a simple PVC endcap glued in place, however we liked the utility of being able to open the housing from the battery side as well. These housings, with a generous safety factor, can be deployed up to 40 meters depth, which encompasses a majority of applications in freshwater and coastal marine ecosystems. We believe that the system is capable of withstanding higher pressures than we tested. The IV valve epoxied in to the acrylic door is likely the weak point in this housing design.

Further testing is needed to ascertain the maximum depth rating of this configuration. In general, we have found this housing design to be extremely useful and adaptable to a wide variety of applications (see figure 9 for an example). Due to the ready availability of PVC unions and tubing in a range of sizes, this design can be used to build capable housings both quickly and inexpensively. Housings for deeper deployments could be constructed using schedule 80 PVC components, and thicker acrylic doors.

4. Sample preservation

Depending on the goals of the study, any number of different tubing and filtration configurations can be easily and securely connected to the sample syringe via the standard Luer lock fitting. Because of the ability of PAWS to collect water slowly over time rather than pushing a large volume of water through a filter all at once, even filters with small pore sizes work well with this system. For example, we deployed PAWS in moderately turbid seawater for nutrient analyses (see 7.3 Field Deployment). For this study, we attached a 0.15 um prefilter to exclude any particulates and microbes which could alter nutrient concentrations in the sample. The system performed as expected even with the small pore size of the filters. If the study is focused on microbial community analyses paired with water samples, Sterivex type filters could be used. For measurements of total suspended solids, or just the exclusion of large particles, GF/F filters could be connected. For sediment pore water studies, Rhizons will connect directly to the Luer lock fittings on the sampler. If chemical preservation of the sample is required, the sample syringe or a length of intake tubing could be prefilled by a small volume of a fixative such as formalin, mercuric chloride, sulfuric acid, or ethanol.

C. Operation Instructions

PAWS was designed for easy deployment and operation in the field with minimal prep in the lab. The PAWS syringe cradle was designed so the 60 ml polycarbonate syringe will slide in easily and rotate ¼ turn to lock into place (figure 3). Make sure that the plunger of the syringe is seated in the plunger flange. Two M3 stainless steel threaded rods and thumb nuts are used as a security measure to hold the syringe in place under pressure as well as provide some structural support for the sampling mechanism (figure 4). Slide the two rods through the two holes at the top on the front face of the syringe carriage, over the syringe. Thread two thumb nuts onto both ends of both M3 threaded rods (total of four nuts). Spin the inner two nuts until they are approximately 1 cm in from the end of the rod. Screw the rod ends into the upper stepper motor mount holes and tighten the nuts against the stepper motor bracket. Finally, tighten the remaining two nuts against the front face of the syringe cradle.

Users interface with PAWS controller using the OLED shield (figure 5). In addition to the screen, the shield has three individually programmable buttons (A, B, and C) and a reset button. In the provided code, the buttons are programed to navigate the PAWS menu system, adjust deployment and delay periods, and start the device. The reset button can be used at any point to restart the menu system with the default duration and delay settings. PAWS turns on immediately once the battery has been connected. After a brief welcome screen, the PAWS menu system goes into the sampling duration page. Here the user can adjust the amount of time it takes to fill the entire syringe (60 ml). In the current firmware, potential durations range between 1 minute and 24 hours. The duration can be increased by 1-minute

increments by pressing button A, and 1-hour increments by pressing button B. The counter cycles back to 0 after 60 minutes, or 24 hours, respectively. As such, the sample collection rate can be set between a max of 60 ml/min and a minimum of 60 ml/24hours or 0.042 ml/min. If longer sampling periods are needed, it is possible to change line 182 in the code to reflect the desired number of hours (up to 112 hours with the current battery). To make set-up faster, we set this value a maximum of 24 hours as all our sampling regimes were 24 hours or less.

Once the desired deployment period is selected, the user presses button C to advance to the delay menu. In this menu, the user can adjust the length of time PAWS delays before starting sample collection. Potential delays in the provided code range between 0 minutes (immediate start) and 24 hours. Again this can be adjusted by modifying line 182 of the code. Once the desired delay has been selected, button C is pressed. This advances the PAWS menu to the start screen which instructs the user to press C to start. If the delay is set to 0-minutes, sampler collection will begin immediately when the user presses C, a useful feature for bench testing. Otherwise pressing C here will start the delay countdown timer (not displayed). If at any point the user would like to stop operation, C can be pressed again. The countdown or sampling will stop immediately, and the user will have the option to press C one last time to return the sampler to its “home” position. This homing function keeps a running tally of steps taken and when activated will reverse the motor at full speed the same number of steps. The homing function is also available once PAWS has completed a programmed sample collection. The homing function is useful for resetting the system to a sampling ready state but could also be used to expel a collected sample without removing the syringe.

Once the sampling duration and delay functions have been set, the tray can

be slid into the pressure housing. The tray and the syringe carriage lock the sampling system into the housing by bracing against the walls of the tube. A short luer extension tube is connected between the syringe and the pass through on the pressure housing door. Once this connection is made, the door can be put in place and the locking collar screwed into place. Note – users should make sure that the o-ring is clean and greased with a thin layer of silicone prior to putting the door in place. Now any external tubing and/or filters can be connected to the exterior Luer lock on the acrylic door. After retrieving the sampler, it is important to remember that part of the sample will be contained in any length of tubing between the inlet and the syringe.

PAWS are approximately 5 lbs (2.25 kgs) positively buoyant in seawater. As such, it is important to secure the samplers in a method that is appropriate for the deployment environment. In low energy environments, a PAWS will sit on the benthos with a couple of dive weights zip-tied onto the pipe section of the housing. Ankle weights for drysuit diving also fit very snugly around the housing (figure 1). In more energetic or turbulent environments it might be necessary to secure the samplers using a post, bracket, or sand anchors.

D. Validation and characterization

1. Pressure design and testing

All of the components of the PAWS system which handle pressure internally, including the extension tubing, pass through, and syringe, are rated by the manufacturer to at least 175 PSI (119 meters water depth) working pressure. We used the Under Pressure™ housing and vessel design software from DeepSea Power and Light to calculate the pressure rating of the external housing (“Under Pressure

Design Software"). The calculated failure pressure for the 3" schedule 40 PVC pipe is 398 PSI (273 meters water depth). The calculated failure pressure for the acrylic doors is 191 PSI (131 meters water depth).

The syringe mechanism was tested for failure in a lab setting under a 60 PSI (40 meters water depth equivalent) pressure differential for 24 hours. We then turned on the PAWS system and simulated water sampling at this pressure over a 24-hour period. In addition, we conducted a repeat stress test of the sampling mechanism consisting of 50 rapid cycles between 0 and 60 PSI. The pressure housing was tested for one hour at a depth of 21 meters in seawater, and during multiple deployments of up to 12 hours at 1 meter depth in seawater. No leaks, mechanical damage, or signs of stress were observed in any of these tests. At the time of publication, we have not conducted failure testing on the sampling mechanism. Though we believe it is capable of withstanding higher pressure, we have rated the pressure limits of the system based on the successful 60 PSI tests that we performed.

2. Simulated environment testing

To test the efficacy of the PAWS system to integrate changes in water chemistry over an extended period of time, we deployed a sampler in a lidded tank containing approximately 44 liters of artificial seawater made from tap water and Instant Ocean®. Over 8 hours, the tank was spiked with phosphorus (Seachem Flourish®), a common macronutrient of concern in both marine and freshwater systems. In an effort to simulate the heterogeneity of natural systems, we varied the volume of phosphorus added between 0 and 10 ml. At hours 0.5, 2.5, and 4.5 the tank was dosed with 5 ml of Seachem Flourish®. At hour 1.5 the tank was dosed with 10 ml.

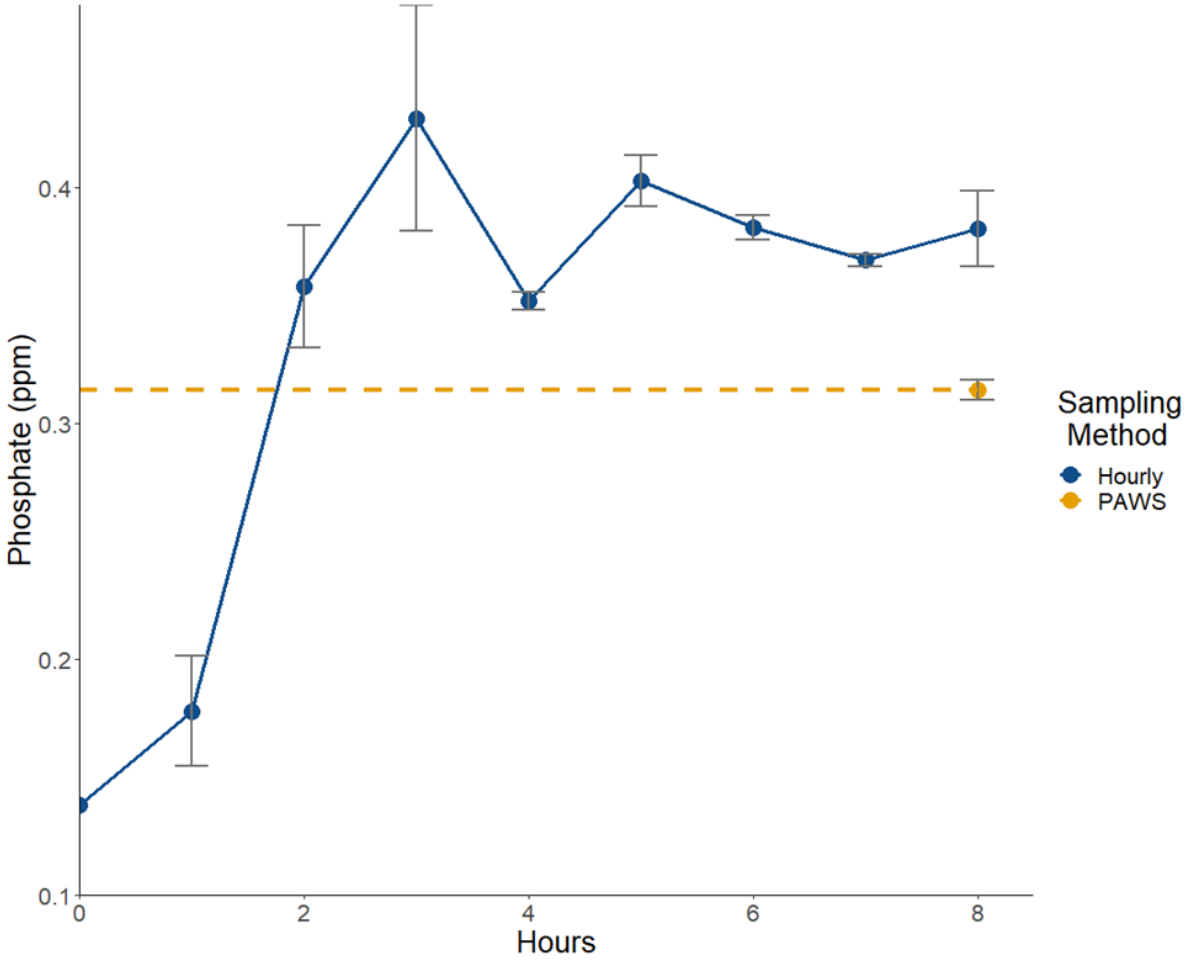

Figure 7. Mean phosphate concentrations, with standard error, from test tank samples collected manually (blue dots) as compared to the integrated sample collected by PAWS (yellow dot). The dotted yellow line indicates the integrated phosphate concentration over the sampling period derived from the PAWS sample. The solid blue line indicates the interpolated trends in phosphate between individual bottle samples. The standard error bars reflect the variation in the three samples collected at each bottle sampling timepoint (with the exception of t=0 which had only one sample), and the three sub-samples that were analyzed from the PAWS syringe. The ~44 L tank was spiked with a 5ml dose of Seachem Flourish® Phosphorus at hours 0.5, 2.5, and 4.5, a 10 ml dose at hour 1.5, and 0 ml at hours 3.5, 5.5, 6.5 and 7.5.

Table 2. Means and standard error (SE) for PO_4 concentrations from PAWS compared to bottle sampling at different frequencies

Sampling Method	**Mean PO_4 Concentration (ppm)**	**SE**
PAWS	0.314	± 0.031
Hourly	0.341	± 0.032
Every 4 hours	0.306	± 0.031
Every 8 hours	0.260	± 0.028

No phosphorus was added at hours 3.5, 5.5, 6.5 and 7.5. The tank was stirred with a small paddle for at least a minute after each addition and then again before sampling. On the hour, three samples were collected by hand adjacent to the PAWS inlet and analyzed using a Hanna Instruments “Checker” Ultra Low Range Phosphorus Colorimeter. After 8 hours, the PAWS system was removed from the tank and the syringe removed from the sampler. The integrated sample from the syringe was then analyzed three times using the colorimeter and compared with the individual samples (figure 7). The mean concentration from the PAWS samples (0.314 ± 0.031 ppm PO_4) is an underestimate as compared to the integrated concentrations from the manual samples (0.341 ± 0.032 ppm PO_4), but the PAWS samples still fall within the standard error of the mean of the manual samples (table 2).

3. Discussion of simulated environment testing

Real world field studies are often limited by time, personnel, or budget constraints which do not allow for high frequency bottle sampling (e.g. hourly). This becomes increasingly more difficult when the number of sampling locations in a study increases. Supposing that our test system could not be sampled hourly, but on 4-hour or 8-hour intervals instead, the PAWS samples do a much better job at captur-

ing a mean PO_4 concentration that is closer to the hourly mean as compared to means calculated from samples collected at lower resolutions (table 2). PAWS cannot capture the high frequency variability of a system, such as that seen at hour 3 of the tank test (figure 1). It is possible that this variability occurred in the test system as a result of chemical interactions between the added phosphorus and the dissolved salts from the Instant Ocean® resulting in a form of phosphorus not detectable by the colorimeter. It could also be the result of insufficient mixing, despite the small tank size and mixing after additions and before sample collection. Similar high frequency variability will also occur in natural systems in the form of inputs, deposition, blooms, or chemical reactions. However, unless a study is particularly concerned with these short-duration events, smoothing the variability using an integrated sample may provide a more representative picture of long-term trends that is not as skewed by extreme events.

4. Field deployment

We deployed a PAWS system alongside three benthic flux chambers in a subsea sediment deposition zone at the mouth of a river in Mo'orea, French Poly-

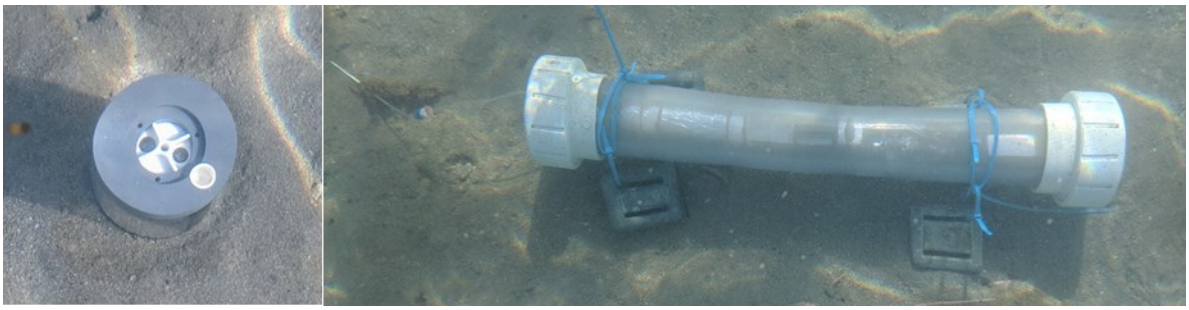

Figure 8. Benthic flux chamber (left) and PAWS (right) deployed at 1m water depth in Mo'orea, French Polynesia. The flux chamber consists of a 10cm clear tube capped with a sealed lid (grey) which contains a manual magnetic stir propellor (center white) and a rubber septum for sampler collection with a syringe (edge white). The chamber is driven into the seafloor to collect potential chemical fluxes over a 12-hour period. The PAWS system was deployed alongside three flux chambers to collect a comparison sample of ambient seawater.

nesia. Benthic flux chambers consisted of a piece of 10 cm inside diameter by 61 cm long clear tubing that was driven at least 5cm into the sediment (Thurber et al. 2020). The upper end of the tube was capped with an o-ring sealed lid that included a septa port for extraction of water samples using a syringe, and a magnetic propellor to mix the fluid within the chamber prior to sampling (figure 8). The goal of this study was to assess what, if any, flux of nutrients (nitrogen and phosphorus species) might be occurring between the sediment and the surrounding seawater. Over 12 hours, the benthic chambers captured seawater exposed to sediment while the PAWS collected ambient seawater for comparison. For this deployment, the PAWS was programmed to fill the syringe over 12 hours and was equipped with a 0.15 uM prefilter on a 15 cm long inlet tube. Once the study area had settled after installation of the flux chambers and sampler, time zero water samples were collected out of the septa of the chambers and directly adjacent to the PAWS inlet using syringes. After 12 hours, samples were again collected from the septa of flux chambers (after mixing with the magnetic stirrer), and adjacent to the sampler inlet. The sampler was then retrieved along with the flux chambers. Back in the lab, the PAWS syringe was removed and the sample was transferred to a storage bottle. All samples were sent to Oregon State University for analysis.

5. Discussion of field deployment

Unfortunately, the results from this study cannot be shared as the samples were lost in a lab fire (Stewart, 2019). However, the study provided an excellent field test for the PAWS system, as the mechanics of system performed faultlessly. Additionally, the study design presents a good example of how PAWS can be used in the field. In this case, we feel that the sample collected by PAWS would have

provided a better comparison to samples collected from the flux chambers, as opposed to bottle samples. This is because both the flux chamber and the PAWS samples are integrated over time, representing an average concentration, or accumulation, of nutrients. Comparing the flux chamber samples to bottle samples, which only provide instantaneous values of the ambient water conditions could skew results as the bottles may be collected during or between peaks and valleys in nutrient concentrations. Despite the loss of the samples, this test deployment, in addition to the lab testing, provided collaborators with sufficient confidence in the system to deploy them in their studies. PAWS will be deployed in the near future to track nutrient cycling inside the cryptic structures of coral reefs.

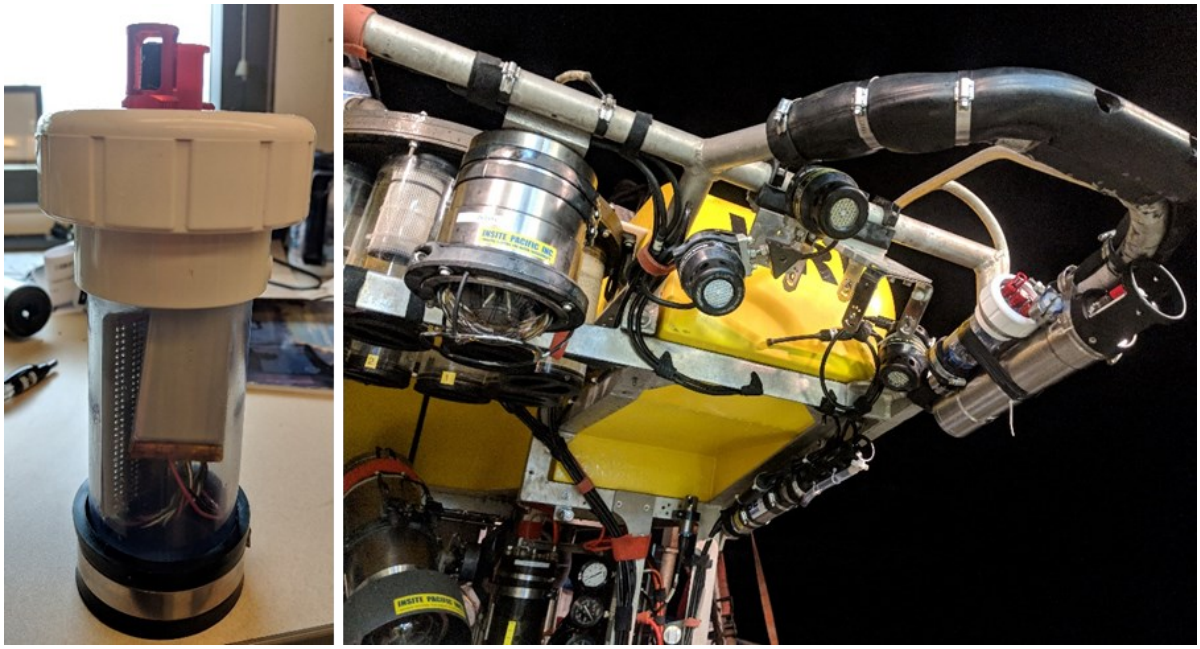

Figure 9. Pressure and temperature logger built with the same general architecture as PAWS sitting on the bench (left). Both the logger and PAWS use an Adafruit M0 express microcontroller. The logger uses temperature and pressure sensors from Blue Robotics. This version of the logger was built in a 2-inch PVC housing with a PVC union and laser cut acrylic door on one end, and a rubber cap on the other. We tested the logger down to 1000m alongside a commercial CTD package on the ROV *Hercules.* To handle the high pressures, the housing was filled with mineral oil and the rubber cap acts as pressure compensator. Future versions of PAWS will incorporate sensors for parallel data logging, or to act as a sampling trigger.

6. Additions and future developments

PAWS was designed as a functional base unit that allows easy opportunity to expand and build upon. The Adafruit Feather microcontroller can communicate with numerous external devices simultaneously using a multitude of communication protocols including I2C and SPI. This functionality allows for the easy addition of sensors (e.g. pressure or temperature sensors) that could trigger PAWS to start sampling in response to physical changes in the environment. For example, a pressure sensor equipped PAWS unit deployed in a stream could wake up and begin sampling when there is an increase in stream depth to capture an integrated water sample during a storm event. Towards this end, we have built and tested a prototype of a temperature and pressure data-logger designed around the Feather M0 express and deployed in the same type of housing used for the PAWS system (figure 9). Future work will integrate these two devices into one unit. Moving forward, we also intend to release an update to the PAWS firmware to improve power management and sleep functionality. This will make PAWS more efficient, reducing battery requirements for longer deployments.

E. Conclusion

Research questions related to water chemistry impacts on aquatic and marine environments are exceptionally varied. They cover a wide range of chemical compounds, time and spatial scales, habitats, depths, flow conditions and organisms. To address these myriad questions it is essential that marine and freshwater scientists have an arsenal of tools at their disposal. It is especially important that these tools are able to provide data on the spatial and temporal scales relevant to rapidly changing and highly heterogeneous conditions. Here we present a Pro-

grammable Autonomous Water Sampler that adds an inexpensive, robust, and highly adaptable tool to the available arsenal. PAWS is capable of capturing an integrated picture of water chemistry conditions over a range of timescales with a price per unit that allows for coordinated widespread deployments either as a standalone sampling device or as a supplement to a larger research program.

Support and Funding:

Funding for this research was provided by the NSF GRFP program, Link Foundation Ocean Instrumentation Fellowship, NSF Career grant OCE—1547952, and the UCSB Coastal Fund Grant.

F. Citations

Albright, R., Langdon, C., Anthony, K.R.N., 2013. Dynamics of seawater carbonate chemistry, production, and calcification of a coral reef flat, central Great Barrier Reef. Biogeosciences 10, 6747–6758. https://doi.org/10.5194/bg-10-6747-2013

Anderson, H.S., Johengen, T.H., Godwin, C.M., Purcell, H., Alsip, P.J., Ruberg, S.A., Mason, L.A., 2021. Continuous In Situ Nutrient Analyzers Pinpoint the Onset and Rate of Internal P Loading under Anoxia in Lake Erie's Central Basin. ACS EST Water 1, 774–781. https://doi.org/10.1021/acsestwater.0c00138

Bird, L., Sherman, A., Ryan, J., 2007. Development of an Active, Large Volume, Discrete Seawater Sampler for Autonomous Underwater Vehicles. pp. 1–5. https://doi.org/10.1109/OCEANS.2007.4449303

Borgwardt, F., Robinson, L., Trauner, D., Teixeira, H., Nogueira, A.J.A., Lillebø, A.I., Piet, G., Kuemmerlen, M., O'Higgins, T., McDonald, H., Arevalo-Torres, J., Barbosa, A.L., Iglesias-Campos, A., Hein, T., Culhane, F., 2019. Exploring variability in environmental impact risk from human activities across aquatic ecosystems. Science of The Total Environment 652, 1396–1408. https://doi.org/10.1016/j.scitotenv.2018.10.339

Carpenter, S.R., Caraco, N.F., Correll, D.L., Howarth, R.W., Sharpley, A.N., Smith, V.H., 1998. Nonpoint Pollution of Surface Waters with Phosphorus and Nitrogen. Ecological Applications 8, 559–568. https://doi.org/10.1890/1051-0761(1998)008[0559:NPOSWW]2.0.CO;2

Carvalho, M.C., 2020. Portable open-source autosampler for shallow waters. HardwareX e00142. https://doi.org/10.1016/j.ohx.2020.e00142

Cassidy, R., Jordan, P., 2011. Limitations of instantaneous water quality sampling in surface-water catchments: Comparison with near-continuous phosphorus time-series data. Journal of Hydrology 405, 182–193. https://doi.org/10.1016/j.jhydrol.2011.05.020

Chapin, T.P., 2015. High-frequency, long-duration water sampling in acid mine drainage studies: A short review of current methods and recent advances in automated water samplers. Applied Geochemistry 59, 118–124. https://doi.org/10.1016/j.apgeochem.2015.04.004

Chemcatcher – Passive water quality sampler, n.d. URL https://chemcatcher.ie/ (accessed 9.10.21).

Enochs, I., Formel, N., Shea, L., Chomiak, L., Piggot, A., Kirkland, A., Manzello, D., 2020. Subsurface Automated Samplers (SAS) for ocean acidification research. Bulletin of Marine Science 96. https://doi.org/10.5343/bms.2020.0018

Fernandes de Barros Marangoni, L., Ferrier-Pagès, C., Rottier, C., Bianchini, A., Grover, R., 2020. Unravelling the different causes of nitrate and ammonium effects on coral bleaching. Sci Rep 10, 11975. https://doi.org/10.1038/s41598-020-68916-0

Garcia, V.E., Liu, J., DeRisi, J.L., 2018. Low-cost touchscreen driven programmable dual syringe pump for life science applications. HardwareX 4. https://doi.org/10.1016/j.ohx.2018.e00027

Haddock, S., Dunn, C., 2015. Fluorescent proteins function as a prey attractant: Experimental evidence from the hydromedusa Olindias formosus and other marine organisms. Biology open 4. https://doi.org/10.1242/bio.012138

Iannone, M., Caccavo, D., Barba, A.A., Lamberti, G., 2022. A low-cost push–pull syringe pump for continuous flow applications. HardwareX 11. https://doi.org/10.1016/j.ohx.2022.e00295

Jaša, L., Sadílek, J., Kohoutek, J., Straková, L., Maršálek, B., Babica, P., 2019. Application of passive sampling for sensitive time-integrative monitoring of cyanobacterial toxins microcystins in drinking water treatment plants. Water Research 153, 108–120. https://doi.org/10.1016/j.watres.2018.12.059

Lewis, S.E., Brodie, J.E., Bainbridge, Z.T., Rohde, K.W., Davis, A.M., Masters, B.L., Maughan, M.,

Devlin, M.J., Mueller, J.F., Schaffelke, B., 2009. Herbicides: A new threat to the Great Barrier Reef. Environmental Pollution 157, 2470–2484. https://doi.org/10.1016/j.envpol.2009.03.006

Li, Y., Migliaccio, K., 2010. Water Quality Concepts, Sampling, and Analyses. CRC Press.

Low cost ISE Ammonium probe (immersion) without RFID, 10 m cable | Hach USA - Details [WWW Document], n.d. URL https://www.hach.com/aise-sc-ise-ammonium-probe/product-details?id=14667082652 (accessed 1.3.22).

Martin, J.B., Thomas, R.G., Hartl, K.M., 2004. An inexpensive, automatic, submersible water sampler. Limnology and Oceanography: Methods 2, 398–405. https://doi.org/10.4319/lom.2004.2.398

Mucciarone, D.A., DeJong, H.B., Dunbar, R.B., Takeshita, Y., Albright, R., Mertz, K., 2021. Autonomous submersible multiport water sampler. HardwareX 9, e00197. https://doi.org/10.1016/j.ohx.2021.e00197

Naidu, R., Arias Espana, V.A., Liu, Y., Jit, J., 2016. Emerging contaminants in the environment: Risk-based analysis for better management. Chemosphere 154, 350–357. https://doi.org/10.1016/j.chemosphere.2016.03.068

Portable Samplers [WWW Document], n.d. URL https://www.teledyneisco.com/en-us/water-and-wastewater/portable-samplers (accessed 9.10.21).

Robertson, D.M., Roerish, E.D., 1999. Influence of various water quality sampling strategies on load estimates for small streams. Water Resour. Res. 35, 3747–3759. https://doi.org/10.1029/1999WR900277

Schulz, R., 2004. Field Studies on Exposure, Effects, and Risk Mitigation of Aquatic Nonpoint-Source Insecticide Pollution: A Review. Journal of Environmental Quality 33, 419–448. https://doi.org/10.2134/jeq2004.4190

Stewart, C., n.d. Burt Hall fire causes lasting damage, sets back research efforts. The Daily Barometer. URL https://dailybaro.orangemedianetwork.com/5468/daily-barometer-news/burt-hall-fire-causes-lasting-damage-sets-back-research-efforts/ (accessed 9.2.22).

SUNA V2 Nitrate Sensor | Sea-Bird Scientific - Overview | Sea-Bird [WWW Document], n.d. URL https://www.seabird.com/nutrient-sensors/suna-v2-nitrate-sensor/family?productCategoryId=54627869922 (accessed 1.3.22).

Thurber, A.R., Seabrook, S., Welsh, R.M., 2020. Riddles in the cold: Antarctic endemism and microbial succession impact methane cycling in the Southern Ocean. Proceedings of the Royal Society B: Biological Sciences 287, 20201134. https://doi.org/10.1098/rspb.2020.1134

Under Pressure Design Software - Complimentary Download [WWW Document], n.d. URL https://www.deepsea.com/knowledgebase/design-tools/under-pressure-design-software/ (accessed 9.20.21).

Vrana, B., Allan, I.J., Greenwood, R., Mills, G.A., Dominiak, E., Svensson, K., Knutsson, J., Morrison, G., 2005. Passive sampling techniques for monitoring pollutants in water. TrAC Trends in Analytical Chemistry 24, 845–868. https://doi.org/10.1016/j.trac.2005.06.006

Wijnen, B., Hunt, E.J., Anzalone, G.C., Pearce, J.M., 2014. Open-Source Syringe Pump Library. PLOS ONE 9, e107216. https://doi.org/10.1371/journal.pone.0107216

Windsor, F.M., Durance, I., Horton, A.A., Thompson, R.C., Tyler, C.R., Ormerod, S.J., 2019. A catchment-scale perspective of plastic pollution. Global Change Biology 25, 1207–1221. https://doi.org/10.1111/gcb.14572

Woodward, G., Gessner, M.O., Giller, P.S., Gulis, V., Hladyz, S., Lecerf, A., Malmqvist, B., McKie, B.G., Tiegs, S.D., Cariss, H., Dobson, M., Elosegi, A., Ferreira, V., Graça, M.A.S., Fleituch, T., Lacoursière, J.O., Nistorescu, M., Pozo, J., Risnoveanu, G., Schindler, M., Vadineanu, A., Vought, L.B.-M., Chauvet, E., 2012. Continental-Scale Effects of Nutrient Pollution on Stream Ecosystem Functioning. Science 336, 1438–1440. https://doi.org/10.1126/science.1219534